ANNUAL REPORT

2022

UNIVERSITY OF OSLO

Above: *CEED members and guests visiting the cobolt mines at Blaafarveværket in June 2022. Photo by:* ***Stephanie Werner.***

Front cover: *A representation of the mountain of achievements by CEED, the sun setting on a glorious decade of science, and the shadow of CEED's legacy.*

Figure by: ***Grace E. Shephard.***

Design by: ***Trond H. Torsvik.***

Back cover from the top:

1. *Participants at the Sundvolden Symposium, November 2022. Photo by: Stéphane Polteau.*
2. *Professors Trond H. Torsvik and Stephanie Werner will lead the new Centre of Excellence PHAB. Photo: UiO.*
3. *Annique van der Boon and Madeleine Vickers on Spirsbergen aa part of the SvalClime workshop, October 2022 Sea. Photo credit: Madeleine Vickers.*

PRIMARY OBJECTIVE:

Develop an Earth model that explains how mantle processes drive plate tectonics and trigger massive volcanism and associated environmental and climate changes throughout Earth history

SECONDARY OBJECTIVES:

(1) Build a consistent global plate tectonic model for the past 1100 Ma

(2) Explore how palaeogeography and True Polar Wander have influenced the long-term climate system

(3) Develop models that link surface volcanism with processes in the deepest mantle

(4) Develop models that link subduction processes in arcs and collision orogens with the mantle

(5) Understand the role of Volumeinous intrusive and extrusive volcanism on global climate changes and extinctions in Earth history

(6) Develop models for mantle structure, composition and material properties

(7) Understand similarities and differences between the Earth and the other terrestrial planets

(8) Develop tools and databases that integrate plate reconstructions with geodynamic and climate modelling

CEED is dedicated to research of fundamental importance to the understanding of our planet, that embraces the dynamics of the plates, the origin of large scale volcanism, the evolution of climates and the abrupt demise of life forms.

This ambitious venture shall result in a new model that explains how mantle processes interact with plate tectonics and trigger massive volcanism and associated environmental and climate changes throughout Earth history.

ACHIEVEMENTS IN 2022

CEED published **112** publications in international journals, **2** books and **3** book chapters. This includes **9 papers in high-impact journals** with **1** as CEED personnel as the **first author**.

Two PhD candidates successfully defended their PhD projects: **Florence Ramirez** (29.11) and **Chloé Markussen Marcilly** (12.12)

Ágnes Király won the 2023 Early Career Scientist Award from the Geodynamics Division of EGU.

Razvan Caracas was awarded the Mineralogical Society of America Dana Medal for 2023.

Annique van der Boon was given the CEED young researcher award.

Manfredo Capriolo won the Tesi di Dottorato 2022 award for the best PhD thesis by the Italian Society of Mineralogy and Petrology (SIMP) .

CEED conferred **The Else Ragnhild Neumann Award** for the fourth time. The 2022-award went to **Jessica Ann McBeck,** UiO.

Mathew Domeier was awarded a Consolidator Grant from the European Research Council and **Annique van der Boon** was awarded a YRT project from the Norwegian Research Council.

Trond H. Torsvik and **Stephanie Werner** were awarded a new Centre of Excellence from the Norwegian Research Council.

Paleontology fieldwork on Malmøya organised by Elizabeth Dowding, summer 2022. Photo by: Elizabeth Dowding.

Organization

Scientfic Advisory Board

Professor **Anny Cazenave**, LEGOS-CNES Toulouse, France

Professor **Claudio Faccenna**, Università Roma TRE, Italy

Professor **Per Barth Lilje**, Department of Astrophysics, UiO

CEED

Centre leader: Professor **Trond H. Torsvik**

Deputy Centre leader: Professor **Stephanie Werner**

Admin. coordinator: **Nina Mino Thorud**, then **Trine Sannesmoen**

41 Professors, Adjunct Professors, Researchers and Research Associates

16 Postdocs

12 PhD fellows

6 Technical-administrative staff members

7 Master students

1 Professor emerita

2 Professor emeritus

In total:

75 paid staff members and 45,5 man-years representing

Centre for Earth Evolution and Dynamics (CEED) was officially opened on 1st of March 2013. Our research includes the dynamics of tectonic plates and Earth history, convection in the mantle, structure of the deep Earth and the origin of mantle plumes and possible connections with large scale volcanism, climate changes through geological time, mass extinctions, and research on planets from our Solar System. To ensure that our scientific vision is effectively met, the activities have been carried out mainly within six research themes, each lead by a Team leader :

The Deep Earth (Team leader Reidar Trønnes, deputy Team leader Chris E. Mohn)

Earth Modelling (Team leader Clint Conrad, deputy Team leader Agnes Kiraly)

The Dynamic Earth (Team leader Valentina Magni, deputy Team leader Grace Shephard)

Earth Crises (Team leader Henrik Svensen, deputy Team leader Morgan T. Jones)

Earth and Beyond (Team leader Stephanie Werner, deputy Team leader Agata Krzesinska)

Earth Laboratory (Team leader Pavel Doubrovine, deputy Team leader Evgeniy Kulakov, then Mathew Domeier)

CEEDlings dressing up at Sundvolden Hotel (Symposium 13-19.11).
Photo by: Ming Geng.

Sundvolden Hotel, location for CEED's international Symposium, November 2022.
Photo by: Sue Webb.

Table of contents

1. Nature Reviews Earth & Environment

"This paper demonstrates that the Permian–Triassic mass extinction (252 million years ago) substantially reduced global biodiversity, with the extinction of 81–94% of marine species and 70% of terrestrial vertebrate families. The environmental changes can be linked to the effects of volcanic emissions during the eruption of the Siberian Traps Large Igneous Province and volcanically driven environmental perturbations included global warming, oceanic anoxia, oceanic acidification, ozone reduction, acid rain and metal poisoning"

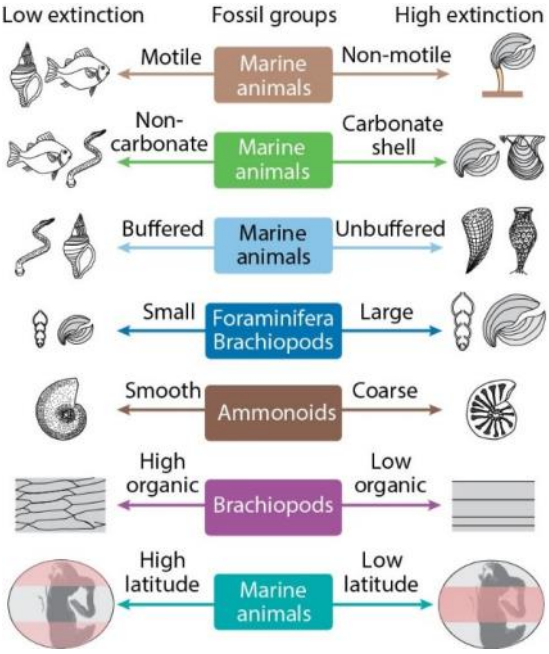

Dal Corso, J., Song, H., **Callegaro, S.**, Chu, D., Sun, Y., Hilton, J., Grasby, S.E., Joachimski, M. & Wignall, P.B. (2022). Environmental crises at the Permian–Triassic mass extinction. **Nature Reviews Earth & Environment** 3, 197-214.

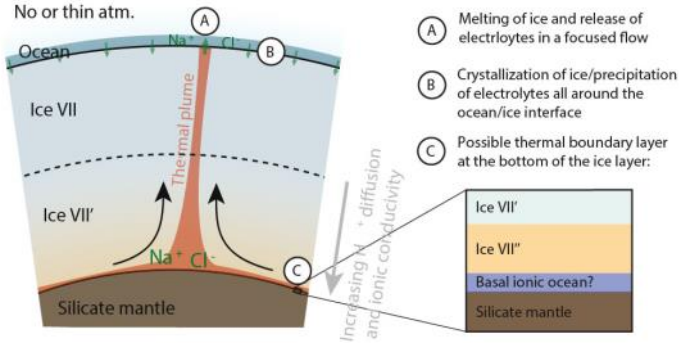

Hernandez, J-A., Caracas, R. & Labrosse, S. (2022). Stability of high-temperature salty ice suggests electrolyte permeability in water-rich exoplanet icy mantles. **Nature Communications** 13, 10.1038/s41467-022-30796-5

2. Nature Communications

"This study shows that up to 2.5 wt% NaCl can be dissolved in dense water ice at interior conditions of water-rich super-Earths and mini-Neptunes. Salt impurities enhance the diffusion of H atoms, extending the stability field of superionic ice, and push towards higher pressures the transition to the stiffer ice X phase. These findings suggest that the high-pressure ice mantle of water-rich exoplanets is permeable to the convective transport of electrolytes between the inner rocky core and the outer liquid layer"

3. Nature Communications

"This study performs ab initio calculations on the partitioning of He, Ne, Ar, Kr and Xe between liquid iron and silicate melt under core forming conditions. For He our results are consistent with previous studies allowing for substantial amounts of He in the core. In contrast, the partition coefficient for Ne is three orders of magnitude lower than He. This very low partition coefficient would result in a $^{3}He/^{22}Ne$ ratio of ~10^{3} in the core, far higher than observed in ocean island basalts (OIBs). We conclude that the core is not the source of noble gases in OIBs"

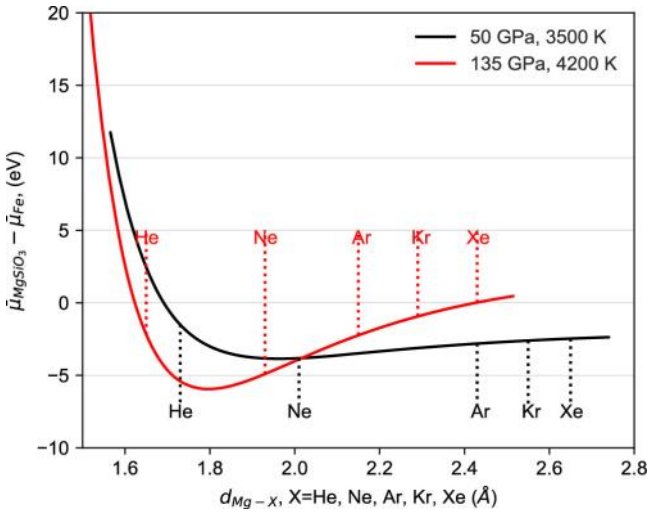

Li, Y., Vocadlo, L., Ballentine, C. & **Brodholt, J.P.** (2022). Primitive noble gases sampled from ocean island basalts cannot be from the Earth's core. **Nature Communications** 13:3770, 10.1038/s41467-022-31588-7.

4. Nature Communications

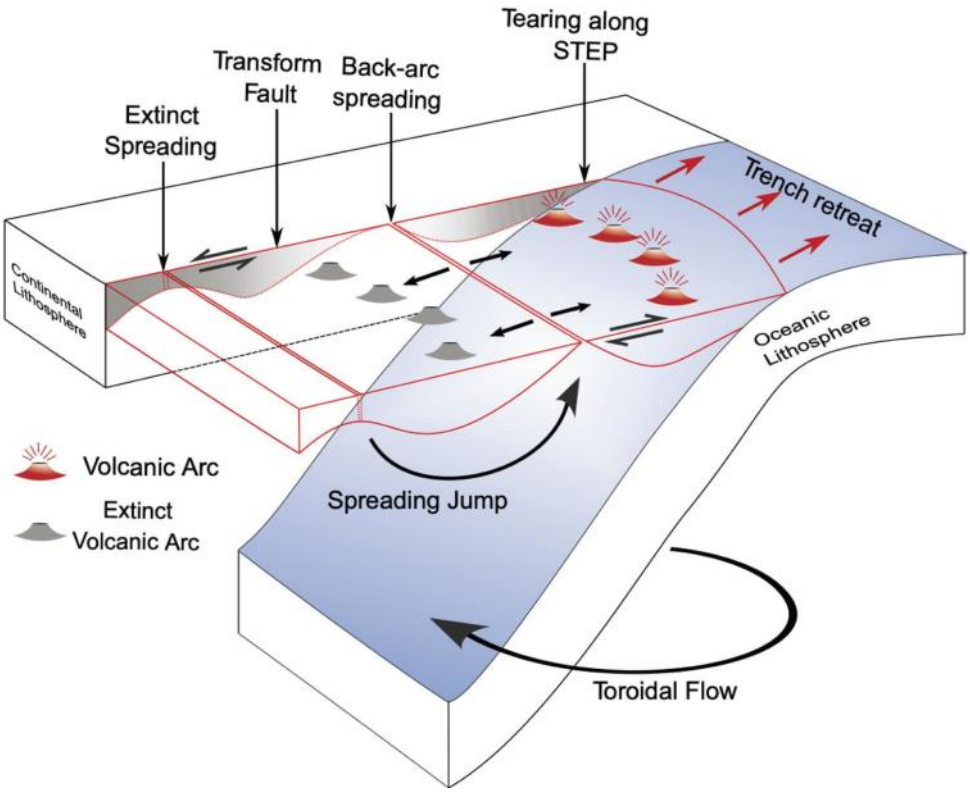

"This paper demonstrates that the time and distance of spreading centres jumps are controlled by the ratio between the transform fault and overriding plate strengths. Despite being less complex than natural systems, our models explain why narrow subducting plates have more frequent and closely spaced spreading jumps than wider subduction zones. It also explains why wide back-arc basins undergo no spreading centre jumps in their life cycle"

Schliffke, N., van Hunen, J., Allen, M.B., **Magni, V.** & Gueydan, F. (2022). Episodic back-arc spreading centre jumps controlled by transform fault to overriding plate strength ratio. **Nature Communications** 13:582, 10.1038/s41467-022-28228-5.

5. Nature Communications

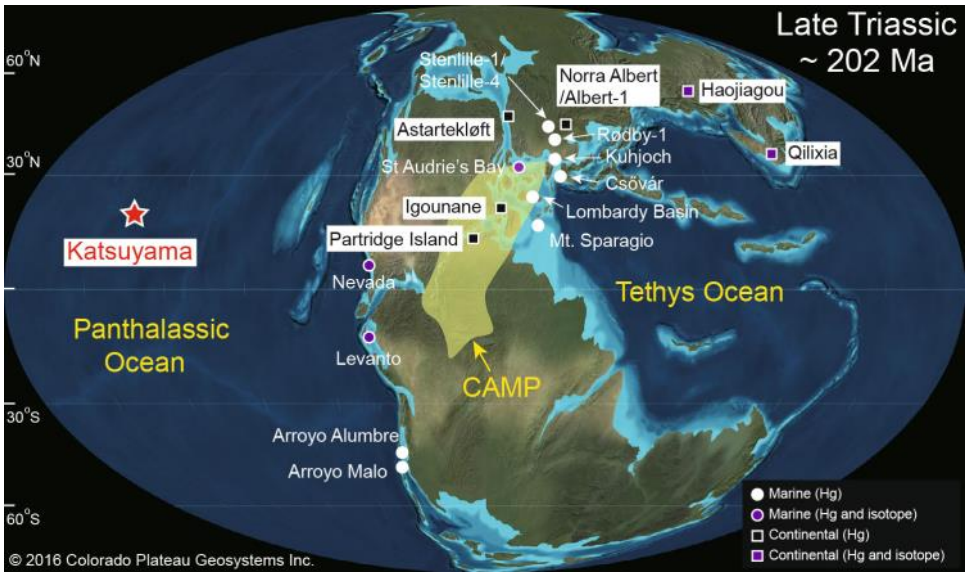

"This study uses mercury (Hg) concentrations and isotopes from a pelagic Triassic–Jurassic boundary section in Japan to track changes in Hg cycling. Hg enrichments are characterized by negative mass independent fractionation of odd Hg isotopes, providing evidence of their derivation from terrestrial organic-rich sediments rather than from deep-Earth volcanic gases. The data provide evidence that combustion of sedimentary organic matter by igneous intrusions and/or wildfires played a significant role in the environmental perturbations accompanying the event"

Shen, J., Yin, R., Algeo, T.J., **Svensen, H.H.** & Schoepfer, S.D. (2022). Mercury evidence for combustion of organic-rich sediments during the end-Triassic crisis. **Nature Communications** 13:1307, 10.1038/s41467-022-28891-8.

6. Nature Astronomy

"This study analysed ROSINA observations and found a previously unrecognized change in the correlations of O_2 with H_2O, CO_2 and CO that contradicts the prevailing notion that the release of O_2 is linked to H_2O at all times. These findings can be explained by the presence of two distinct reservoirs of O_2: a pristine source in the deeper nucleus layers dating back to before nucleus formation, and an H_2O-trapped secondary reservoir formed during the thermal evolution of the nucleus. These results imply that O_2 must have been incorporated into the nucleus in a solid and distinct phase during accretion in significantly lower abundances than previously assumed"

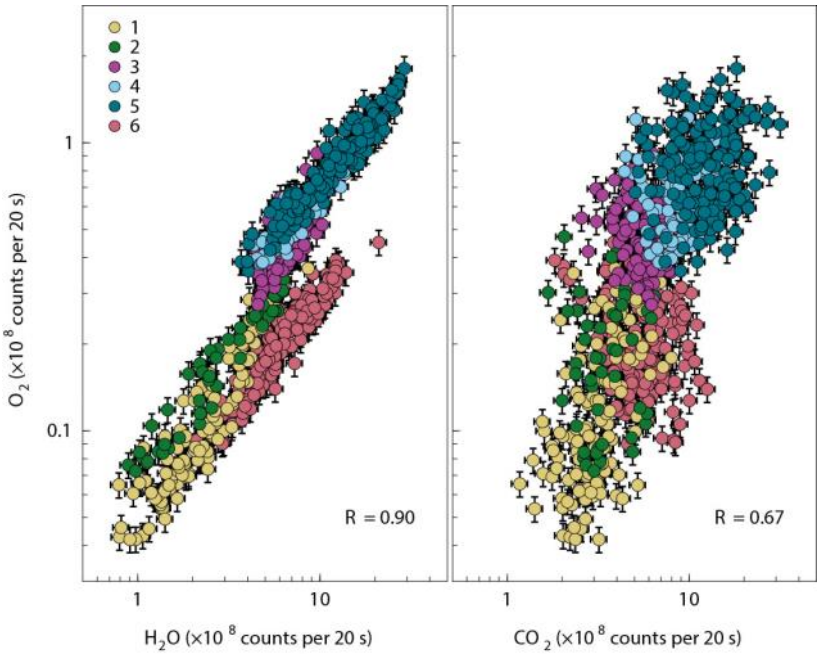

Luspay-Kuti, A., Mousis, O., Pauzat, F., **Ozgurel, O.**, Ellinger, Y., Lunine, J.I., Fuselier, S.A., Mandt, K.E., Trattner, K.J., Petrinec, S.M. (2022). Dual storage and release of molecular oxygen in comet 67P/Churyumov–Gerasimenko. **Nature Astronomy** 6, 724-730.

7. **Communications** Earth & Environment (Nature)

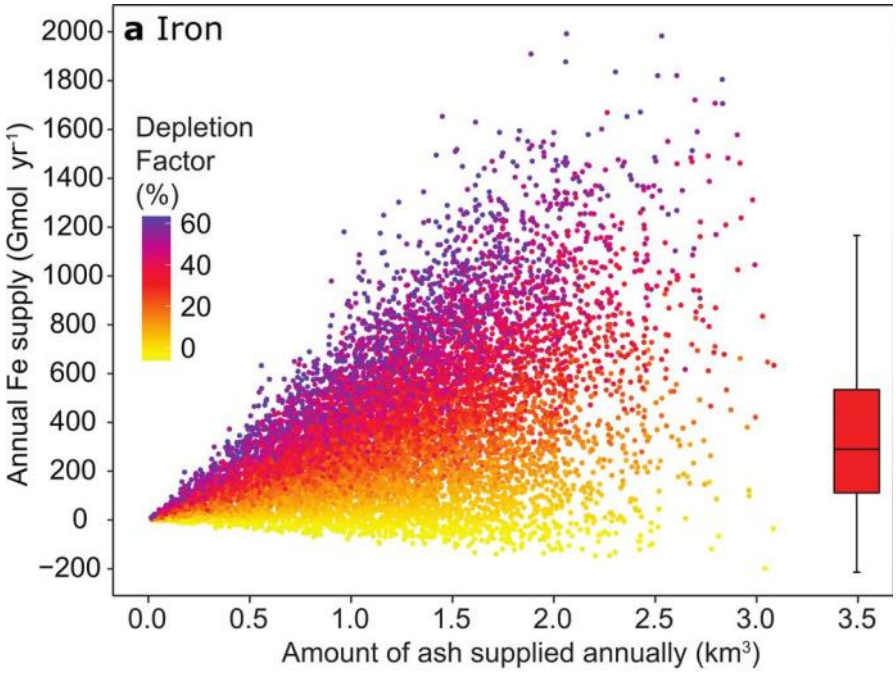

Longman, J., Palmer, M.R., Gernon, T.M., Manners, H.R. & **Jones, M.T.** (2022). Subaerial volcanism is a potentially major contributor to oceanic iron and manganese cycles. **Communications** Earth & Environment 3:60, 10.1038/s43247-022-00389-7.

"This paper uses marine sediment-hosted ash composition data from ten volcanic regions, and subaerial volcanic eruption volumes, to estimate global ash-driven nutrient fluxes. We estimate average fluxes of dissolved Iron and Manganese from volcanic sources to be between 50 and 500 (median 180) and 0.6 and 3.2 (median 1.3) Gmol yr^{-1}, respectively. Much of the element release occurs during early diagenesis, indicating ash-rich shelf sediments are likely important suppliers of aqueous iron and manganese. Estimated ash-driven fluxes are of similar magnitude to aeolian inputs. We suggest that subaerial volcanism is an important, but underappreciated, source of these micronutrients to the global ocean"

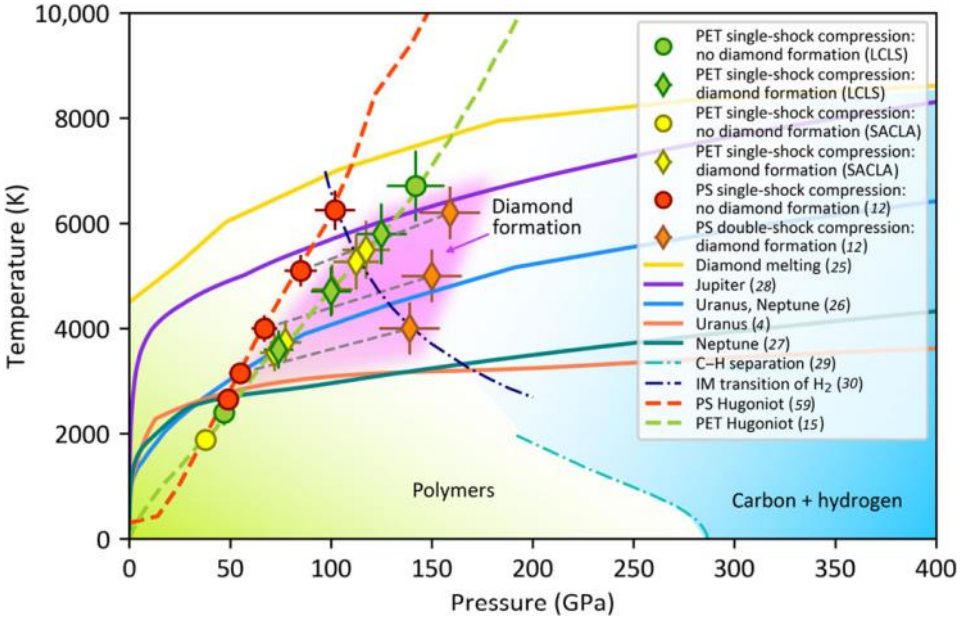

He Z. *et al.* (including **Hernandez, J-A.**) (2022). Diamond formation kinetics in shock -compressed C─H─O samples recorded by small-angle x-ray scattering and x-ray diffraction. **Science Advances** 8, eabo0617.

8. Science Advances

"This study investigates a stoichiometric mixture of C and H2O by shock-compressing polyethylene terephthalate plastics and performing in situ x-ray probing. We observe diamond formation at pressures between 72 ± 7 and 125 ± 13 GPa at temperatures ranging from ~3500 to ~6000 K. Combining x-ray diffraction and small-angle x-ray scattering, we access the kinetics of this exotic reaction. The observed demixing of C and H_2O suggests that diamond precipitation inside the ice giants is enhanced by oxygen, which can lead to isolated water and thus the formation of superionic structures relevant to the planets' magnetic fields"

9. Proceedings of the National Academy of Sciences (PNAS)

"This paper demonstrates that dynamic variations in the Earth's interior could have played a key role in the Eocene–Oligocene climatic transition (~33.9 Ma) and the inception of glaciations. Pulsations in the Iceland mantle plume modified the bathymetry of the Greenland–Scotland Ridge, which affected deep water formation in the North Atlantic. Our model simulations show that the changes in the Atlantic–Arctic oceanic gateways cooled the Southern Hemisphere, and later the Northern Hemisphere, paving the way for the growth of major land-based ice sheets. This supplements the current view that decreasing atmospheric CO2 concentrations and/or changes to the Southern Ocean gateways or the Tethys Seaway dominated climate changes and the inception of glaciations at the time"

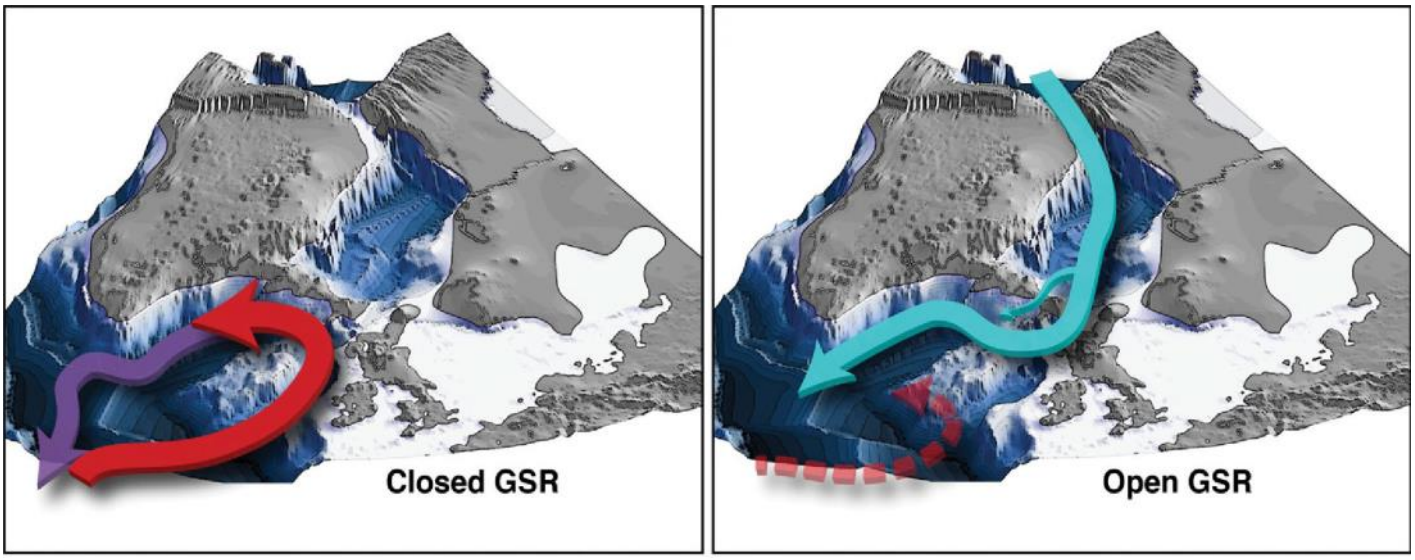

Straume, E.O., Nummelin, A.H., **Gaina, C.**, **Nisancioglu, K.H.** (2022). Climate transition at the Eocene-Oligocene influenced by bathymetric changes to the Atlantic-Arctic oceanic gateways. Proceedings of the National Academy of Sciences of the United States of America 119 (17), e2115346119.

From the Director

The Centre for Earth Evolution and Dynamics (CEED) started in 2013, originally located in the Physics Building, but in 2014 we got our own fortress in the ZEB building. This is the 10th annual report and the end of a long journey with substantial scientific results documented in a large number of articles and books (Box 1). CEED was dedicated to research of fundamental importance to the understanding of the Earth's evolution, which embraced the paleogeography and dynamics of the plates, the origin of large-scale volcanism, the evolution of climates and the abrupt demise of life forms. CEED has bridged the knowledge gap between plates and plumes, and the processes leading to the rapid changes in the atmospheric concentration of greenhouse gases documented in the geological record. We also successfully extended our research to other planets and this provided the fundament for a new Centre of Excellence (Centre for Planetary Habitability), in short PHAB.

BOX 1: CEED numbers 2013-2023

- *~900 articles (67 in the high-profile 'Nature-Science-PNAS' journals).*
- *~24,000 citations, h-index=64 (Scopus).*
- *2 scientific books.*
- *7 popular science books.*
- *60 new projects, including seven Young Talent Grants, two ERC grants, one Norwegian Research School (DEEP), one National Infrastructure (Ivar Giæver Geo-magnetic Laboratory) and a new Centre of Excellence (PHAB).*
- *29 PhD and 41 Master students.*
- *62 postdocs and researchers.*
- *Arranged 60 seminars/workshops.*
- *125 field campaign and cruises.*
- *16 Awards, 10 Medals and 12 Elected Fellows.*
- *Students and researchers from 30 countries.*

During CEED's lifetime, we have published around 900 articles and arranged 60 seminars, workshops and international conferences. The largest of these was held at Sundvollen in November 2022 with around 150 participants. Here we summarized our findings that were discussed with a large number of invited scientists. The program was spread over five days: On day one we outlined the general motivation and history for starting CEED, followed by lectures by keynote speakers that either were involved in the planning of CEED or whose scientific contributions very much stimulated us to establish CEED. The program for the following three days were arranged according to the CEED research themes: Each team leader provided an overview of the main CEED findings, followed by invited keynote lectures on relevant theme issues. There were also two afternoon poster-sessions presenting the most recent finds.

A final debate on the CEED vision, our main hypotheses (Box 2) and successes (/ disappointments) was stimulating, and notably lively concerning postulated links between surface and deep mantle process, and environmental consequences of large igneous provinces (LIPs). Two antipodal regions of slower than average shear-wave velocities (Fig. 1) have for long been imaged in the lowermost mantle, and named the African and Pacific large low shear-wave velocity provinces (LLSVPs). How the LLSVPs formed, what they are made up of and whether they represent long-lived (stable) or dynamic features was lively debated at the Sundvollen meeting, but there was some consensus (at least by some of us) that *most* hotspot lavas and LIPs are the surface manifestations of deep mantle plumes and *largely* sourced from the edges of the LLSVPs (Fig. 1). Combining slab-sinking times and plume ascent times, suggests that 250 ± 50 million years may elapse from initial surface subduction until the eruption of hotspot lavas or a LIP. Interestingly, the subduction pattern between 300 and 200 Ma (Fig. 1) show that the LLSVPs have

largely been devoid of surface subduction, and where it have occurred, slabs have not penetrated the lowermost mantle and modified their shape.

During CEED we have generated 60 new projects. The most important is a new Center of Excellence (PHAB) awarded in 2022, and on the final day of the Sundvollen conference we had invited a number of keynote speakers that addressed topics of relevance to the new PHAB venture. In addition to PHAB, we also received two other prestigious grants in 2022, namely an ERC Consolidator grant (Mathew Domeier) and a young outstanding talent grant from the Norwegian Research Council (Annique van der Boon). These grants, in addition to several other ongoing grants, will form part of the PHAB portfolio in the opening years.

On February 28th 2023 CEED officially ended as a Centre of Excellence (CoE), not all will actually leave physically since some have changed to other sections in the department, have their own projects, or continue to work on other projects. Some also have or will submit new proposals that might be incorporated in the new Centre. PHAB, however, is very different from CEED and is the first Centre in Norway dedicated to research on the habitability of star-planet systems.

CEED has employed a large number of (temporal) postdoctoral workers and researchers, 62 in total over 10 years. I wish to thank you all for your important contributions and hope you enjoyed your time at CEED. Finally, I thank all our students, staff members, adjunct professors and international collaborators for making CEED a wonderful and memorable scientific and social voyage.

BOX 2: CEED Vision 2013

To develop an Earth model that explains how mantle processes drive plate tectonics and trigger massive volcanism and associated environmental and climate changes throughout Earth history.

Main Hypotheses

1. *Mantle plumes are generated from the edges of the Large Low Shear Velocity Provinces (LLSVPs) that on Earth have been stable for the entire Phanerozoic.*
2. *Deep mantle plumes explain the surface distribution of most hotspots, Large Igneous Provinces (LIPs) and kimberlites.*
3. *Mantle plumes explain long-lived massive volcanism on other planets.*
4. *Mantle dynamics have a first-order impact on the motion of lithospheric plates.*
5. *Plate tectonics and True Polar Wander (TPW) influence the long-term climate system and major changes in Earth's life.*
6. *LIPs have been involved in continental break-up and have caused most of the mass extinctions and rapid climate changes of Phanerozoic times.*
7. *The environmental consequences of LIP volcanism are strongly dependent on the magma emplacement environment, with severe impact when magma intrudes organic- and evaporite-rich sedimentary basins.*

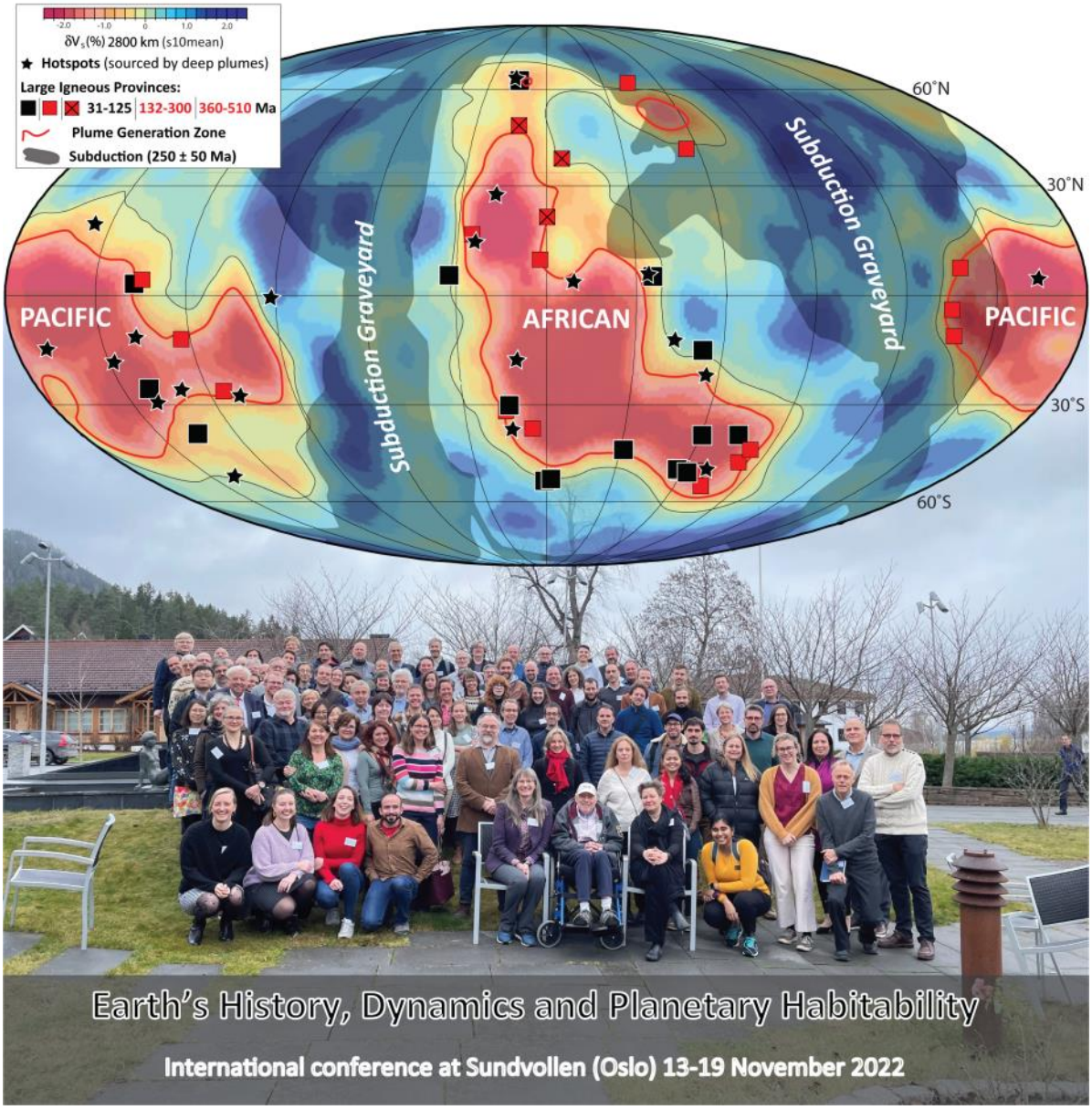

Figure 1. Top panel: *Main CEED hypotheses (Box 2) are centred around mantle plumes and LLSVPs (large low shear-wave velocity provinces) in the lowermost mantle beneath Africa and the Pacific, and links to volcanic systems that may provide a direct link between plume-generation processes in the deep mantle, and changes in the atmosphere-hydrosphere-biosphere system. We have shown for long that that most reconstructed large igneous provinces (LIPs) overlie a contour of constant velocity (the plume generation zone) that correspond to the largest horizontal velocity gradient in the lowermost mantle at ~2800 km depth. That is the 0.9% slow contour in the s10mean tomography model that averages 10 global shear-wave-velocity models. About 250 Myrs must elapse from the subduction of oceanic crustal materials until eruption of recycled crustal components in hotspot lavas. This time could be much longer or shorter and reconstructed surface subduction zones between 200 and 300 Myrs may have been the original slab-sources for active hotspots (black stars) and LIPs dating back to say 125 Ma (squared black symbols). Hotspots argued to have been sourced by deep mantle plumes and are spatially linked to the LLSVPs; the hotspot pattern is similar to that for reconstructed LIPs but unlike LIPs — preferentially erupting above the LLSVP edges — a few Pacific hotspot locations are displaced toward the interior of the LLSVP.* **Bottom panel:** *Group photo at the Sundvollen conference 2022.*

Above: Trond H. Torsvik, Sundvolden 2022. Photo by: Trine Sannesmoen

Below: A final debate on the CEED vision, Sundvolden 2022. Photo by: Sue Webb.

1. Deep Earth: Materials, structure and dynamics

The Deep Earth team members have continued their efforts to disentangle the structure, composition, materials and dynamics of the lower mantle and outer core. In 2022, we published 19 peer-reviewed articles, including two in Nature Communications, one in Nature Astronomy and one in Science Advances. One example of these is the quantum-chemical contribution by Li et al. on the partitioning of the noble gases He and Ne between silicate melt and Fe-metallic melt at pressures and temperatures corresponding to the core-mantle boundary. Both He and Ne prefer the silicate melt in the basal magma ocean, and because the Ne-partitioning to silicate melt is very strong, the core cannot be the source of the primordial He and Ne isotopic signal carried by deep-rooted and vigorous mantle plumes sampled by oceanic island basalts.

Articles published in 2022

Material properties at extreme conditions during planetary accretion and within Super-Earths and giant planets. **Bögels & Caracas (2022)** investigated the critical point and supercritical regime of MgO in order to characterise the thermo-physical properties of a fundamental oxide component in the Earth and other rocky planets. This is part of an ongoing ab initio characterisation of the proto-lunar disk of silicate vapour and liquid, formed as a result of the Earth -Theia collision about 100-150 My after the start of the Solar nebula. By laser-shock compressing a stoichiometric mixture of C and H_2O in starting materials of polyethylene terephthalate (PET) plastics, **He et al. (2022)** observed diamond precipitation by in situ X-ray probing, using a combination of X-ray diffraction (XRD) and small-angle X-ray scattering (SAXS) at the X-ray free energy laser (XFEL) facilities at the Linac Coherent Light Source (LCLS) of SLAC National Accelerator Laboratory in California and at the Super photon ring, 8 GeV (Spring-8) in Hyogo, Japan. Similar diamond precipitation accompanied by C-H-separation and H_2O release inside ice giants may be important for superionic structures and magnetic field generation. The research also indicates the potential to fabricate tailor-sized nanodiamonds with an increasing number of technological applications in medicine, catalysis, and electronics. **Hernandez et al. (2022a)** investigated the NaCl-solubility (about 2.5 wt%) and properties of salty water ice at 1600 K and the pressure conditions of water-dominated exoplanets (super-Earths). They concluded that ice mantles of such planets may be permeable to convective transport of salty electrolytes between inner rock cores and outer liquid layers.

Silicate melting and melt properties and processes. Using two different ab initio atomistic simulation approaches, Braithwaite & Stixrude (2019) and Wilson & Stixrude (2021) obtained surprisingly low melting temperatures for davemaoite (cubic perovskite-structured $CaSiO_3$), e.g. about 5600 K at 136 GPa. Because such a low melting curve would conflict with the experimentally derived melting phase relations of basaltic composition, **Hernandez et al. (2022b)** investigated the davemaoite melting curve further, using five different ab initio atomistic simulation methods. The resulting strong increase in the davemaoite melting temperatures with increasing pressure, to about 7000 K at 136 GPa, is consistent with experimentally derived phase relations in basaltic and picritic compositions. A further account of these phase relations and their implications for the materials of the lowermost mantle is presented in the following section on "Dense residual davemaoite in the lowermost mantle: implications for ULVZs and LLSVPs". **Huang et al. (2022a; 2022b)** investigated the physical properties and nitrogen speciation in a pyrolitic magma ocean (MO) melt by experiments and atomistic simulations. With increasing pressure, the MO melt densifies by bond length reductions and coordination number increase. Whereas the O-O bond length decreases from 2.56 to 2.36 Å (7.8%) in the 36-136 GPa range at 4000 K, the shorter Mg-O

and Fe-O lengths (1.88 and 1.80 Å, respectively at 136 GPa) are compressed by 4.2 and 4.1%, respectively. The shortest Si-O bond length remains constant at 1.64 Å in the entire 36-136 GPa range. Whereas the average O-O coordination number decreases from 12.2 to 10.7 in the 36-136 GPa range, the cation-oxygen coordination numbers increase, e.g. from about 5 to 6 for Si-O. The pressure-induced melt densification of 40% is accompanied by a 28% shear velocity increase in a corresponding pyrolitic glass. Under the relatively oxidised conditions expected for a hot pyrolitic magma ocean, the nitrogen speciation is in the form of dissoved N_2-units. Degassing near the surface may therefore produce a N_2-rich early atmosphere. **Davis et al. (2022)** investigated element speciation, coordination and bond lengths in silicate-carbonate melts with excess metallic Fe, using ab initio molecular dynamics covering the 1-148 GPa range at 3000 and 4000 K. The results are largely similar to those of Huang et al. (2022a,b). Additional findings are that increasing pressure promotes C-C and C-Fe bonding and the gradual replacement of carbonate groups with carbon polymers and C-Fe clusters.

Core materials, properties and distribution of water and noble gases. In order to elucidate candidate materials for the inner and outer core, **Zurkowski et al. (2022)**, performed laser-heated diamond anvil cell experiments with Fe_2S up to 194 GPa and 2500 K, using synchrotron X-ray diffraction for phase identification and equation-of-state determination. They inferred the C23-C37 phase transition in the 120-150 GPa range. Based on the density-pressure relations derived by Zurkowski et al. (2022), S cannot be the only core-alloying light element, but possibly a minor contributor. With first principles molecular dynamics calculations, **Li et al. (2022a)** determined the liquid state diffusivity, viscosity and density in the systems Fe-H and Fe-H_2O. Hydrogen has a large leverage on the physical properties of liquid core alloys, e.g. density and seismic velocity (e.g. Umemoto & Hirose, 2020). The Li et al. (2022a) results involve higher Fe self-diffusivity than those of previous studies and diffusivities for O and H (diffusing "interstitially") that are about 2 and 11 times larger the Fe diffusivity. The associated viscosity reduction in an outer core fluid with or without H, will suppress viscous entrainment, promoting small-scale turbulent convection, as well an outermost stagnant E'-layer below the core-mantle boundary, indicated by seismology, core dynamics modelling and mineral physics (Lay & Young 1990). From the Wang et al. (2021) results based on an equivalent ab initio approach, Li et al (2022a) used the density contrast at the inner core boundary to estimate the maximum H-content in the core. With excess O relative to stoichiometric H_2O composition, the maximum H-content would be 0.1 wt%, and with the unlikely scenario with no O in the core, the maximum would be 0.3 wt% H. In order to put further constraints on the origin and source of primordial-like isotopic compositions of He and Ne characteristic of high plume-flux oceanic island basalts, **Li et al (2022b)** investigated the partitioning of the these elements between silicate ($MgSiO_3$) melt and Fe-metallic melt. In the 50-135 GPa range, He is moderately and Ne is strongly lithophile ($D_{He}^{met/sil}$ and $D_{Ne}^{met/sil}$ are 10^{-2}-10^{-3} and 10^{-6}, respectively). This implies that the core cannot be the source for the primordial-like noble gas composition, because the metal-silicate partitioning would have imposed an unacceptably high $^3He/^{22}Ne$-ratio in the core.

Hydrogen in mantle silicates – water content of the mantle and the core. Using particle swarm optimisation with density functional theory and the quasi-harmonic approximation, **Solomatova et al. (2022)** investigated the crystallography, crystal chemistry, elasticity and relative stability of three $MgSiO_2(OH)_2$-phases. Phase H remains the energetically favoured

polymorph compared to the Mg-endmember of phase egg and phase $P4_32_12$ to pressures of at least 300 GPa, indicating that it might be a hydrous mineral in large exoplanets. However, because the relative stabilities of phase egg and phase $P4_32_12$ may be higher in more realistic Al-bearing compositions, the system $MgSiO_2(OH)_2$-$AlSiO_3(OH)$ should be investigated further. **Drewitt et al. (2022)** derived densities of hydrous silicate melts in the system MgO-SiO_2-H_2O at deep upper mantle to shallow lower mantle p-T condition by ab initio atomistic simulations. Based on a comparison of their results with experimentally derived melt densities, they concluded that the hydrous melts derived by dewatering of wadsleyite during its phase transition to olivine at 410 km depth are positively buoyant for a wide range of Mg# (100-50). Their results also indicate that hydrous melts generated by water-saturation in sinking lithosphere below the 660 km seismic discontinuity will rise buoyantly into the transition zone. The buoyancy-driven melt percolation is facilitated by the very low viscosity of such hydrous melts. Consequently, the Drewitt et al. results disproves the proposed trapping of dense hydrous melt just above the 410 km discontinuity and imply that the relatively dry transition zone cannot accumulate water. The entire convecting mantle must therefore have a water content similar to that of the average upper mantle (the asthenospheric MORB source) of about 0.03 wt%. Such an average water concentration is equivalent to a total mantle water mass of 0.5-1 times the present ocean water mass. By comparison, a possible, and maximum, water concentration of 0.12 wt% in the core (Li et al. 2022a), would correspond to about 22 ocean masses.

Meteorites, comets and asteroids – materials and properties. Jadeite reported in shocked meteorites are often characterised only by micro-Raman spectroscopy. Based on crystal chemical analyses of shocked meteorites, combined with ab initio atomistic simulations, **Baziotis et al. (2022)** demonstrated that such "jadeites" identified by Raman spectroscopy commonly contain 15-35 mol% of the end member components $Vacant^{M2}\,Si^{M1}\,Si_2{}^{T}\,O_6$ (Si-pyroxene) and $Ca^{M2}\,Al^{M1}\,AlSi^{T}\,O_6$ (Ca-tschermak's or kushiroite component) and only 50-75% of the jadeite component. Based on the Rosetta spacecraft data, **Luspay-Kuti et al. (2022)** measured high cometary O_2-release from comet 67P/Churyumov-Gerasimenko and used ab initio atomistic simulations to model the interactions between H_2O ice with O_2 adsorbed on the surface, or trapped in gas inclusions or cracks. The Rosetta data indicate that the O_2 is associated mainly with H_2O, rather than with CO and CO_2. The oxygen is probably sourced in deeper parts of the nucleus, as well as in shallower secondary H_2O-ice reservoirs, formed by thermal alteration of the nucleus.

Ocean-atmosphere interaction. Using classical molecular dynamics combined with ab initio-based polariseable force fields, **Ozgurel et al. (2022)** investigated the process of sea-spray aerosol (SSA) emission into the air. They focussed on mono- and di-carboxylates, containing 4, 6 or 8 carbon atoms, which comprise a large fraction of SSA surfaces, and recorded the structural and dynamical properties of Na^+, K^+, Mg^{2+} and Ca^{2+} cations interacting with monocarboxylates and dicarboxylates of various lengths in a simulation box containing 2000 water molecules. Whereas K^+ is more prone to reside at the SSA-surface, Na^+ will be transported in the aerosol to a greater extent.

Experimental and theoretical method developments. In a lattice dynamical study of the phonon spectrum of an Y-Al-garnet (YAG, $Y_3Al_5O_{12}$), **Poulos et al. (2022)** compared the

experimental methods of IR spectroscopy, Raman scattering and neutron scattering with atomistic density functional theory and classic potential theory. The agreement between the experimental and theoretical approaches was excellent, and the atomistic simulations allowed an accurate calculation of the thermodynamic and elastic properties of YAG. The compact and dense crystal structure of YAG enabled the calculation of these properties, even at temperatures close to the melting point, by the quasi-harmonic approximation. **Li et al. (2022c)** developed the Fortran-based toolkit, ElasT, which simplifies the calculation of solid-state elastic constants at finite temperatures. These theory-based stress-strain methods were successfully applied to crystals of different materials and lattice types, and the agreement with other experimental and theoretical elasticity data is excellent.

References to 2022-articles from the Deep Earth team

Baziotis I, Xydous S, Papoutsa A, Hu J, Ma C, Klemme S, Berndt J, Ferriere L, **Caracas R**, Azimow PD, 2022. Jadeite and related species in shocked meteorites: Limitations on inference of shock conditions. Am. Mineral. 107, 1868-1877.

Bogels TFJ, **Caracas R**, 2022. Critical point and supercritical regime of MgO. Phys. Rev. B. 105, 064105.

Davis AH, Solomatova NV, Campbell AJ, **Caracas R**, 2022. The speciation and coordination of a deep Earth carbonate-silicate-metal melt. J. Geophys. Res. 127, e2021JB023314.

Drewitt JWE, Walter MJ, **Brodholt JP**, Muir JMR, Lord, OT, 2022. Hydrous silicate melts and the deep mantle H_2O cycle. Earth Planet. Sci. Lett. 581, 117408.

Ezad IS, Dobson DP, Thomson AR, Jennings ES, Hunt SA, **Brodholt JP**, 2022. Kelyphite textures experimentally reproduced through garnet breakdown in the presence of a melt phase. J. Petrol. 63, 1-22.

Ezad IS, Einsle JF, Dobson DP, Hunt S, Thomson AR, **Brodholt JP**, 2022. Improving grain size analysis using computer vision techniques and implications for grain growth kinetics. Am. Mineral. 107, 262-273.

He Z et al., incl. **Hernandez**, 2022. Diamond formation kinetics in shock-compressed C─H─O samples recorded by small-angle x-ray scattering and x-ray diffraction. Sci. Adv. 8, eabo0617.

Hernandez, J-A, Caracas R, Labrosse, S, 2022a. Stability of high-temperature salty ice suggests electrolyte permeability in water-rich exoplanet icy mantles. Nat. Comm. 10.1038/s41467-022-30796-5.

Hernandez J-A, Guren MG, Mohn CE, Baron MA, Trønnes RG, 2022b: Ab initio atomistic simulations of Ca-perovskite melting. Geophys. Rev. Lett., 49, e2021GL097262.

Huang D, Murakami M, **Brodholt JP**, McCammon C, Petitgirard S, 2022a. Structural evolution in a pyrolitic magma ocean under mantle conditions. Earth Planet. Sci. Lett. 584, 117473.

Huang D, **Brodholt JP**, Sossi P, Li Y, Murakami M, 2022b. Nitrogen speciation in silicate melts at mantle conditions from ab initio simulations. Geophys. Res. Lett. 49, e2021GL095546.

Li Y, Guo X, Vocadlo L, **Brodholt JP**, Huaiwei N, 2022a. The effect of water on the outer core transport properties. Phys. Earth Planet. Int. 329-330, 106907.

Li Y, Vocadlo L, Ballentine C, **Brodholt JP**, 2022b. Primitive noble gases sampled from ocean island basalts cannot be from the Earth's core. Nat. Comm. 10.1038/s41467-022-31588-7.

Li Y, Vocadlo L, **Brodholt JP**, 2022c. ElasT: A toolkit for thermoelastic calculations. Computer Phys. Comm. 273, 108280.

Luspay-Kuti A, Mousis O, Pauzat F, **Ozgurel O**, Ellinger Y, Lunine JI, Fuselier SA, Mandt KE, Trattner KJ, Petrinec SM, 2022. Dual storage and release of molecular oxygen in comet 67P/Churyumov–Gerasimenko. Nat. Astron. 6, 724-730.

Ozgurel O, Duflot D, Masella M, RealF, Toubin C, 2022. A Molecular Scale Investigation of Organic/Inorganic Ion Selectivity at the Air−Liquid Interface. ACS Earth Space Chem. 2022, 6, 1698−1716.

Poulos M, Giaremis S, Kioseoglou J, Arvanitidis J, Christofilos D, Ves S, Hehlen MP, Allan NL, **Mohn CE**, Papagelis K, 2022. Lattice dynamics and thermodynamic properties of $Y_3Al_5O_{12}$ (YAG). J. Phys. Chem. Solids 162, 110512.

Solomatova NV, **Caracas R**, Bindi L, Asimow P, 2022. Ab initio study of the structure and relative stability of $MgSiO_4H_2$ polymorphs at high pressures and temperatures. Am. Mineral. 107, 781-789.

Zurkowski CC, Lavina B, Brauser NM, **Davis AH**, Chariton S, Tkachev S, Greenburg E, PrakapenkaVB, Campbell AJ, 2022. Pressure-induced C23–C37 transition and compression behavior of orthorhombic Fe_2S to Earth's core pressures and high temperatures. Am. Mineral. 107, 1878-1885.

Additional references

Braithwaite J, Stixrude L, 2019. Melting of $CaSiO_3$ perovskite at high pressure. Geophys. Res. Lett. 46, 2037-2044.

Lay T, Young CJ, 1990. The stably stratified outermost core revisited. Geophys. Res. Lett. 17, 2001-2004.

Umemoto K, Hirose K, 2020. Chemical compositions of the outer core examined by first principles calculations. Earth Planet. Sci. Lett., 531, 116009.

Wang W, Li Y, Brodholt JP, Vočadlo L, Walter MJ, Wu Z, 2021. Strong shear softening induced by superionic hydrogen in Earth's inner core. Earth Planet. Sci. Lett. 568, 1170142.

Wilson A, Stixrude L, 2021. Entropy, freezing and dynamics of $CaSiO_3$ liquid, Geochem. Cosmochem. Acta, 302, 1-17.

Dense residual davemaoite* in the lowermost mantle: implications for ULVZs and LLSVPs

(*cubic perovskite-structured $CaSiO_3$, formerly termed Ca-perovskite)

Partial preprint of manuscript to be submitted: Trønnes RG, Mohn CE, Grømer B, Hernandez J-A, Guren MG, Baron MA: Dense residual davemaoite in the lowermost mantle.

Significance

Davemaoite, which is the third most abundant mineral in the lower mantle, is also the last mineral to be consumed during partial melting of recycled oceanic crust of basaltic and picritic composition. Because of its residual nature and high density, davemaoite, accompanied by iron-rich melts, may sink towards the core-mantle boundary after partial melting of recycled oceanic crust. There, they may form the main ingredients of partially molten, 5-40 km thick lenses, recognized by slow seismic wave propagation. Such ultra-low velocity zones (ULVZs) at the bottom of the mantle may represent partially open "windows" to the outer core of molten iron-dominated liquid. Minor melt mixing and element diffusion via the ULVZs may transfer characteristic isotopic fingerprints on basalts erupted on volcanically active oceanic islands (like Hawaii, Galapagos and Iceland), which are formed above buoyant columnar plumes rooted in the ULVZs.

Summary

The liquidus field of davemaoite (dm) expands with increasing pressure, making it the most residual phase during partial melting of recycled oceanic crust (ROC) of basaltic to picritic composition. ROC slivers, which have higher density and lower solidus temperature than peridotite, may sink relative to peridotite in the lateral low-viscosity flow above the core mantle-boundary towards the large low S-wave velocity provinces (LLSVPs) and undergo partial melting in the hottest regions near their margins. Partial ROC melting above the ULVZs, preferentially located at or near LLSVP margins, may disaggregate the source lithology, causing dense dm-rich residues and even denser silicate and metallic melts to sink relative to buoyant seifertite and Fe-poor post-bridgmanite. The ULVZs may thereby become enriched in refractory dm with interstitial silicate melt and tiny fractions of Fe-dominated metallic melt. During the late-stage crystallization of a basal magma ocean, dm was probably also incorporated into dense cumulates dominated by Fe-rich post-bridgmanite (converted from bridgmanite in the solid state). Such cumulates might be an essential part of the two antipodal LLSVP base layers, in addition to accumulated piles of ROC and some ROC residues. The high dm-melt partition coefficient for radioactive U and Th, which produces radiogenic He and nucleogenic Ne, imply that the primordial He and solar Ne isotopic compositions in deep-rooted plumes are unlikely to be sourced in either the ULVZs, the LLSVPs or in the core.

The melting curve of davemaoite

In order to put constraints on the melting phase relations of basaltic to peridotitic compositions, Hernandez al. (2022) investigated the melting curve of pure $CaSiO_3$ davemaoite, using five different first principles methods (Figure 1.1). An important motivation to clarify the davemaoite melting curve was the two recent ab initio investigations of Braithwaite & Stixrude (2019) and Wilson & Stixrude (2021), resulting in a surprisingly low melting temperature of 5600 K at the core-mantle boundary (CMB) pressure of 136 GPa. As shown in Figure 1.1, Hernandez et al. (2022) obtained a melting curve of about 7000 K at 136 GPa. The two-phase thermodynamics approach with the assumption that the melt has ideal atomic mixing, increases the Gibbs free energy of the melt, resulting in a strongly underestimated melting temperature (Wilson & Stixrude 2021, Hernandez et al. 2022). In order to assess the problematically low melting temperatures of Braithwaite & Stixrude (2019), Hernandez et al. determined the melting temperature at 105 GPa, using the Z-method with and without the waiting time analysis. The resulting melting temperature of about 6580 K is in very good agreement with the TI-curve and the curves from the solid-liquid coexistence calculations, using 120- and 720-atom cells. Because the method description of Braithwaite and Stixrude (2019) is incomplete, the reason for their low melting temperatures (e.g. 5230 K at 105 GPa) is unclear. However, Hernandez et al. (2022) emphasised that in order to avoid premature melting and drift in the electronic entropy, frequent updates (about every 1 ps) of the electronic entropy along the ionic trajectory will ensure that the ionic kinetic energy plus the electronic free energy is conserved.

The liquidus phase relations in the pseudoternary system CMS at 24-136 GPa

Figure 1.2, middle panel, which is based on a range of experimental phase equilibrium data on peridotitic, basaltic and simplified MgO-SiO_2-system compositions, illustrates the expansion of the dm liquidus field with increasing pressure in the 27-136 GPa range in the system CMS, where C=Ca+Na+K, S=Si+0.9Al and M=100-(C+S), in atom%. The expansion of the dm liquidus field is in accordance with the strongly increasing melting temperature of dm with

increasing pressure and with the experimentally determined phase relations of basaltic, peridotitic and MgO-SiO_2-system compositions. The left panel shows T-X liquidus to solidus diagrams along the $MgSiO_3$-$CaSiO_3$ join at 24 and 136 GPa, illustrating the effects of the steeply rising melting temperature of dm compared to the less steep melting curve of bridgmanite (Figure 1.1a). The middle and right panels of Figure 1.2 show that dm is the first liquidus phase and last residual phase during crystallisation and partial melting, respectively, of basaltic and picritic compositions. In peridotites, however, the first liquidus phase is ferropericlase (fp) at pressures corresponding to the shallowest regions of the lower mantle (24-31 GPa) and bridgmanite in the deeper parts (136 GPa). The komatiite range bridges the two former compositional and phase equilibrium domains.

During partial melting of picritic and basaltic lithologies near the CMB, the first mineral to be completely consumed is the Ca-ferrite-structured Al-rich phase (cf-phase, e.g. Pradhan et al., 2015; Tateno et al., 2018). The next phases to disappear will be seifertite, followed by bridgmanite (bm) or post-bridgmanite (pbm). As shown in Figure 1.2, right and middle panels, the early disappearance of the silica minerals (after the cf-phase) is likely in picritic compositions during the entire lower mantle pressure range. Basaltic melt compositions, however, are close to cosaturation with dm and stishovite (or β-stishovite) at 27 GPa, and β-stishovite remains the second most residual phase through the lower mantle to about 100 GPa, where bm comes closer to the liquidus.

Partial melting of recycled oceanic crust in the lowermost mantle and the composition of ULVZs

The solidus of basaltic and picritic compositions appears to be lower than that of peridotite (Fiquet et al., 2010; Andrault et al. 2011, 2014; Pradhan et al. 2015), presumably related to a more complex mineralogy and relative enrichments in melt-loving elements like Al, Ti, Fe and Na, compared to peridotite. This is likely be confirmed by further melting studies on basaltic and picritic compositions, using similar experimental approaches to those of Kuwayama et al. (2022) and Pierru et al. (2022), who recently lowered the peridotite solidus estimates (see below).

Extensive research on the origin, materials and dynamics of the ULVZs over the last three decades has revealed that they are mostly characterised by V_S and V_P reductions of about 30 and 10%, respectively, and density increases of mostly 5-15% relative to the ambient D" zone (e.g. Williams & Garnero, 1996; Thorne et al., 2004; McNamara et al. 2010; Yu & Garnero, 2018; Chen, 2021). The ULVZ thicknesses are generally in the 5-40 km range, and recently some stratification in density and velocities have been observed (e.g. Pachai et al. 2022). A gradual stratification could for instance span a 5-20 % density excess range from the upper ULVZ-surface to the CMB (Table 1.1) Previously, the lack of detectable stratification and the indications of dense interstitial melt, led to the inference that the ULVZs must have a vigorous internal convection, in order to prevent solid-melt separation (Hernlund & Jellinek, 2010). Significant internal convective flow in the ULVZs are likely even if some internal stratification has now been observed. The root zones of most of the high-flux mantle plumes feeding the volcanism of major oceanic islands appear to coincide with the thickest ULVZs.

The type, composition, phase relations and density of candidate residual minerals are essential information to establish simple petrological models for the origin, structure and dynamics of ULVZs. The observation of positively correlated plume flux and $^{3}He/^{4}He$-ratios with negative $^{182}W/^{184}W$ anomalies may indicate a minor core-mantle chemical exchange through the ULVZs.

Mineral and melt density, seismic velocity and models for the ULVZs

Figure 1.3 shows recently acquired and compiled mineral and melt densities. The upper panel displays mineral densities along a hot mantle adiabat (500 K above the Stixrude et al. 2009 adiabat), calculated by the BurnMan software (left), as well as mineral and melt densities at 3500 K and approximately 136 GPa, calculated by ab initio atomistic simulation in the NVT ensemble (right side). The lower panel, based largely on the ab initio calculations of Wang et al. (2020), shows mineral densities along the Brown & Shankland (1981) adiabat, which is 30-50 K below the Stixrude et al. (2009) adiabat. The main residual mineral, dm, is slightly denser than residual pbm (1.2%), seifertite (3.2%) and about 4.9% less dense than the pseudo-eutectic melt. The seismic velocity reduction ratio $\Delta V_S/\Delta V_P$ of about 3 for dm (e.g. Thomson et al. 2019), as well as for mineral aggregates with interstitial melt (e.g. Williams & Garnero 1996), matches closely the velocity reduction ratio recorded in the ULVZs.

Figure 1.4 is a model of a ULVZ located in the main plume generation zone at an LLSVP-margin (e.g. Torsvik et al., 2006; Burke et al., 2008). Partial melting of ROC slivers near the top of the hot ULVZ-surface (e.g. Liu et al. 2016) may disaggregate the source and enable density-driven partial separation of buoyant seifertite and residual, Fe-poor post-bridgmanite, and sinking of dense Fe-dominated metallic melt, FeO- and Fe_2O_3-rich silicate melt and dm. The three sinking phases will migrate downwards into the ULVZs, and some of the metallic melt may sink into the core. Using the calculated densities at 3500 K and 136 GPa and the outermost core PREM-density of 9904 kg/m^3, Trønnes et al. (in prep.) show four simple density models, illustrating some phase assemblage options that brackets the ULVZ density excess of roughly 10% relative to the ambient peridotite-dominated lowermost mantle (Table 1.1). The latter lithology was modelled as a mildly depleted peridotite with 4, 76 and 21 mol% dm, bm, and fp, respectively (Trønnes & Mohn, in prep.).

Table 1.1. ULVZ phase proportions and density excess ($\Delta\rho$%)

	dm	res-pbm	sil-melt	met-melt	$\Delta\rho$%
Model 1	80	10	10	5	5.7
Model 2	70	10	12	8	9.5
Model 3	60	15	15	10	9.7
Model 4	60	10	15	15	13.7

Abbreviations: res-, residual; sil-, silicate; met-, metallic

Table 1.1 shows that the expected ULVZ density excess of roughly 10 % can be obtained by a reasonable combination of 60-80 % dm, 10-15 % residual pbm, 10-15% silicate melt and 5-15 % metallic melt. The metallic melt, which has a density of 1.77 and 1.68 times those of dm and the silicate melt, respectively, has the greatest leverage on the bulk ULVZ-density. ULVZs with gradually or discontinually stratified structures with a density excess increasing from about 5 % at the top to e.g. 15% at the bottom, will likely have lower parts (layers) with elevated metallic melt

content (e.g. Figure 1.4, Panel D, upper right). The metallic melt fraction is unlikely to exceed 8-10 % in the upper parts, but might be considerably higher in the lowermost parts near the CMB. Although the degree of internal ULVZ-convection is unresolved, the convection of ULVZs with a considerable melt fraction is likely to be extensive (Hernlund & Jellinek, 2010).

The two main LLSVP material types

Davemaoite is relatively abundant in both of the two most likely material types comprising the large low S-wave provinces (LLSVPs). In an unmelted state, primitive basaltic to pictitic ROC would contain 27-23 mol% dm. Although residual ROC, subsequent to melt extraction, would be even more enriched in dm, the partial disintegration and sinking of dense melt and dm towards the CMB and ULVZs would reduce a potential dm enrichment in the LLSVPs.

The second LLSVP candidate material is remnants of relatively late-stage cumulates from the basal magma ocean (BMO) crystallisation. With the assumptions that the CMB temperature is 4000 K, that bm would be stable in the hottest regions of the D" zone and that such LLSVP regions could be about 750 K hotter than the coolest areas of the D" thermal boundary layer (i.e. in areas of subducted slabs), Trønnes et al. (2019) used the excess temperature and excess density versus mol% $FeSiO_3$ relations (Wolf et al. 2015, Fig. 8) to estimate that bm with 16 mol% $FeSiO_3$ would correspond to a density excess of 1.25%. This thermally adjusted density excess, corresponding to an intrinsic material density difference of about 2.2%, is consistent with the geophysical observations and models of Ishii & Tromp (1999), Moulik & Ekström (2016) and Lau et al. (2017).

Recent determinations of the melting curve of iron and the solidus of peridotite (Sinmyo et al. 2019; Kuwayama et al. 2021; Pierru et al. 2022), however, indicate that the CMB temperature is about 3700 rather than 4000 K and that the peridotite solidus is about 3800 K. These results, combined with new determinations of the bm-pbm phase transition in peridotite and the systems $MgSiO_3$-$FeSiO_3$, MS-$FeAlO_3$ and MS-Al_2O_3 (Kuwayama et al., 2021; Mohn, in prep.), demonstrate that pbm is omnipresent in the lowermost 200-300 km of the mantle, even the hottest D" regions, and especially in basaltic and picritic ROC, but also in magma ocean cumulates with a combined content of the $FeSiO_3$- and $FeAlO_3$-components exceeding 10-15 mol%. Whereas the density effect is quite similar from substitutions of either of the $FeSiO_3$ and $FeAlO_3$ components (Figure 1.3) and both components stabilises pbm at the expense of bm, the $FeSiO_3$ component stabilises pbm more than that of $FeAlO_3$ (Mohn in prep.). This implies that the double-crossing scenario (Hernlund et al., 2005) with re-stabilisation of the high-entropy phase bm is no longer tenable.

The protracted BMO solidification, probably ongoing at least into the Proterozoic, proceeded downwards from the top ceiling and was accompanied by core-BMO chemical exchange involving FeO-transfer from to the BMO to the core and SiO_2 in the opposite direction. This core-BMO exchange would have "buffered" or moderated the evolving BMO composition at relatively high Si/(Mg+Fe) and Mg/Fe ratios, resulting in suppression of fp-crystallisation and promotion and prolongation of the mainly-bm-crystallisation in spite of the extraction of large volumes of $MgSiO_3$-rich bm. The resulting BMO-enrichment of Na, Ca, Al and other incompatible minor and trace elements would promote the precipitation of the aluminous Ca-ferrite-structured phase (cf) and dm. Whereas cf has low density, allowing its incorporation

into the solidifying BMO-ceiling (Figure 1.3, lower panel), the dense dm would initially sink into the hot BMO melt and dissolve.

Figure 1.3 indicates that the dm-bm-BMO neutral buoyancy would be reached only when the BMO melt was sufficiently dense and Fe-rich to crystallise bm with a combined $FeSiO_3$+$FeAlO_3$ content of about 16 mol%, according to BurnMan calculations, or 18-19 mol%, according to the ab initio DFT results. Such evolved BMO cumulates would have an appropriate density for relatively thin base layers in the LLSVPs (e.g. Lau et al. 2017; Robson et al., 2022). The solid-state and nearly isochemical bm- to pbm-conversion involves an additional density increase of 1.5-1.6% for either a pure MS composition or the $MS_{81.25}FS_{18.75}$ or $MS_{81.25}FA_{18.75}$ compositions (Figure 1.3). The mostly isochemical and abrupt nature of the bm-pbm-transition results from relatively flat and narrow phase loops in pressure-composition -space (Mohn, in prep.), as well as from the rheological features of this transition (Amman et al. 2010).

Implications for Earth's geochemical reservoirs

The distinct negative correlation between $^{3}He/^{4}He$ and $^{182}W/^{184}W$ ratios and less distinct negative correlation between $^{136}Xe/^{130}Xe$ and $^{129}Xe/^{130}Xe$ in basalt generated above deep-rooted, high-flux mantle plumes support dynamical ULVZs acting as partially open windows to the core. Whereas the low $^{182}W/^{184}W$ and $^{129}Xe/^{130}Xe$ ratios are core signatures (e.g. White, 2015; Mundl et al., 2017, Jackson et al. 2018; Mundl-Petermeier et al. 2020; Jackson et al. 2020), the high $^{3}He/^{4}He$ ratios are probably not. Because dm contains very high concentrations of U and Th, the high dm contents in both the ULVZs and the LLSVPs will preclude high $^{3}He/^{4}He$ ratios in these reservoirs. The decay of these elements yields radiogenic ^{4}He and nucleogenic ^{21}Ne, which would obliterate any primordial He-Ne isotopic signal (e.g. Hernandez et al., 2022). According to Li et al. (2022), the core is also an inappropriate source for the primordial He– and Ne-isotopic composition [see Ferrick & Korenaga (2023) for an opposimg view]. Such primordial light noble gas isotopic signals found in high plume-flux oceanic island, are strongly associated with residual source characteristics (e.g. Class and Goldstein 2005; Albarede, 2008). Considerable plume entrainment of early refractory and bridgmanitic lithologies, which was diffusionally recharged with primordial He and Ne during the Hadean, and remains neutrally buoyant, and to a large extent convectionally inert, in the middle part of the lower mantle, can explain this core and refractory mantle dichotomy.

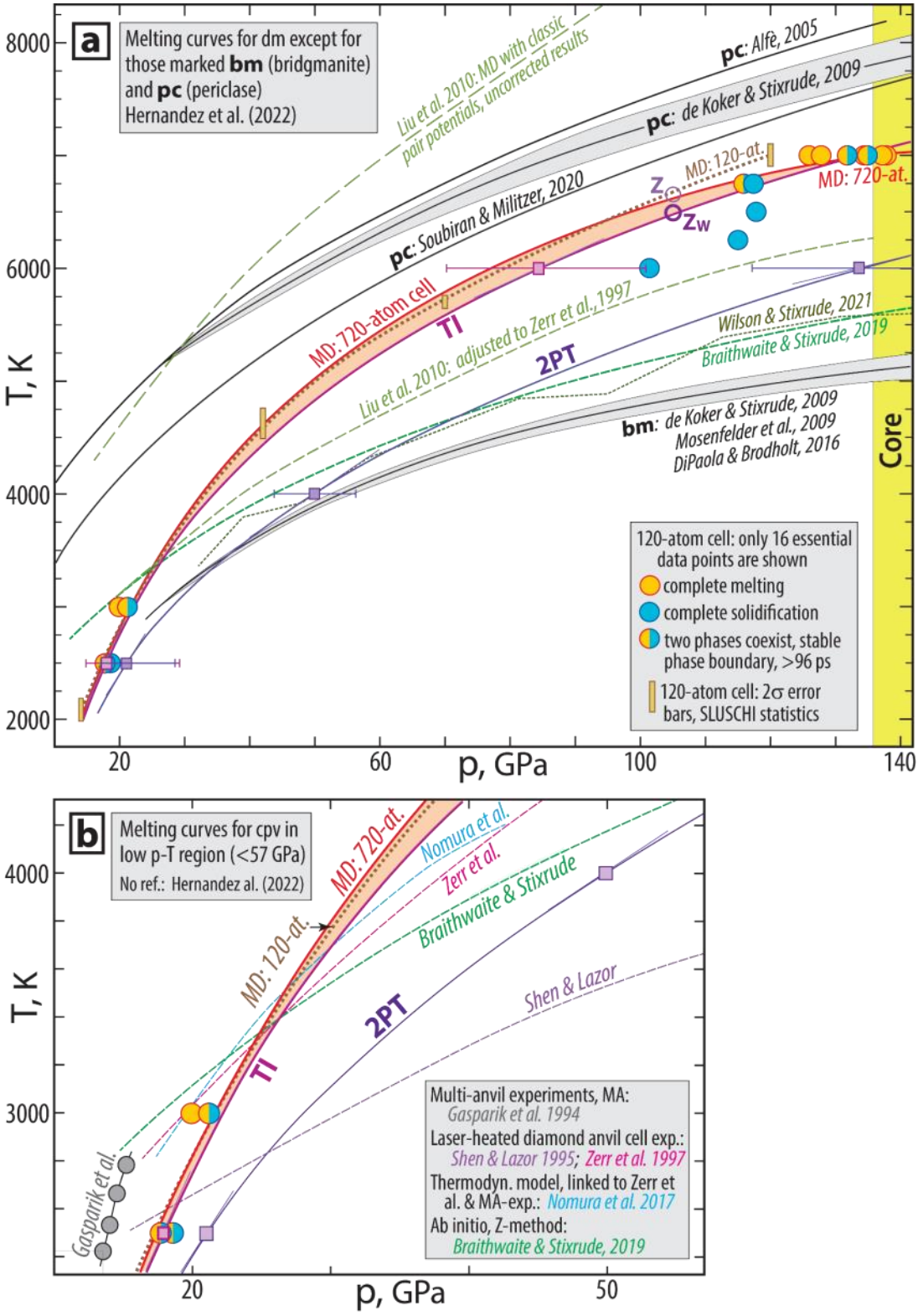

Figure 1.1. *Melting curves for davemaoite (dm, $CaSiO_3$), bridgmanite (bm, $MgSiO_3$) and periclase (pc, MgO), slightly modified from Hernandez et al. (2022).*

Previously published melting curves. ***Panel a***: *The $MgSiO_3$ melting curve of de Koker and Stixrude (2009) has a grey uncertainty envelope, encompassing the melting curves of Mosenfelder et al. (2009) and Di Paola and Brodholt (2016). A corresponding MgO melting curve with a gray uncertainty envelope (de Koker and Stixrude, 2009) is shown together with the Alfè et al. (2005) and Soubiran and*

Militzer (2020) curves. Dm-curves: Two melting curves, based on classic pair potential MD simulation by Liu et al. (2010) include an upper curve, which is uncorrected for overheating, and a lower curve, corrected for 48% overheating by linking it to Zerr et al. (1997). The melting curves of Braithwaite and Stixrude (2019) and Wilson and Stixrude (2021) are based on the Z method and 2PT (two-phase thermodynamics) method, respectively. ***Panel b****: The grey circular symbols represent melting points determined by multianvil experiments by Gasparik et al. (1994). The curves from Shen and Lazor (1995) and Zerr et al. (1997) are based on one-sided laser-heated diamond anvil cell experiments, and the Nomura et al. (2017) curve is a thermodynamic model linked to 24 GPa multianvil experiments and the Zerr et al. (1997) curve.*

The four different Ca-perovskite melting curves from Hernandez et al. (2022) *include curves based on two-phase thermodynamics (2PT), thermodynamic integration for the melt, combined with 2PT-method free energy for Ca-perovskite (labelled TI), as well as molecular dynamics (MD) solid-melt coexistence simulations with 120- and 720-atom cells. Orange shading marks the p-T region between the 720-atom cell and TI curves. The TI and 2PT curves are Simon and Glatzel (1929) regressions based on the melting points and their dp/dT slopes. The 120- and 720-atom cell solid-liquid coexistence curves are drawn with a smooth cubic spline-like function, with the 720-atom cell curve weighted by the point clusters at 18-21 GPa and 116-135 GPa. The two Z-method melting temperatures of Hernandez et al. (2022) at 105 GPa with and without the waiting time analysis are marked as Z_W and Z, respectively. It is evident that these melting temperatures of about 6580 K at 105 GPa are in excellent agreement with the TI-curve and the curves from the solid-liquid coexistence calculations, using 120- and 720-atom cells. Although the very large difference (1300-1400 K) from the low melting temperature of Braithwaite and Stixrude (2019) is uncertain, Hernandez et al. emphasised that frequent updates (about every 1 ps) of the Fermi-Dirac smearing to match the average temperature of the previous run is required to avoid premature melting and drift in the electronic entropy.*

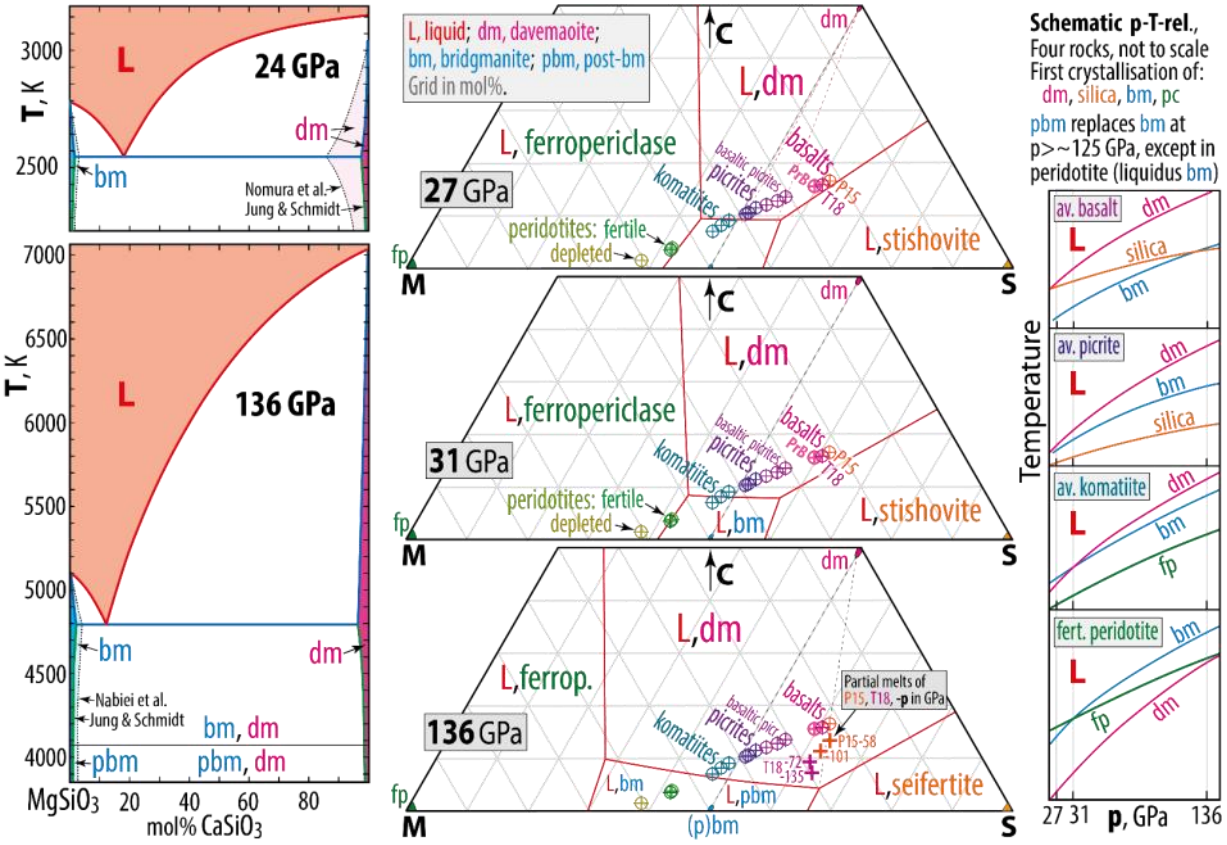

Figure 1.2. ***Left panels****: Approximate phase relations along the $MgSiO_3$-$CaSiO_3$ join at 24 and 136 GPa. The melting points of bridgmanite (bm) and davemaoite (dm) are from the melting curves of de*

Koker and Stixrude (2009) and Hernandez et al. (2022) in Fig. 1. The inferred bm and dm compositional ranges along the $MgSiO_3$-$CaSiO_3$ join are based on ab initio theory (Jung and Schmidt, 2011) and high-p-T experiments at at 24 GPa (Nomura et al., 2017) and close to 136 GPa, at 129 GPa (Nabiei et al., 2021). The 24 GPa eutectic composition is from Nomura et al. (2017). The liquidi, solidi and solvi are indicated by red, blue and green curves, respectively, and the horizontal black line at 136 GPa and 4075 K, indicating the post-bridgmanite (pbm) transition for $MgSiO_3$ is from Tsuchiya et al. (2004) and Mohn (in prep).

***Middle panels**: Liquidus phase relations in parts of the pseudoternary system CMS at 27, 31 and 136 GPa. Complex natural compositions are projected into the CMS-plane as in Fig. 13 in Trønnes et al. (2019). The rock compositions are recast to a CMS projection with the components calculated from atom%: C=Ca+Na+K, S=Si+0.9Al and M=100-(C+S). Small coloured fields indicate the inferred mineral compositional ranges. The two binary MS-eutectics are based on the experimental results of Ozawa et al. (2018). The liquidus phase boundaries in the CMS ternary are inferred from the experimentally derived phase relations of natural peridotite and basalt compositions (mainly Zhang and Herzberg, 1994; Hirose and Fei, 2002; Trønnes and Frost, 2002; Ito et al., 2004; Fiquet et al., 2010; Andrault et al., 2011; Andrault et al., 2014; Tateno et al., 2014, 2018; Pradhan et al., 2015; Nabiei et al., 2021). The displayed bulk lithologies are detailed by Trønnes & Mohn (in prep). At 136 GPa, dm is the first and pbm is the second phase to precipitate below the liquidus for basaltic and picritic compositions. The komatiites might have bm or pbm as the second phase after dm below the liquidus, whereas bm is the first liquidus phase (at considerably higher T) for the peridotitic compositions. Accordingly, the common phase field surrounding MS is labelled L,bm (left part) and L,pbm (right part). The third phase to precipitate below the liquidus is seifertite for the basalts and picrites and ferropericlase for the komatiites. The two pseudoternary eutectics are located based on the observed phase relations. The 136 GPa pbm-seifertite-dm eutectic is placed exactly where simultaneous pbm-seifertite-dm co-precipitation follows the initial dm crystallization for the P15 composition, but where the T18 and PrB compositions crystallise pbm as the second liquidus phase after dm (Tateno et al., 2018).*

***Right panels**: Schematic p-T melting relations for average basalt, picrite, komatiite and fertile peridotite, based on the CMS liquidus relations in the middle panels. Although post-bridgmanite (pbm) will be present at low subsolidus temperature for all the compositions above 120-130 GPa, it may reach the melting range only for the basaltic and picritic compositions. Tateno et al. (2018) found a 135 GPa (erroneously marked 125 GPa in their Fig. 3) crystallization sequence of dm, followed by post-bridgmanite (pbm) and then seifertite. Because the bm-pbm (for $MgSiO_3$) transition has a large dp/dT-slope of about 7 MPa/K (Oganov & Ono, 2004; Tsuchiya et al., 2004; Mohn, in prep.), and their synchrotron-based XRD recordings at 135 GPa and 300 K also include strong bm peaks, it seems likely that the second phase to crystallize is bm. At subsolidus conditions, the $FeAlO_3$ and $FeSiO_3$ components, partition from bm into coexisting pbm, stabilizing pbm to lower pressures (e.g. Mohn, in prep). The $K_D^{bm/melt}{}_{Fe/Mg}$ and $K_D^{pbm/melt}{}_{Fe/Mg}$, however, are very low (about 0.1 and 0.04 for bm and pbm, respectively) in the lowermost mantle (e.g. Tateno et al., 2014). In the lowermost mantle, $MgSiO_3$-rich bm might therefore crystallise after dm, even from natural basaltic and picritic melts, but will certainly be replaced by pbm below the melting range.*

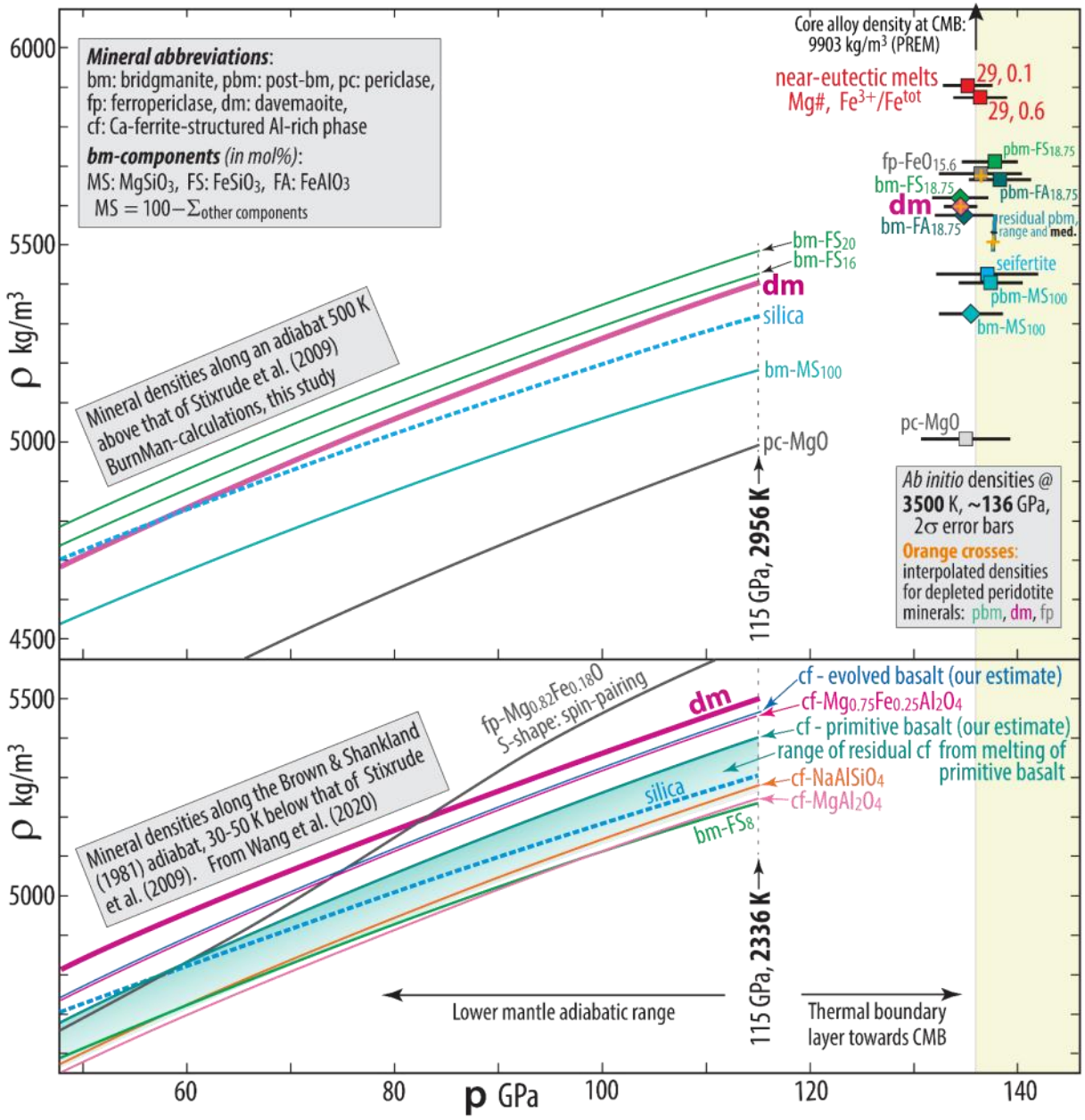

Figure 1.3. *Mineral and melt densities.* ***Upper panel****: Mineral density curves calculated with the BurnMan software along an adiabat 500 K above the Stixrude et al. (2009) adiabat (left) and mineral and melt densities calculated at 3500 K and about 136 GPa, using ab initio atomistic simulations (right).* ***Lower panel****: Mineral density curves along the Brown and Shankland (1981) adiabat from Wang et al. (2020). The estimated composition and density of the Ca-ferrite-structured Al-rich phases in basaltic lithologies (thin blue curve for evolved basalt and green curve for primitive basalt) is based on mineral analyses of experimental run products (Kesson et al., 1994; Ricolleau et al., 2010; Hirose et al., 2005), combined with linear interpolations between the curves for the three Ca-ferrite-type components* $NaAlSiO_4$*,* $MgAl_2O_4$ *and* $Mg_{0.75}Fe_{0.25}Al_2O_4$ *(Wang et al., 2020). A wide, light green field fot the density of inferred residual cf generated during incipient melt extraction from the primitive basalt is also indicated. Experimental phase relations indicate that the Al-rich Ca-ferrite phase is the first one to disappear from the residue during partial melting (Pradhan et al., 2015; Tateno et al., 2018).*

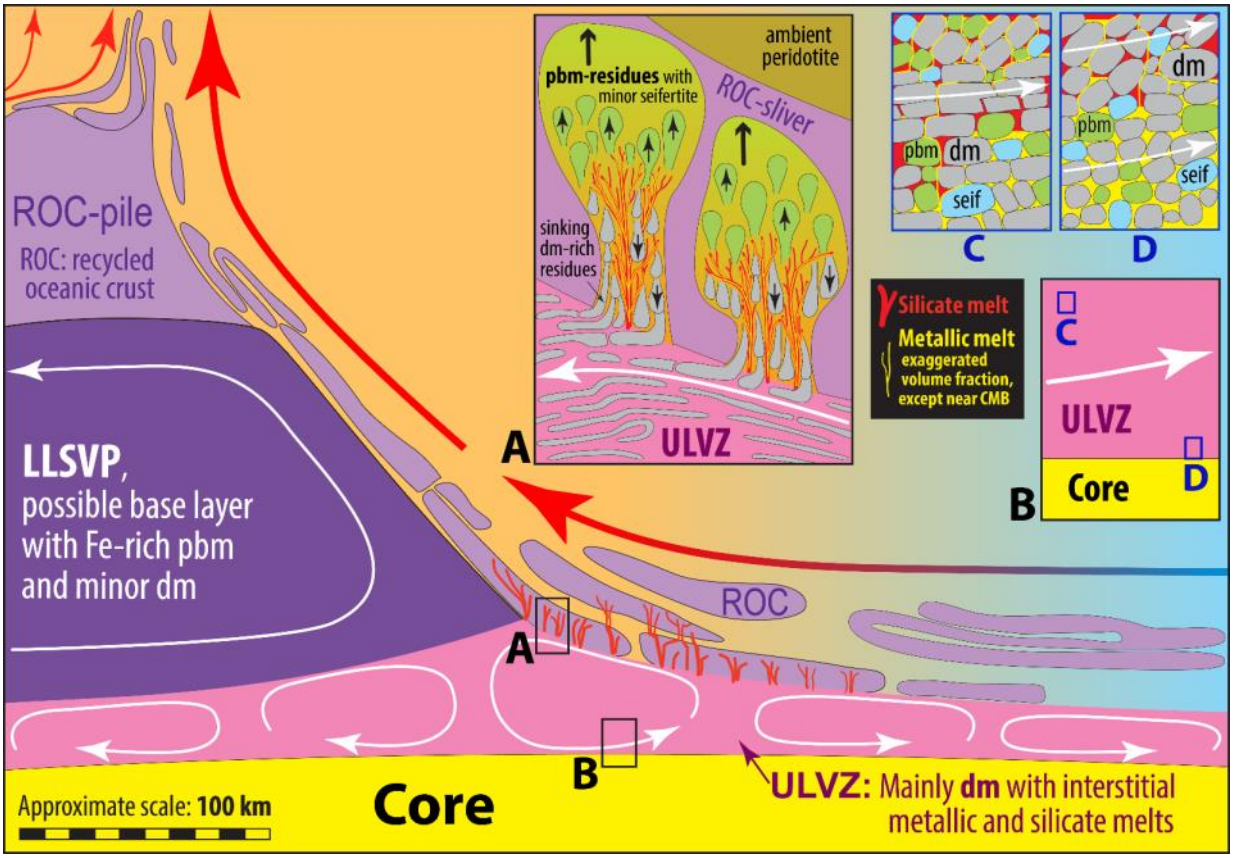

Figure 1.4. *Conceptual model for the inferred structure, materials and dynamics near the margin of a large low S-wave velocity province (LLSVP). The wide liquidus stability field at lowermost mantle pressure conditions and high-density of davemaoite (dm) make it the favoured main mineral in ultra-low velocity zones (ULVZs), as well as an important minor phase in a high-density lower LLSVP-layer, dominated by $FeAlO_3$-rich bridgmanite (bm) formed as late-stage cumulates of the basal magma ocean (Trønnes et al., 2019). Piles of recycled oceanic crust (ROC) of inferred picritic composition on top of the lower LLSVP-layer is also expected to be dm-rich (20-25 mol%).* ***Inset panel A*** *illustrates the dynamics of partial melting of picritic ROC-slivers in contact with ULVZs and density-driven separation of sinking dm-dominated residues, as well as immiscible silicate (red/magenta) and Fe-dominated metallic (yellow) melts, from rising bm-dominated residues.* ***Panels C and D*** *(locations shown in* ***panel B****) illustrate the dynamics of convective crystal mush deformation and the separation and core segregation of dense metallic melt from the dm-dominated ULVZ. The sinking metallic melt might extract sufficient FeO from the silicate melt to become O-saturated on its way to the core. A Si-saturated outer core alloy might supply SiO_2 to the interstitial silicate ULVZ-melt (Trønnes et al., 2019), making it neutrally or even positively buoyant relative to dm, due to decreasing Fe/Mg and (Mg+Fe)/Si ratios.*

References

Albarede F, 2008, Rogue mantle helium and neon. Science 319, 943-945.

Alfè D, 2005, Melting curve of MgO from first-principles simulations. Physical Review Letters, 94, 4–7.

Amman, M.W., Brodholt, J.P., Wookey, J., Dobson, D.P., 2010. First-principles constraints on diffusion in lower-mantle minerals and a weak D″ layer. Nature 465, 462–465.

Andrault, D., Bolfan-Casanova, N., Nigro, G.L., Bouhif, M.A., Garbarino, G., Mezouar, M., 2011. Melting curve of the deep mantle applied to properties of early magma ocean and actual core-mantle boundary. Earth Planet. Sci. Lett. 304, 251–259.

Andrault, D., Pesce, G., Bouhifd, M.A., Bolfan-Casanova, N., Hénot, J.-M., Mezouar, M., 2014. Melting of subducted basalt at the core-mantle boundary. Science 344, 892–895.

Braithwaite, J. and Stixrude, L. (2019). Melting of CaSiO3 perovskite at high pressure. Geophysical Research Letters 46, 2037-2044.

Brown, J.M., Shankland, T.J., 1981. Thermodynamic parameters in the earth as determined from seismic profiles. Geophys. J. R. Astron. Soc. 66 (3), 579–596.

Burke, K., Steinberger, B., Torsvik, T.H., Smethurst, M.A., 2008. Plume generation zones at the margins of large low shear velocity provinces on the core-mantle boundary. Earth Planet. Sci. Lett. 265, 49–60.

Chen J, 2021, Tracking the origin of ultralow velocity zones at the base of Earth's mantle. Nat. Sci. Rev. 8, nwaa308.

Class C, Goldtein SL, 2005, Evolution of helium isotopes in the Earth's mantle. Nature, 436, 1107-1112.

de Koker, N., Karki, B. B., and Stixrude, L. (2013). Thermodynamics of the MgO-SiO2 liquid system in Earth's lowermost mantle from first principles. Earth and Planetary Science Letters, 361, 58–63.

de Koker, N. and Stixrude, L. (2009). Self-consistent thermodynamic description of silicate liquids, with application to shock melting of MgO periclase and MgSiO3 perovskite. Geophysical Journal International, 178, 162-179.

Di Paola C, Brodholt JP, 2016. Modeling the melting of multicomponent systems: the case of MgSiO3 perovskite under lower mantle conditions. Scientific Reports, 6, 29830.

Ferrick AL, Korenaga J, 2023. Long-term core-mantle interaction explains W-He isotope heterogeneities. Proc. Nat. Acad. Sci. 120, e2215903120.

Fiquet, G., Auzende, A.L., Siebert, J., Corgne, A., Bureau, H., Ozawa, H., Garbarino, G., 2010. Melting of peridotite to 140 GPa. Science 329, 1516–1518.

Gasparik, T., Wolf, K., and Smith, C. M. (1994). Experimental determination of phase determination in the CaSiO3 system from 8 to 15 GPa. American Mineralogist 79, 1219–1222.

Hernandez J-A, Guren MG, Mohn CE, Baron MA, Trønnes RG, 2022: Ab initio atomistic simulations of Ca-perovskite melting. Geophys. Rev. Lett., 49, e2021GL097262.

Hernlund, J.W., Jellinek, M., 2010. Dynamics and structure of a stirred partially molten ultralow-velocity zone. Earth Planet. Sci. Lett. 296, 1–8.

Hernlund, J.W., Thomas, C., Tackley, P.J., 2005. A doubling of the post-perovskite phase boundary and structure of the Earth's lowermost mantle. Nature 434, 882–886.

Hirose, K., Fei, Y., 2002. Subsolidus and melting phase relations of basaltic composition in the uppermost lower mantle. Geochim. Cosmochim. Acta 66, 2099–2108.

Ishii, M., Tromp, J., 1999. Normal-mode and free-air gravity constraints on lateral variations in velocity and density of Earth's mantle. Science 285, 1231–1236.

Ito, E., Kubo, A., Katsura, T., Walter, M.J., 2004. Melting experiments of mantle materials under lower mantle conditions with implications for magma ocean differentiation. Phys. Earth Planet. Inter. 143–144, 397–406.

Jackson, C.R.M., Bennett N.R., Du Z., Cottrell E., and Fei Y., 2018, Early episodes of high-pressure core formation preserved in plume mantle. Nature, 553, 491-495.

Jackson, M.G., Blichert-Toft J., Halldórsson S.A., Mundl-Petermeier A., Bizimis M., Kurz M.D., Price A.A., Harðardóttir S., Willhite L.N., Breddam K., Becker T.W., and Fischer R.A., 2020, Ancient helium and tungsten isotopic signatures preserved in mantle domains least modified by crustal recycling. Proc. Nat. Acad. Sci.117, 30993-31001.

Jung DY, Schmidt MW (2011) Solid solution behavior of CaSiO3 and MgSiO3 perovskites, Physics and Chemistry of Minerals, 38, 311–319

Kuwayama Y, Hirose K, Cobden L, Kusakabe M, Tateno S, Ohishi Y, 2022. Post-perovskite phase transition in the pyrolitic lowermost mantle: Implications for ubiquitous occurrence of post-perovskite above CMB. Geophys. Res. Lett. 49, e2021GL096219.

Lau, H.C.P., Mitrovica, L.X., Davis, J.L., Tromp, J., Yang, H.-Y., Al-Attar, D., 2017. Tidal tomography constrains Earth's deep-mantle buoyancy. Nature 551, 321–326.

Li Y, Vocadlo L, Ballentine C, Brodholt JP, 2022. Primitive noble gases sampled from ocean island basalts cannot be from the Earth's core. Nat. Comm. 10.1038/s41467-022-31588-7.

Liu, Z. J., Yan, J., Duan, S. Q., Sun, X. W., Zhang, C. R., and Guo, Y. (2010). The melting curve of CaSiO3 perovskite under lower mantle pressures. Solid State Communications, 150, 590–593.

McNamara, A.K., Garnero, E.J., Rost, S., 2010. Tracking deep mantle reservoirs with ultra-low velocity zones. Earth Planet. Sci. Lett. 299, 1–9.

Mosenfelder, J. L., Asimow, P. D., Frost, D. J., Rubie, D. C. & Ahrens, T. J. (2009). The MgSiO3 system at high pressure: thermodynamic properties of perovskite, postperovskite, and melt from global inversion of shock and static compression data. Journal of Geophysical Research 114, B01203.

Moulik, P., Ekström, G., 2016. The relationships between large-scale variations in shear velocity, density, and compressional velocity in the Earth's mantle. J. Geophys. Res. 121, 2737–2771.

Mundl, A., Touboul M., Jackson M.G., Day J.M.D., Kurz M.D., Lekic V., Helz R.T., and Walker R.J., 2017, Tungsten-182 heterogeneity in modern ocean island basalts. Science, 356, 66-69.

Mundl-Petermeier, A., Walker R.J., Fischer R.A., Lekic V., Jackson M.G., and Kurz M.D., 2020, Anomalous 182W in high 3He/4He ocean island basalts: Fingerprints of Earth's core? Geochim. Cosmochim. Acta, 271, 194-211,

Nabiei, F., Badro J., Boukare C.-E., Hebert Cecile, Contoni, M., Borensztjan, S., Wehr, N., Gillet, P. (2021) Zerr, A., Serghiou, G., & Boehler, R. (1997). Melting of CaSiO3 perovskite to 430 kbar and first in-situ. Geophysical Research Letters, 24(8), 909–912.

Nomura, R., Zhou, Y., and Irifune, T. (2017). Melting phase relations in the MgSiO3-CaSiO3 system at 24 GPa. Progress in Earth and Planetary Science, 4, 34.

Oganov, A.R., Ono, S., 2004. Theoretical and experimental evidence for a post-perovskite phase of MgSiO3 in Earth's D" layer. Nature 430, 445-448.

Ozawa, K., Anzai, M., Hirose, K., Sinmyo, R., & Tateno, S. (2018). Experimental determination of eutectic liquid compositions in the MgO-SiO2 system to the lowermost mantle pressures. Geophysical Research Letters, 45, 9552–9558.

Pachhai S, Li M, Thorne MS, Dettmer J, Tkalcic H, 2022. Internal structure of ultralow-velocity zones consistent with origin from a basal magma ocean. Nat. Geosci. 15, 79-84.

Pierru R, Pison L, Mathieu A, Gardes E, Garbarino G, Mezouar M, Hennet L, Andrault D, 2022. Solidus melting of pyrolite and bridgmanite: Implication for the thermochemical state of the Earth's interior. Earth Planet. Sci. Lett. 117770.

Pradhan, G. K., Fiquet, G., Siebert, J., Auzende, A. L., Morard, G., Antonangeli, D., and Garbarino, G. (2015). Melting of MORB at core-mantle boundary. Earth and Planetary Science Letters, 431, 247–255.

Robson A, Lau HCP, Koelemeijer P, Romanowicz B 2022. An analysis of core-mantle boundary Stoneley mode sensitivityy and sources of uncertainty. Geophys. J. Int. 228.1962-1974.

Shen, G., and Lazor, P. (1995). Measurement of melting temperatures of some minerals under lower mantle pressures. Journal of Geophysical Research: Solid Earth, 100, 17699–17713.

Simon, von F., and Glatzel, G. (1922). Bernerkungen zur Schmelzdruckkurve. Zeitschrift Für Anorganische Und Allgemeine Chemie, 178, 309–316.

Sinmyo, R., Hirose K., and Ohishi Y., 2019. Melting curve of iron to 290 GPa determined in a resistance-heated diamond-anvil cell. Earth Planet. Sci. Letters 510, 45-52.

Soubiran, F., & Militzer, B. (2020) Anharmonicity and phase diagram of magnesium oxide in the megabar regime. Physical Review Letters, 125, 175701.

Stixrude L, de Koker N, Sun N, Mookherjee M, Karki BB, 2009. Thermodynamics of silicate liquids in the deep Earth. Earth Planet. Sci. Lett. 278, 226–232.

Tateno, S., Hirose, K., Sata, N., and Ohishi, Y. (2009). Determination of post-perovskite phase transition boundary up to 4400 K and implications for thermal structure in D″ layer. Earth and Planetary Science Letters, 277(1–2), 130–136.

Tateno, S., Hirose, K., and Ohishi, Y. (2014). Melting experiments on peridotite to lowermost mantle conditions. Journal of Geophysical Research, 119, 4684–4694.

Tateno, S., Hirose, K., Sakata, S., Yonemitsu, K., Ozawa, H., Hirata, T., et al. (2018). Melting Phase Relations and Element Partitioning in MORB to Lowermost Mantle Conditions. Journal of Geophysical Research, 123(7), 5515–5531.

Thomson, A.R., Crichton, W.A., Brodholt, J.P., Wood, I.G., Siersch, N.C., Muir, J., Dobson, D.P., Hunt, S.A. (2019) Calcium silicate perovskite's seismic velocities can explain LLVPs in Earth's lower mantle. Nature 572, 645-647.

Thorne, M.S., Garnero, E.J., Grand, S.P., 2004. Geographic correlation between hot spots and deep mantle lateral shear-wave velocity gradients. Phys. Earth Planet. Inter. 146, 47–63.

Torsvik TH, Smethurst MA, Burke K, Steinberger B (2006) Large Igneous Provinces generated from the margins of the large low velocity provinces in the deep mantle. Geophys. J. Int. 167,1447-1460.

Trønnes, R.G., Baron M.A., Eigenmann K.R., Guren M.G., Heyn B.H., Løken A., and Mohn C.E., 2019, Core formation, mantle differentiation and core-mantle interaction within Earth and the terrestrial planets. Tectonophys. 760, 165-198.

Trønnes, R.G., Frost, D.J., 2002. Peridotite melting and mineral-melt partitioning of major and minor elements at 22–24.5 GPa. Earth Planet. Sci. Lett. 197, 117–131.

Tsuchiya, T., Tsuchiya, J., Umemoto, K., Wentzcovitch, R.M., 2004. Phase transition in MgSiO3 perovskite in the earth's lower mantle. Earth. Planet. Sci. Lett. 224, 241-248.

Wang W, Xu Y, Sun D, Ni S, Wentzcovitch R, Wu Z, 2020, Velocity and density characteristics of subducted oceanic crust and the origin of lower-mantle heterogeneities. Nat. Comm. 11, 64.

White WM, 2015, Isotopes, DUPAL, LLSVPs, and Anekantavada. Chem. Geol. 419, 10-28.

Williams, Q., Garnero, E.J., 1996. Seismic evidence for partial melt at the base of Earth's mantle. Science 273, 1528–1530.

Wilson, A., Stixrude, L. (2021). Entropy, freezing and dynamics of CaSiO3 liquid, Geochemical et Cosmochemica Acta, 302,1-17.
Wolf, A.S., Jackson, J.M., Dera, P., Prakapenka, V.B., 2015. The thermal equation of state of (Mg,Fe)SiO3 bridgmanite (perovskite) and implications for lower mantle structures. J. Geophys. Res. 120, 7460–7489.
Yu, S. & Garnero, E. J. 2018, Ultralow velocity zone locations: a global assessment. Geochem. Geophys. Geosyst. 19, 396–414.
Zerr, A., Serghiou, G., & Boehler, R. (1997). Melting of CaSiOs perovskite to 430 kbar and first in-situ. Geophysical Research Letters, 24, 909–912.
Zhang, J.Z., Herzberg, C., 1994. Melting experiments on anhydrous peridotite KLB-1 from 5 to 22.5 GPa. J. Geophys. Res. 99, 17729–17742.

CEED members celebrating 10 years of CEED on the CEED closure: All things must pass, 28.02.23. Photo credit: Ming Geng.

A picture of Georg Sverdrups hus—University Library at night time. Photo by: Ming Geng.

2. Earth Modelling: Numerical Models of Earth Dynamics

The Earth Modelling Team uses a variety of modeling approaches to understand the geodynamics of Earth's lithosphere and mantle, with an overall goal toward deciphering the relationships between mantle dynamics, plate tectonics, and Earth's surface environment, across Earth history. In 2022 the group was active in a wide variety of projects including: plume interactions with the continental lithosphere, the geodynamics of viscosity anisotropy, patterns seismic attenuation and surface volcanism resulting from upper mantle hydration, and the development of numerical codes to model mantle deformation extending from the Earth's surface to the core-mantle boundary (from plumes). Earth Modellers also contribute to CEED's broader efforts in education, computational methods, and scientific visualization.

The Earth Modelling Team had a successful "last year" as part of CEED. We brought some projects toward their close (MAGPIE and 3D-Earth-Greenland) while other projects are continuing (ANIMA) or will be kicking off soon (4D-Earth and BALCONY). We also enjoyed some exciting events:

- **Florence Ramirez** defended her PhD in November.

- **Ágnes Király** won the 2023 Early Career Scientist Award from the Geodynamics Division of EGU.

In 2022 the Earth Modelling Team continued to further the overall goals of CEED. **Florence Ramirez** discovered that the so-called "low-Q Zone", a sub-lithospheric region of high seismic attenuation, is caused by active deformation associated with "plug flow" in the upper mantle (*Ramirez et al.,* submitted). **Bernhard Steinberger** looked at the impact of a potential plume beneath West Antarctica (*Bagge et al.,* 2022; *Bredow et al.,* 2022; *Steinberger et al.*, submitted). As part of the ANIMA project, **Ági Kiraly** and **Yijun Wang** examined the formation of anisotropic fabrics in the upper mantle. **Björn Heyn** examined the interaction of melted mantle with the continental lithosphere, with potential implications for heat flow in Greenland (*Heyn and Conrad*, 2022). **Maaike Weerdesteijn** developed a new numerical code for high-resolution modelling of glacial isostatic adjustment (*Weerdesteijn et al.,* 2023), and showed that contemporary melting in Greenland may drive significant surface uplift above a confined "pocket" of reduced mantle viscosity (*Weerdesteijn et al.,* 2022). **Valerie Maupin** worked with colleagues and CEED PhD student **Annie Jerkins** to use seismic observations to better understand the upper mantle structure and dynamics of Scandinavia (*Bulut et al.,* 2022; *Mauerberger et al.,* 2022). **Robin Watson** continued development on CeedPlates (an in-house tool based on the open-source GPlates software), focussing on build system improvements and arm architecture support (for newer mac hardware). **Helene Wang** showed that continental intraplate volcanism preferentially occurs above regions of elevated water content in the mantle transition zone, which hints at the cause of this volcanism (*Wang et al.,* in preparation). **Björn Heyn** developed a new numerical implementation of a "free base" for a mantle convection calculation (*Heyn et al.,* in preparation). **Jyotirmoy Paul** showed that global mantle flow serves to compress continents, potentially stabilizing them (*Paul et al.,* 2023). **Florence Ramirez** developed a method to use geophysical observations to constrain mantle viscosity (*Ramirez et al.,* 2022), and started applying this method to Scandinavia (*Ramirez et al.,* in preparation). Finally, **Kate Selway** led the MAGPIE fieldwork in Central Greenland, completing the first-ever magnetotellurics survey of this region.

Here is a synopsis of the Earth Modelling Team's most important activities during 2022.

The "Low-Q" zone in the upper mantle explained by plug flow and grain-size reduction

The seismic low-velocity zone (LVZ) beneath the oceanic plates (100 to 250 km depth) has been well known for some time. What is less appreciated is that the LVZ is approximately coincident with a zone of high seismic attenuation (or low seismic quality factor, known as Q). CEED PhD student **Florence Ramirez** set out to explain the low-Q zone by developing an analytical 1-D channel flow model that accounts for upper mantle rheology and its dependence on the many factors that influence it: temperature, flow-modified grain-sizes, water content, and melt fraction. The model predicts seismic velocity and Q, which can be compared to seismic observations. Florence tested her model for flow driven by surface plate motions (Couette flow, Figure 2.1a) and found that the model did not produce a low-Q zone (Figure 2.1c). However, upper mantle flow driven by horizontal pressure gradients (Poiseuille flow, Figure 2.1b) does produce a low-Q zone, especially for wet conditions (Figure 2.1d) and if the flow configuration is plug-like (Figure 2.1b.2). This is because stresses are small in the middle of a plug-flow, which leads to grain-growth and larger Q. These models suggest that the low-Q zone in the upper mantle can be explained by shearing above a plug-like flow that spans the upper 670 km of a wet upper mantle (*Ramirez et al.,* submitted).

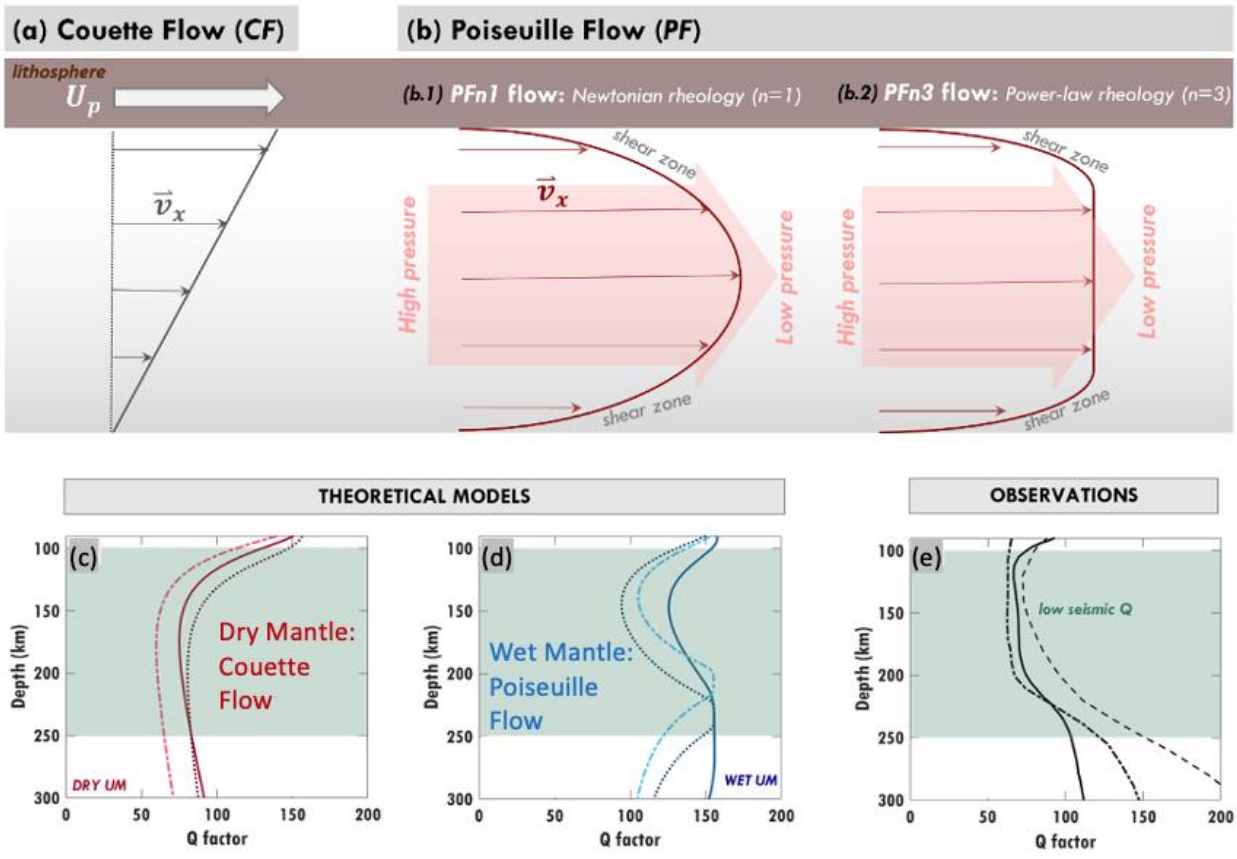

Figure 2.1. *Flow configurations (a-b), seismic Q (reciprocal of attenuation) resulting from these flows (c-d), and observations of Q (e). Couette flow (a) is driven by surface plate motions, while Poiseuille flow (b) is driven by horizontal pressure gradients, and can be plug-like for non-Newtonian rheology (b.2). Couette flow, common for dry conditions, does not produce a low-Q zone (c) while Poiseuille flow, appropriate for wet conditions, does make a low-Q zone (d), especially if the flow is plug-like.*

A potential plume beneath West Antarctica: Inferences from geoid, topography, and numerical models

The West Antarctic Ice Sheet is one of the tipping elements in the Earth's climate system. The behavior of the ice sheet is affected by postglacial rebound, which drives surface uplift following ice sheet melting: Reduced mantle viscosity beneath Antarctica, possibly due to a hot mantle plume, could allow for faster uplift following melting, somewhat counteracting the instability. CEED Associate Professor **Bernhard Steinberger** and collaborators have studied related processes, using geoid and topography as constraints to their models.

Relative to equilibrium shape, the geoid is deepest worldwide (~ –130 m) in the Ross Sea area (Figure 2.2A). Nearby, residual topography is high peaking at ~2 km (Figure 2.2B). Following the approach of Steinberger et al. (2021) the geoid low may be caused by the superposition of a large-scale trough ~70 m caused by lower mantle slabs and Large Low Shear Velocity Provinces (LLSVPs) (Figure 2.2C), and a smaller-scale residual low ~70 m deep due to hot materials in the upper mantle (Figure 2.2D). *Steinberger et al.* (submitted) show that realistic density anomalies in the upper mantle can simultaneously explain the residual geoid low and the topographic high. However, forward plume models tend to predict flattened plume heads beneath the lithosphere whereas geoid modeling requires low-density anomalies also at greater depths.

The influence of hot low-viscosity materials in the upper mantle – in this case, inferred from seismic tomography – on glacial-isostatic adjustment in Antarctica is studied by *Bagge et al.* (2022), which builds upon the workflow developed by Bagge et al. (2021).

Bredow et al. (2022) put the idea of a mantle plume beneath West Antarctica into the larger context of a diverse set of observations, and global geodynamic models. In particular, their models predict that such a plume, if it originates in the lowermost mantle, would be tilted with its base displaced about half-way towards the Pacific LLSVP boundary. Yet, this is an unlikely source location for a lower mantle plume.

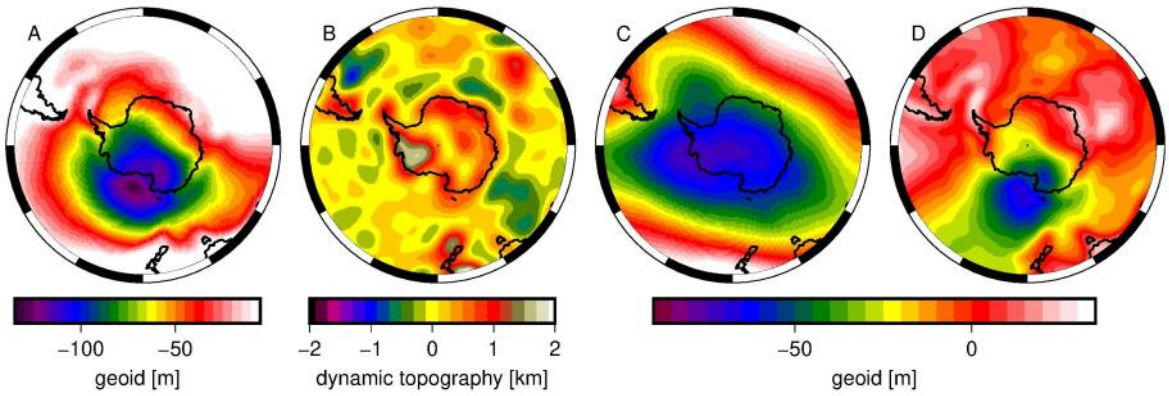

Figure 2.2. *Geoid and residual topography in and around Antarctica. A: Observed geoid relative to the equilibrium spheroid, with contributions from crust and the effect of ocean floor age removed. B: Residual topography (i.e. observation-based dynamic topography) derived in Steinberger et al. (2019). C: Geoid contribution from slabs and LLSVPs after Steinberger and Torsvik (2010). D: Remaining (residual) geoid after contribution in C has been subtracted from A.*

The ANIMA Project

CEED researcher **Ágnes Király**, in collaboration with CEED Professor **Clint Conrad** and CEED Ph.D. student **Yijun Wang**, continues to work on the NFR funded Young Talent Project ANIMA (ANIsotropic viscosity in MAntle dynamics). Progress in the last year followed three main themes within ANIMA:

Theme 1: Implementation of anisotropic viscosity (AV) into the finite element code ASPECT. ASPECT (Bangerth et al., 2020) is an open-source geodynamic software, actively developed by the geodynamic modelling community. Progress has been made in the development of AV in ASPECT. Now, it is possible to track crystallographic orientation (CPO) on particles across the model domain (Fraters and Billen, 2021), and calculate their anisotropic response to the strain rate that each particle experiences (Figure 2.3). Using a large number of particles across the model domain, this response can be interpolated onto the field domains and used to calculate a viscosity tensor that can then be used in the solution. This latter part is still in progress. In this year both PI **Ágnes Király** and Ph.D. student, **Yijun Wang** contributed to ASPECT by developing multiple plugins that are either merged into the main version of ASPECT or available on GitHub (see https://github.com/KiralyAgi/aspect).

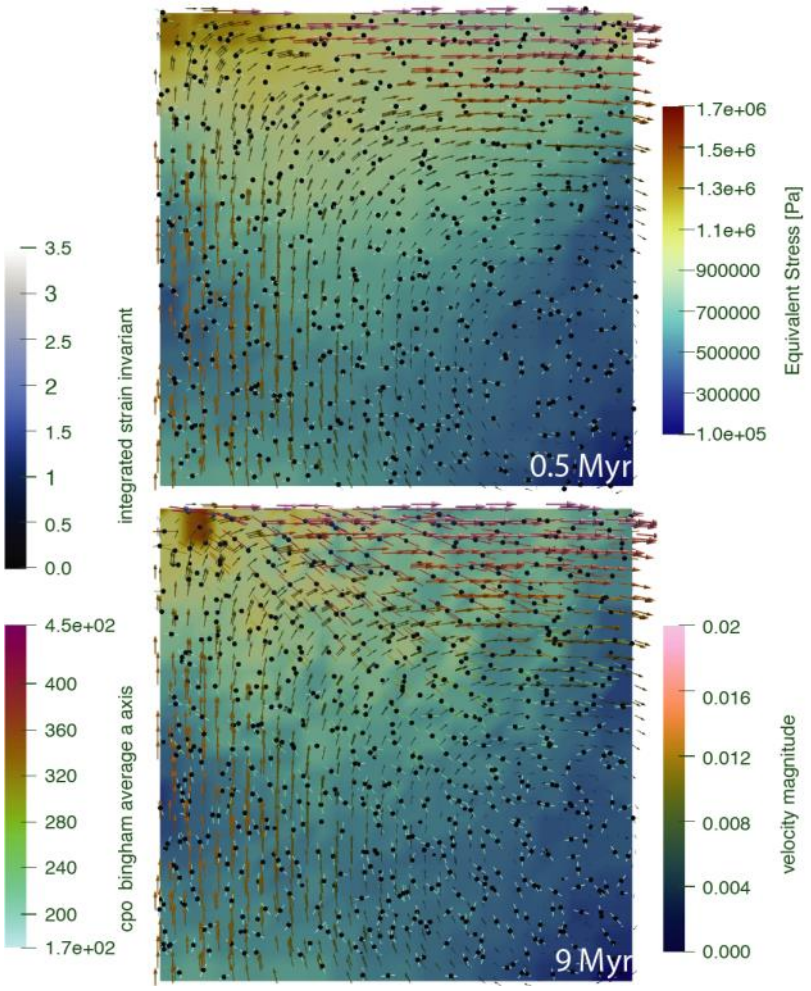

Figure 2.3. *A corner flow model, where CPO development and anisotropic viscosity are tracked on the particles. Dots are showing the particles, and the lines across them show the mean orientation of the olivine a-axis. The arrows show the velocity field, while the background color shows the equivalent stress required to achieve the imposed strain rate based on the anisotropic viscous rheology.*

Theme 2: Comparing numerical methods for calculating CPO and the effect of anisotropic viscosity on CPO evolution.

CEED PhD student **Yijun Wang** has been comparing different numerical methods for tracking olivine CPO: D-REX (Kaminski et al., 2004), the modified director method (MDM)

(Hansen et al., 2016), and the MDM model with anisotropic viscosity (MDM+AV, Király et al., 2020).

For simple deformation paths (e.g. simple shearing), the three models produce similar results, with D-REX predicting slightly faster development and stronger textures with respect to MDM (Figure 2.4a).

On the contrary, when a particle undergoes more a complex deformation (e.g. in a subduction zone) differences between the models are more significant (Figure 2.4b). While D-REX still predicts a slightly stronger texture, we also find that the mean orientation of the CPO can be significantly modified by AV. Thus, not only does olivine CPO affect AV in the mantle, but AV subsequently affects the development of CPO.

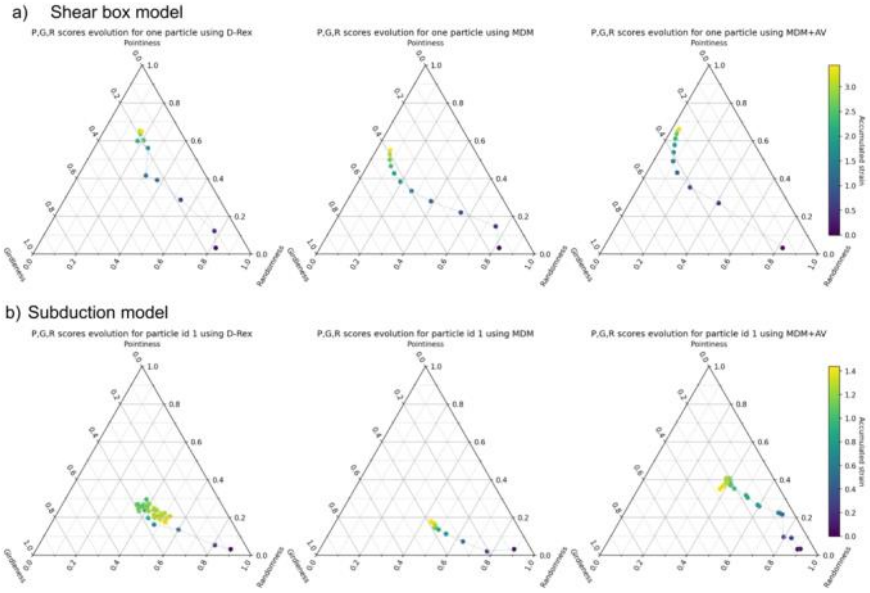

Figure 2.4. *Ternary diagrams showing the pointedness, girdleness, and randomness (P, G, R) scores for olivine particles in a) a shear box model and b) a subduction model. Colors show the degree of accumulated strain. P, G, and R are computed using the eigenvalues of the orientation tensor.*

Theme 3: Developing a new method for constructing the full anisotropic viscosity tensor.

Anisotropic viscosity of textured olivine affects processes where the mantle deforms under dislocation creep. Because dislocation creep deformation depends on stress in a non-linear way (power-law or non-Newtonian viscosity) the definition of the full viscosity tensor is not obvious. Currently, we are working on a method that will allow us to remove the stress-dependency from the viscosity tensor and to define all of its components. This will allow us to develop a fast implementation of anisotropic viscosity within ASPECT, letting us examine the role of anisotropic viscosity on a wide variety of geodynamic problems.

The effect of melt intrusions on plume-induced surface heat flux and lithosphere erosion

Mantle plumes are major sources of extrusive volcanism, as observed at hotspots such as Hawaii and Iceland. Yet for these systems large portions of the generated melt may not reach the surface, especially for continental or cratonic settings. However, even in the absence of extrusive volcanism, the interaction of a plume with continental lithosphere will cause elevated surface heat flux and reduced lithospheric thickness for millions of years after the plume has passed beneath lithosphere. As part of the NFR-funded project MAGPIE, CEED Postdoc

Björn Heyn used numerical models and an analytical solution to show that the maximum relative heat flux anomaly and the maximum relative lithosphere thinning are directly related to each other (Figure 2.5). Moreover, the observed trend is independent of model geometry, plate motion and model parameters, although the anomalies increase with decreasing asthenosphere viscosity or increasing plume excess temperature. The maximum heat flux is observed about 40-140 Myr after the maximum lithosphere thinning during plume passage. This work was demonstrated in a recent publication (*Heyn and Conrad*, 2022).

In a new set of models, Björn Heyn tracked the generation of melt, and its interaction with the lithosphere. These models show that melt only slightly increases the predicted heat flux anomalies as long as does not reach shallow depths (<30 km). Lithosphere thinning becomes much more localized and locally can reach much larger values, but is usually short-lived and therefore is not reflected in elevated heat flux (Figure 2.5, red dots). The delay time between maximum heat flux and maximum lithosphere thinning is reduced. Overall, melt generation and migration cause a much more time-dependent behaviour of surface heat flux and lithosphere thinning. Non-uniform depth of the lithosphere - asthenosphere boundary can cause multiple sequences of melt generation, and therefore multiple events of increased lithosphere thinning and surface heat flux over time spans of ~60-100 Myr. Björn Heyn will continue to work on this topic under the NFR-funded POLARIS project, with a more detailed focus on the evolution of the Arctic and the connection between the Iceland plume and the large igneous provinces NAIP (North Atlantic Igneous Province), HALIP (High Arctic Large Igneous Province), and Siberian Traps.

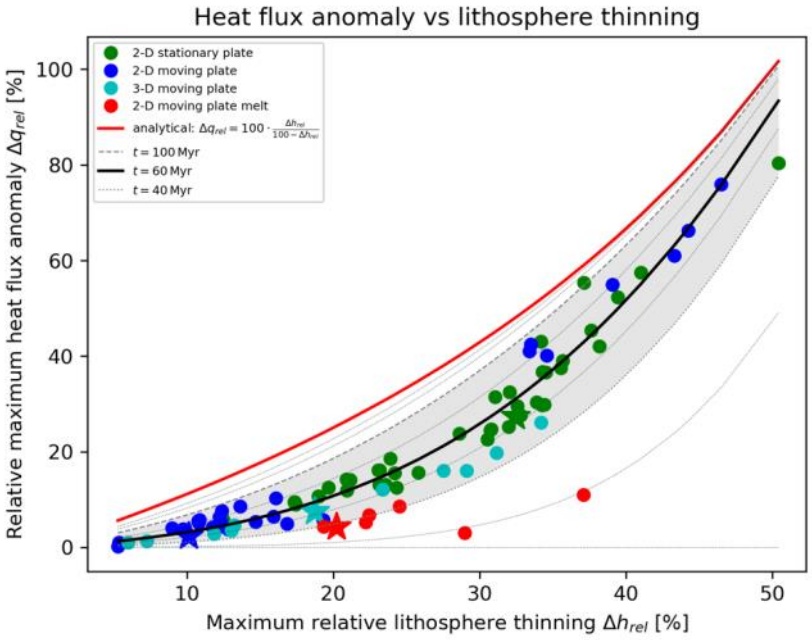

Figure 2.5. *Maximum relative heat flux as a function of maximum relative lithosphere thinning for different model geometries and model parameters. Stars mark the reference models, which only differ by the explanation given in the legend. Note that the maximum heat flux typically follows the maximum thinning by several tens of millions of years and that melting (red symbols) typically produces smaller heat flow because it produces more localized and short-lived lithospheric thinning.*

Solid earth uplift due to contemporary ice melt above low-viscosity regions of the upper mantle

Ice melting in Antarctica and Greenland causes ground motion as Earth's interior deforms in response to ice mass changes at the surface. The timescale for this deformation depends on the viscosity of mantle rocks. It is commonly thought that the high viscosity of the mantle leads to deformation timescales of thousands of years. However, some regions of the upper mantle may have unusually low viscosity, particularly if a mantle plume has introduced heat beneath the lithosphere. For example, this may have been the case for Greenland (Figure 2.6a). CEED PhD student **Maaike Weerdesteijn** has led the development of a new numerical code that can

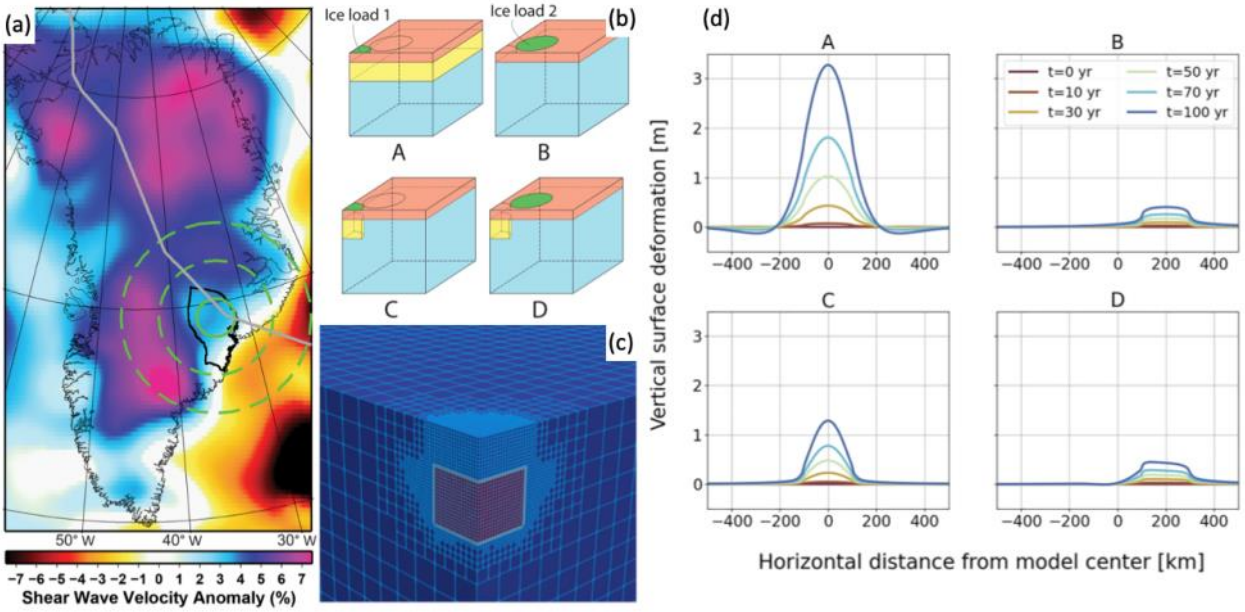

Figure 2.6. *Variations in seismic velocity beneath Greenland at 150 km depth (a) show large lateral variations that may have been induced by passage of Greenland over the Iceland plume (track shown by the grey line). Such variations (shown by colors) may be associated with large variations in mantle viscosity beneath Greenland's lithosphere. Green circles have radii of 100, 300, and 500 km for scale. Deglaciation above this laterally-varying viscosity structure may induce surface uplift also with large lateral variations. To examine such variations, we set up a series of numerical models (b) driven by a circular load of ice melting (green circles, 100 km in radius). Here only a quarter of the model is shown (because of reflexive symmetry), and colors indicate viscosity (pink for high viscosity lithosphere and yellow for low-viscosity regions). Our new numerical code handles large lateral viscosity variations by assigning high resolution to rapidly deforming regions (c). The uplift patterns for 100 years of melting (at rates of 1 m/yr) are shown in (d) for the four scenarios described in (b). A comparison of four models (labelled A, B, C, and D) shows that contemporary ice melt, when positioned above a low-viscosity region of the mantle, can produce uplift rates of cm/yr. Such rates are comparable to present-day observed rates in Greenland.*

compute ground uplift rates following deglaciation. This new code (*Weerdesteijn et al.,* 2023) is based on the mantle convection code ASPECT, and can model deformation while incorporating large variations in mantle viscosity (Figure 2.6b) by adaptively refining the finite element mesh near regions of high deformation (Figure 2.6c).

By applying surface loads consistent with ice loss of 1 meter per year (reasonable for modern Greenland melting), Maaike's new code predicts uplift of ~1 meter above a confined low vis-

cosity region of the mantle (Figure 2.6d.C) following 100 years of melting (*Weerdesteijn et al.,* 2022). The predicted uplift rate (~ 1 cm/yr) is much faster than rates predicted for regions that are not above low-viscosity mantle (Figures 2.6d.B and 2.6d.D) but slower than rates predicted for deglaciation above an entire layer of low-viscosity mantle (Figure 2.6d.A). This work demonstrates the importance of the detailed viscosity structure beneath Greenland, where lateral viscosity variations, such as those associated with the earlier passage of Greenland over the Iceland Plume (Figure 2.6a), exert an important control on present-day uplift patterns. It also shows that contemporary ice melt, when positioned above a low-viscosity region of the upper mantle, may induce rapid uplift of the ground surface at rates of a few cm/yr. Such rates are comparable to the fastest rates observed in Greenland today, which means that contemporary ice melt above low-viscosity mantle is an important contributor to present-day ground deformation in Greenland.

Hydrous regions of the mantle transition zone affect patterns of intraplate volcanism

The Earth's mantle transition zone (MTZ) can store a large amount of water, which is transported into the deep mantle by subducting oceanic lithosphere. The presence of water has the potential to generate melting in the upper mantle that could promote the occurrence of intraplate volcanism (IPV). Despite its importance, the amount and spatial distribution of water within the mantle, and its effect on the origin of volcanism far from plate boundaries, are poorly constrained (Figure 2.7).

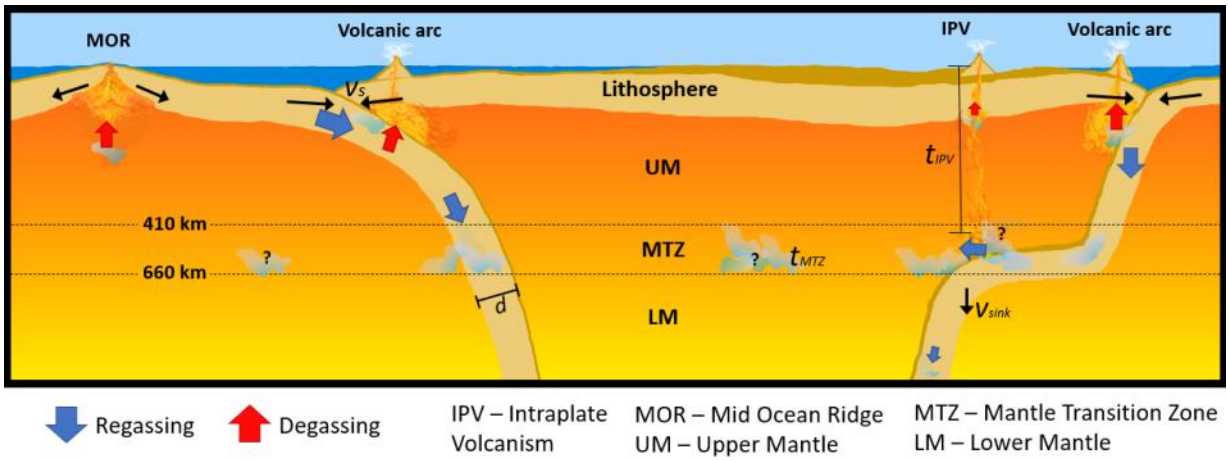

Figure 2.7. *Schematic of Earth's deep water cycle showing water transport into the Earth at subduction zones (regassing) and export out of Earth's interior by volcanism (degassing). Water may be stored for long periods (time t_{MTZ}) in the mantle transition zone (MTZ). The regionally hydrous MTZ might induce melting, hydrous upwellings, and subsequent intra-plate volcanism (IPV) that is not plume-related. Eruptions at intraplate locations above water-rich locations in the MTZ could occur after an unknown IPV delay period (t_{IPV}).*

CEED master's student **Helene Wang**, along with CEED Researchers **Valentina Magni** and **Mat Domeier**, and CEED Professor **Clint Conrad,** developed models of the spatial and temporal heterogeneity of water in the MTZ during the past 400 Myr. Helene Wang compared predicted regions of wet and dry MTZ with the locations of past and present IPV, and discovered a statistically-significant correlation between them. This work was developed as part of

Helene's 2022 master's thesis and is being prepared for publication (*Wang et al.,* in preparation). These findings suggest a link between the formation of volcanism far from plate boundaries and the presence of water within the MTZ (Figure 2.7). This discovery is important for developing new understanding of Earth's deep water cycle.

A freely deformable lower boundary for numerical models with ASPECT

Numerical mantle flow models typically predict topography using vertical stresses, which are converted into dynamic topography during post-processing. While this approach is easy and numerically cheap, the derived topography does not affect the calculated mantle flow, and is always an instantaneous reaction to any flow in the mantle. However, a free surface is required to fully reproduce predicted topography for complex settings, e.g. subduction zones. As a consequence, a free surface has been implemented in various numerical mantle convection codes, including ASPECT. Despite recognition of the importance of a free surface, this approach has not yet been implemented and tested a the lower boundary of numerical models, i.e. the core-mantle boundary (CMB) beneath mantle convection.

Using the existing framework of ASPECT, CEED Postdoc **Björn Heyn** has developed an implementation of a free base that can be used as an analogue to a free surface (*Heyn et al.,* in preparation). However, in contrast to assuming zero stress at the boundary (as is applicable for the surface), the free base must account for hydrostatic pressure of the material overlying the (deformed) lower boundary. Benchmark tests have shown the feasibility and accuracy of this method, but also highlighted some differences in expected amplitudes and timings. As a next step, the method will be made available within future releases of open source code ASPECT. The first models with a free base have reproduced the CMB dynamic topography that Björn Heyn discovered during his PhD work (Figure 2.8).

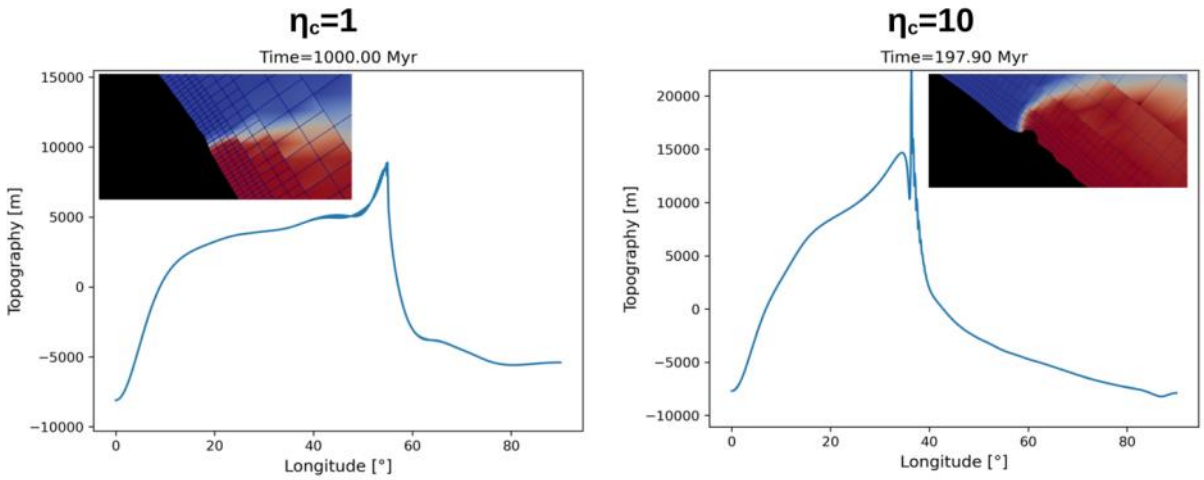

Figure 2.8. *Free base CMB topography for LLSVPs with no intrinsic viscosity increase (left) and with one order of magnitude viscosity increase (right). The inlays show the compositional field, with red as LLSVP material.*

Convective self-compression of cratons and the stabilization of old lithosphere

Despite being exposed to convective stresses for much of the Earth's history, cratonic roots appear capable of resisting mantle shearing. Some cratons have remained stable for more than ~3 billion years. This tectonic stability can be attributed to the neutral density and higher strength of cratons compared to the surrounding mantle. However, the excess thickness of cratons amplifies their coupling to underlying mantle flow, which could be destabilizing. To investigate the stresses that a convecting mantle exerts on cratons that are both strong and thick, Bayreuth postdoc **Jyotirmoy Paul** worked with CEED professor **Clint Conrad** and other collaborators to analyze numerical models of mantle flow that includes stiff cratons. These models show that mantle flow is diverted downward beneath the thick cratonic roots (Figures 2.9c-2.9f), giving rise to a ring of elevated and inwardly-convergent forces along the periphery of most cratons (compare Fig. 2.9a to Fig. 2.9b). These inward forces compress cratonic interiors, as Paul and Conrad discuss in their new paper on this topic (*Paul et al.,* 2023). Such compression could serve to stabilize older continental lithosphere against mantle shearing, thus adding an additional factor that promotes cratonic longevity.

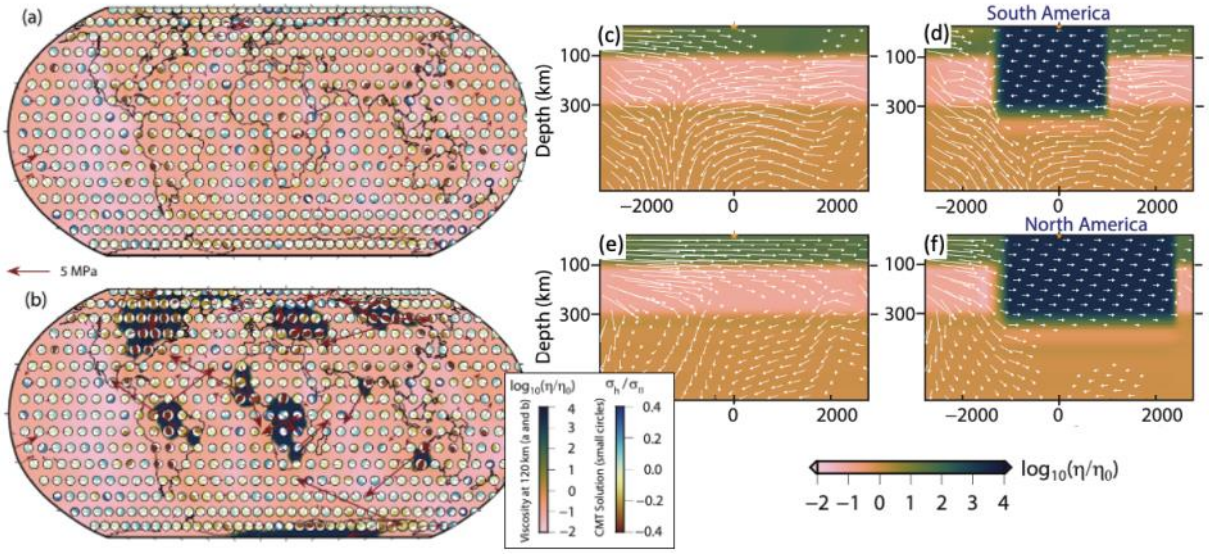

Figure 2.9. *The stress state (CMT stress state solutions and arrows) of the lithosphere at 120 km depth for mantle flow models both without cratons (a) and with cratons (b). Viscosity is shown by background colors while stress state is shown by both colors in small circles (CMT solutions) and arrows. The flow fields (c through d) are shown for cross sections across South America (c and d) and North America (e and f), with colors showing viscosity. Flow for models without cratons (c and e) should be compared to flow for models with cratons (d and f).*

Jyotirmoy Paul was recently awarded a Marie Sklodowska-Curie Award from the Horizon Europe program of the European Commission. He will be joining the remainder of the Earth Modelling Team in 2024 to work on his proposed BALCONY project: BALancing Craton thickness by self-cOmpression, grain size evolution and viscous anisotropY.

The MAGPIE Project

Researchers with the Earth Modelling Team continued to work on the NFR-funded **MAGPIE project** (Magnetotelluric Analysis for Greenland and Postglacial Isostatic Evolution, 2019-2023). MAGPIE returned to the Greenland ice sheet in May of 2022, after a 2-year COVID-

related delay. CEED adjunct professor **Kate Selway** organized a 2-part field project out of SUMMIT and RAVEN stations in central Greenland (Figure 2.10). We collected magnetotellurics (MT) data at 6 sites out of RAVEN station and 7 sites out of SUMMIT station in Greenland, each site spaced about 100 km apart. Together with the data collected out of EastGRIP station in 2019, the survey gives us excellent coverage across the center of Greenland (Figure 2.10). These data will provide valuable constraints on the upper mantle structures beneath central Greenland, including those influenced by the passage of the Iceland plume.

The fieldwork lasted about 6 weeks, with 3 weeks working out of both RAVEN and SUMMIT stations. We drove between MT sites on snowmobiles and camped on the ice while transiting between stations. Temperatures fell below -30°C at times and we encountered some rather harsh conditions. It was an exciting and challenging adventure (Figure 2.11), and is described in more detail here:

The MAGPIE blog:

https://magpiegreenland.wordpress.com/

Video Diary:

https://www.youtube.com/watch?v=fLzWPcyAH7c

Back in the friendly climate and solid ground of CEED, the members of the MAGPIE group progressed with other aspects of the project in 2022. These include:

CEED PhD student **Florence Ramirez** published her method to estimate mantle viscosity using geophysical constraints on seismic wave speed (e.g., from a seismic survey) and electrical conductivity (e.g., from a magnetotellurics survey) (*Ramirez*

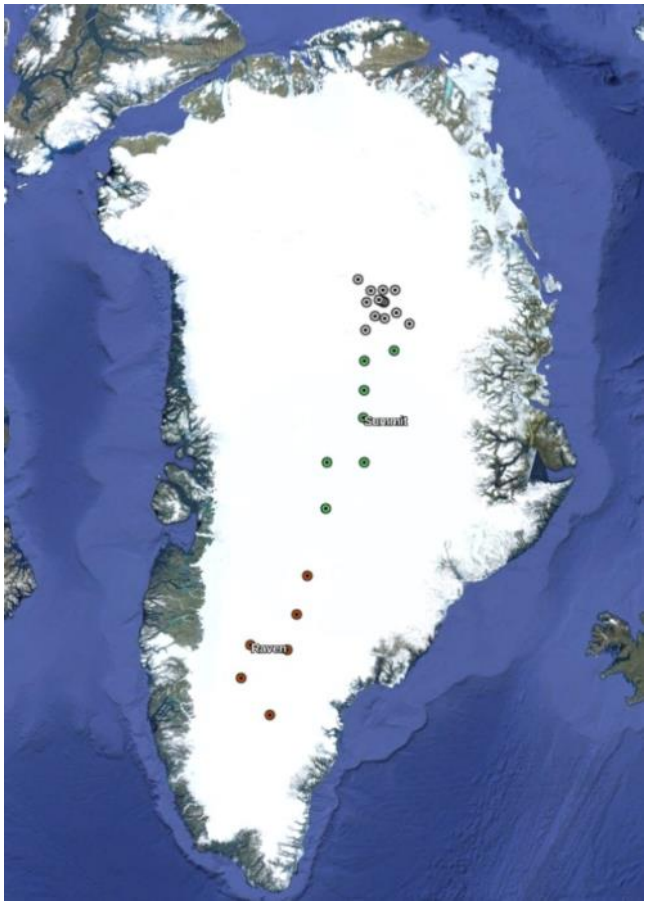

Figure 2.10. *Map of the MAGPIE field work. Magnetotellurics data were collected in 2019 out of EastGRIP station (grey dots) and in 2022 out of RAVEN station (red dots) and SUMMIT station (green dots).*

Figure 2.11. *The MAGPIE team operating out of RAVEN station. Shown (left to right) are Kate Selway, Andreas Bergström, and Clint Conrad. Johanna Eclancher (not shown) joined the team for the work out of SUMMIT, replacing Conrad.*

et al., 2022). This work continued with an application of the method to Scandinavia, where the method can be tested against independent constraints on viscosity from glacial isostatic adjustment (GIA). This work is being prepared for publication (*Ramirez et al.,* in preparation). Florence also used seismic attenuation observations to constrain patterns of mantle flow in the upper mantle (see more details earlier in the Earth Modelling report). These 3 projects formed the chapters of her PhD thesis, which she successfully defended in November.

CEED Postdoc **Björn Heyn** published a new analytical model for the evolution of heat flow following the passage of a plume (*Heyn and Conrad*, 2022). This work continues with an examination of how melting in the upper mantle can affect plume-lithosphere interaction and heat flow (see more details in the Earth Modelling report).

CEED PhD student **Maaike Weerdesteijn** published an analysis for how a small low-viscosity region of the mantle can affect uplift patterns following ice sheet melting (*Weerdesteijn et al.,* 2022) and a technical paper describing the new GIA model that she developed by adapting the mantle convection code ASPECT. See the special writeup about Maaike's work in the Earth Modelling Report. Maaike's work continues with an application of her model to Greenland, where she has found that low mantle viscosity associated with the Iceland plume, coupled with rapid recent melting of the ice sheet, could explain observations of rapid uplift in eastern Greenland. This work will form the third chapter of Maaike's PhD thesis, which Maaike is planning to defend in the spring of 2023.

The MAGPIE project will close later in 2023, after wrapping up these sub-projects.

References

Note: Only 2022 articles by CEED authors (denoted in boldface) are listed here. References for other articles cited above can be found within these articles.

Bagge, M., V. Klemann, **B. Steinberger**, and C. Haeger (2022), Improving the glacial-isostatic adjustment in Antarctica by means of geodynamically constrained structural models of the lithosphere and upper mantle, *ESA Living Planet Symposium*.

Bredow, E., B. **Steinberger,** R. Gassmöller, and J. Dannberg (2022), Mantle convection and possible mantle plumes beneath Antarctica - insights from geodynamic models and implications for topography, *Geological Society of London, Memoirs, 56*, doi:10.1144/M56-2020-2.

Bulut, N., H. Thybo, and **V. Maupin** (2022), Highly heterogeneous upper-mantle structure in Fennoscandia from finite-frequency P-body-wave tomography, *Geophysical Journal International*, *230*(2), 1197-1214, doi:10.1093/gji/ggac107.

Heyn, B. H., and **C. P. Conrad** (2022), On the Relation Between Basal Erosion of the Lithosphere and Surface Heat Flux for Continental Plume Tracks, *Geophysical Research Letters*, *49*(7), e2022GL098003, doi:https://doi.org/10.1029/2022GL098003.

Mauerberger, A., H. Sadeghisorkhani, **V. Maupin,** Ó. Gudmundsson, and F. Tilmann (2022), A shear-wave velocity model for the Scandinavian lithosphere from Rayleigh waves and ambient noise - Implications for the origin of the topography of the Scandes mountain range, *Tectonophysics*, *838*, 229507, doi:https://doi.org/10.1016/j.tecto.2022.229507.

Paul, J., C. P. Conrad, T. W. Becker, and A. Ghosh (2023), Convective self-compression of cra-

tons and the stabilization of old lithosphere, *Geophysical Research Letters*, *50*(4), e2022GL101842, doi:https://doi.org/10.1029/2022GL101842.

Ramirez, F.D.C., C.P. Conrad, and **K. Selway** (submitted), Grain size reduction by plug flow in the wet oceanic upper mantle explains the asthenosphere's low seismic Q zone, *Earth and Planetary Science Letters*.

Ramirez, F. D. C., K. Selway, C. P. Conrad, and C. Lithgow-Bertelloni (2022), Constraining Upper Mantle Viscosity Using Temperature and Water Content Inferred From Seismic and Magnetotelluric Data, *Journal of Geophysical Research: Solid Earth*, *127*(8), e2021JB023824, doi:https://doi.org/10.1029/2021JB023824.

Steinberger, B., M.-L. Grasnick, and R. Ludwig (submitted), The deepest geoid low on Earth and its possible relation to the instability of the West Antarctic Ice Sheet, *Tektonika*.

Weerdesteijn, M. F. M., C. P. Conrad, and J. B. Naliboff (2022), Solid earth uplift due to contemporary ice melt above low-viscosity regions of the upper mantle, *Geophysical Research Letters*, *49*, e2022GL099731, doi:https://doi.org/10.1029/2022GL099731.

Weerdesteijn, M. F. M., J. B. Naliboff, **C. P. Conrad,** J. M. Reusen, R. Steffen, T. Heister, and J. Zhang (2023),Modeling Viscoelastic Solid Earth Deformation Due To Ice Age and Contemporary Glacial Mass Changes in ASPECT, *Geochemistry*, *Geophysics*, *Geosystems*, *24(3),* e2022GC010813, doi:https://doi.org/10.1029/2022GC010813.

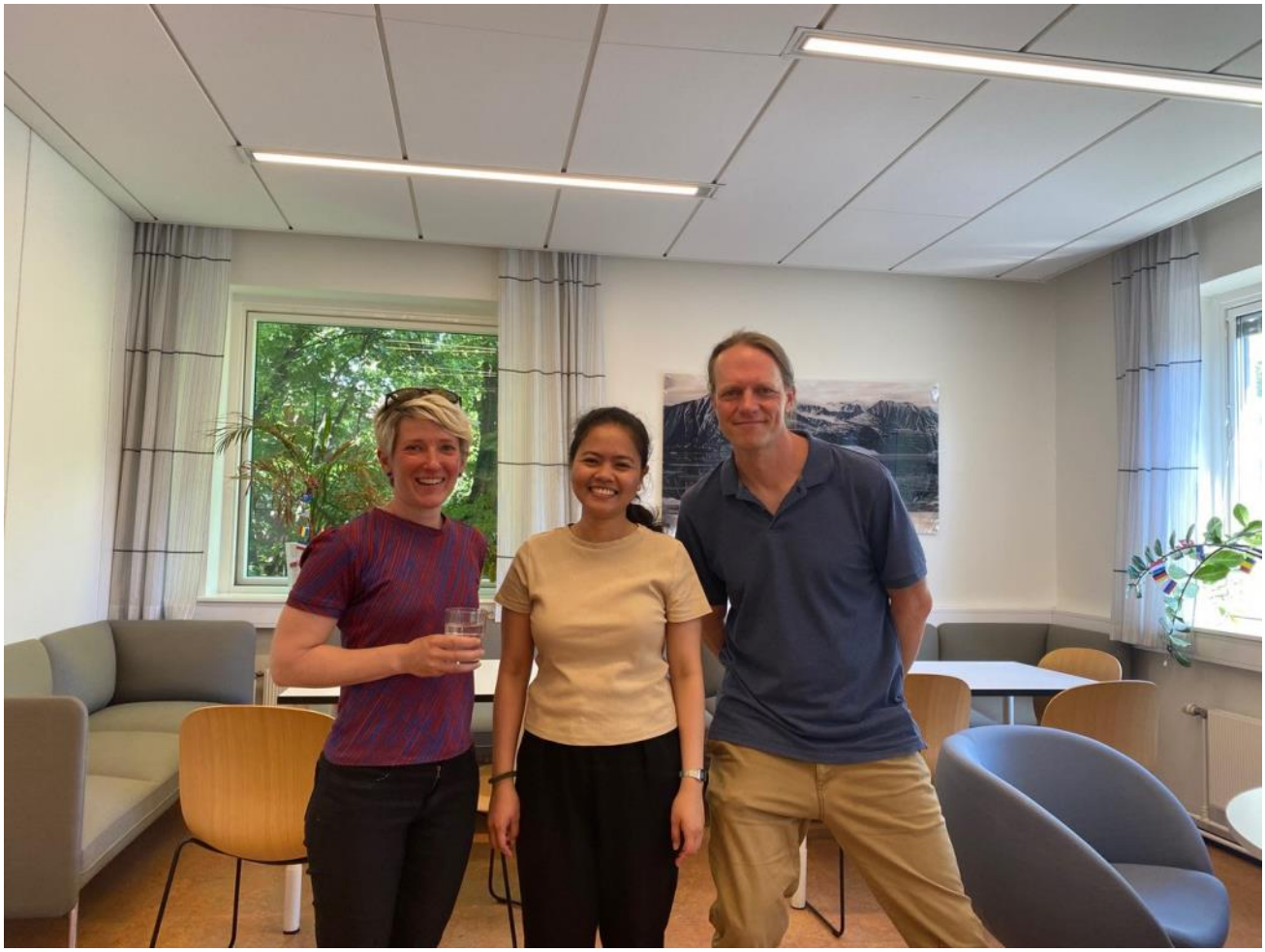

CEED PhD student Florence Ramirez (center) with her two supervisors (Kate Selway and Clint Conrad). Due to corona-related travel restrictions, Florence was only able to meet with both supervisors together for a few hours during Kate's only (and brief) visit to Oslo. This photo was taken during that visit, about 6 months before Florence successfully defended her thesis (in November, 2022). Photo by: Clint Conrad.

Above: Björn Heyn, Florence Ramirez and Yijun Wang during the CEED closure: All things must pass, 28.02.23. Below: Night time at UiO. Photos by: Ming Geng.

3. Dynamic Earth: Plate motions and Earth history

The mission of the Dynamic Earth team is to explore the link between the lithosphere and the convecting mantle, as well as its interactions with the climate and oceans. We achieve this largely through the large-scale framework of Plate Tectonics and the Wilson Cycle. In 2022, Dynamic Earth members and their collaborators published articles on a variety of topics, including: magnetotelluric and seismic data, the NE Atlantic and Eurasia Basin, the Wilson Cycle, rifted margins mantle properties and seismology, and carbon cycling. The Dynamic Earth team members are also involved in a number of collaborative projects with the other CEED teams, the GEO department, as well as numerous national and international collaborations. Throughout the year, the team participated in a number of marine and terrestrial expeditions including several featured below. As expected with the final year of CEED, the Dynamic Earth Team reduced in size due to a number of positions retiring or gaining employment elsewhere. As at the end of 2022 it comprised 14 members, including adjunct and Emeritus positions. A new guest researcher, ***Paul Wessel*** *joined us from Hawaii. One new PhD student,* ***Juan Camilo Meza Cala*** *joined us as part of the NFR-funded DYPOLE project. It was also the final year for Team Leader* ***Valentina Magni*** *who took a position at the Norwegian Geophysical Institute (NGI).*

A few highlights of our research from the 2022 calendar year are below:

The Geysir-BaiaMare EEA project.

A CEED quest for searching relevant geological structures that may be used to harness geothermal energy has continued in 2022. As part of Geysir-BaiaMare project (including **Minakov, Neukirch, Gaina**) funded by EEA, CEED researcher **Alexander Minakov**, and collaborators from Sweden and Romania collected a new set of geophysical data in the intra-Carpathian region of Baia Mare (Romania). The Baia Mare region is a Neogene depression in the larger Pannonian Basin, developed in the vicinity of a large strike-slip fault and the Middle Miocene Tibles-Gutai volcanic mountains.

The international team collected additional magnetotelluric data that will complement the studies undertaken in 2021. Seismic data collected in 2021 revealed a fault zone that most probably controlled the tectonic evolution of the eastern Pannonian and Transylvanian basins, and may help evaluating the geothermal potential of the region (Panea et al., in review). Preliminary results from the MT data analysis were presented at the EGU and AGU (Neukirch et al.) conferences, as well as preliminary 3D model of the lithospheric structure at AGU 2022 (Minakov et al.). The 3D model helps to explain the observed temperature anomalies in the region by: i) transient heat transfer due to large intrusive bodies (possibly extending down to the Moho boundary) and ii) groundwater flow controlled by surface topography, rock permeability changes due to contrasting lithology and regional strike-slip shear zones and decollement horizons. These results and future plans were discussed in a joint online workshop (Norway-Romania) in December 2022.

GoNorth-2022 Expedition: New Deep Seismic Data Acquired at Ice-Covered Northern Barents Sea Continental Margin.

Several CEED researchers, including those related to the DYPOLE project (**Faleide, Minakov, Meza Cala**) were involved in the large Norwegian expedition **GoNorth**. The northern Barents Sea-Svalbard continental margin is a unique laboratory for studying a complex pattern of lithospheric deformation during early Cenozoic continental fragmentation. Recent studies postulated that corridors of exhumed mantle imaged by seismic reflection data in the Nansen Basin were formed in the Eurasia Basin since its inception. Now, new deep seismic data have been acquired to test the existing hypotheses of the margin's geological evolution

and to explore the links between the present-day segmentation of the ultraslow Gakkel Ridge and the inherited crustal structure of the passive margin.

Figure 3.1*: Acquisition of deep seismic data at the northern Barents Sea continental margin using the research icebreaker Kronprins Haakon in October-November 2022.*

The first GoNorth expedition acquiring wide-angle seismic data was performed in October-November 2022 using the new Norwegian research vessel Kronprins Haakon. The new deep seismic refraction data provide control on seismic velocities, that combined with seismic reflection, gravity and magnetic data can be used to determine the crustal and upper mantle structure of the northern Barents Sea continental margin and the character of the continent-ocean transition zone.

The seismic refraction/wide-angle reflection data were obtained along a 240-km-long profile using 24 ocean bottom seismometers (OBS). The OBS deployed at the sites under the sea ice were deployed/recovered using the University of Bergen remotely operated vehicle Ægir6000 that was operated via the moonpool. The OBS data provided information on crustal and mantle seismic phases. Seismic reflection data were also collected during the expedition. Two lines were achieved, oriented N-S and NE-SW, respectively. The N-S seismic reflection profile provides an image of the sedimentary structure of the northern Barents Sea shelf,

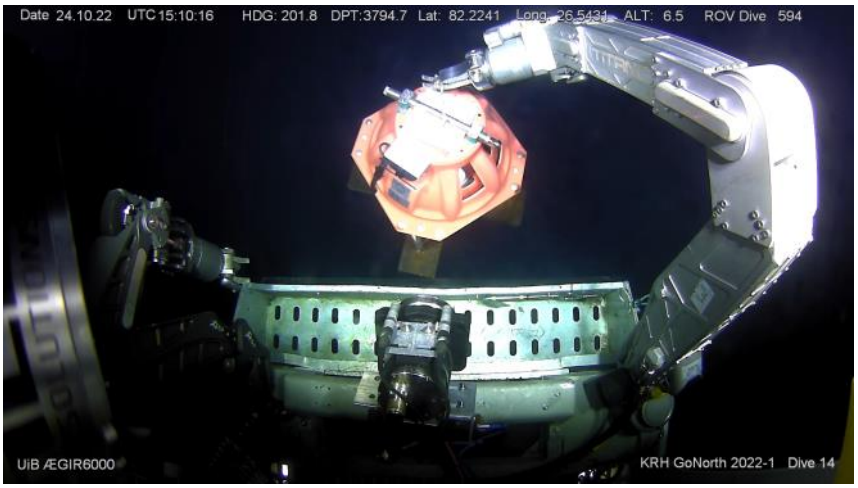

Figure 3.2. *Recovery of GEUS OBS 19 using remotely operated vehicle (water depth 3794 m). The OBS at the sites under the sea ice were recovered using the University of Bergen remotely operated vehicle (ROV) Ægir6000 that was operated from the moonpool of RV Kronprins Håkon.*

the continent-ocean transition, and the southwestern part of the Nansen Basin whereas the southern flank of the Sophia Basin and northwest Svalbard continental margin was imaged along the second reflection profile.

What is lurking on the below of the Barents.

Continuing the Barents and Arctic theme of activities, **Grace Shephard, Juan Camila Meza Cala,** and **Adriano Mazzini** (Earth Crises) group also participated on a teaching and research cruise to the Barents Sea in August 2022. The team went onboard R/V Helmer Hanssen, to exploring the Barents Sea in the region south of Svalbard. The main aim of the cruise "CAGE -22-6-HH", was to map and study sites of fluid flow on the seafloor, which can be related to natural methane and gas seeps, and link to their geological setting. They were scientific party of 13 people, plus two instrument engineers, and the ship's crew, and included nine nationalities – Australia, Brazil, Britain, Columbia, Denmark, Italy, Germany, Norway, Russia – and from four universities (UiT, UiO, Bologna and Kiel).

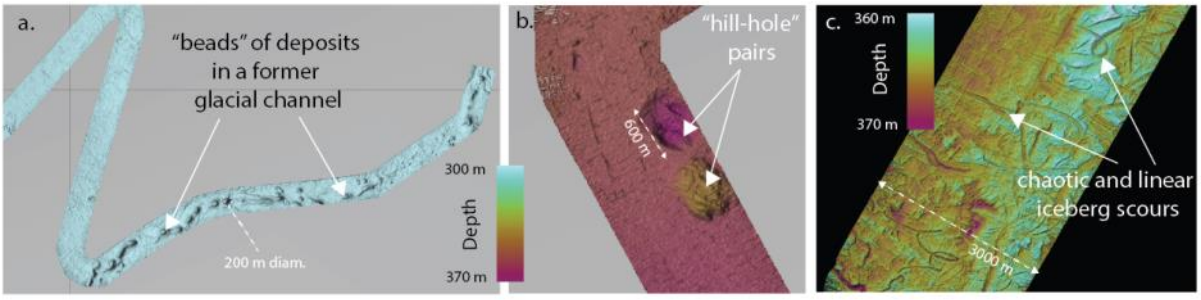

Figure 3.3. *Some of the newly mapped features on the Barents seafloor during the cruise. Including a) annual sedimentary deposits from past glacial channels, b) "hill-hole" pairs possibly formed when sediment blocks freeze onto the base of the ice sheet before being dumped downstream and c) some of the many iceberg scours that wiggle in all directions. These images are made from the multibeam data as the ship passes overhead and are loaded into the software, Fledermaus. From blog entry by Grace Shephard* https://cage.uit.no/2022/09/02/whats-lurking-on-top-of-the-below/

Multi-rifting episodes in the North Atlantic.

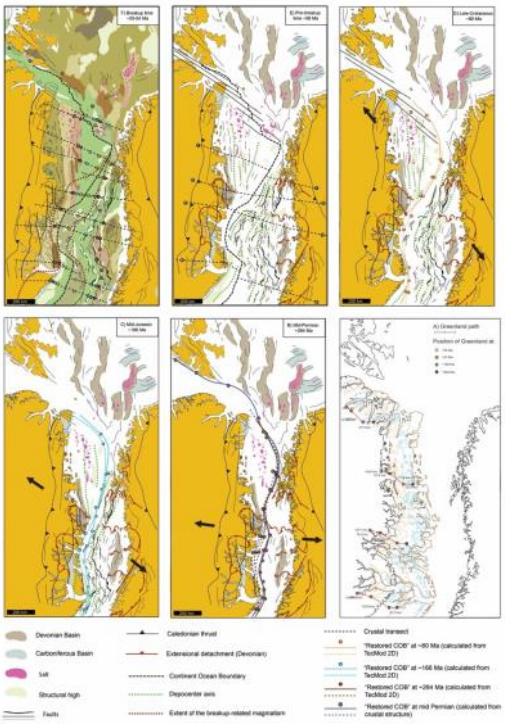

Figure 3.4. *Palinspastic plate reconstruction maps of the NE Atlantic realm from breakup until the mid-Permian time.*

Moving to the shelf east of Norway, several team members (**Abdelmalak, Gac, Faleide, Shephard, Torsvik**) collaborated to constrain pre-drift opening of the NE Atlantic. Restoring the effect of the multi-rifting phases is challenging because it is difficult to quantify the individual phases to the total extension estimates. This is mainly due to the lack of extensive data coverage and variable stratigraphic interpretations. An extensive amount of seismic reflection and refraction data covering the NE Atlantic was used to build a set of eight conjugate crustal transects and their corresponding stratigraphic models (Abdelmalak et al. 2022). The observed crustal thickness is used to quantify the cumulative pre-drift extension since the mid-Permian. Following on. for-

ward basin modelling is used to calculate the incremental crustal stretching factors for each of the main rifting phases. The results are used to establish and present a full-fit palinspastic plate kinematic model for the NE Atlantic since the mid-Permian, and will be the base for future work on more elaborated models in order to build accurate paleogeographic and tectonic maps.

Understanding the early Paleozoic carbon cycle balance and climate change from modelling.

Chloé M. Marcilly (who was awarded her PhD in 2022), examined the sensitivity of the Earth's climate to paleogeography and carbon degassing during the Ordovician global cooling by using the spatially resolved GEOCLIM model. Using refined continental reconstructions and new estimates of solid Earth degassing between 490 and 430 Ma, Chloé and collaborators (including **Torsvik**) performed new simulations of pCO2 and surface temperatures. First, the impact of continental drift alone was investigated throughout the studied period by calculating its imprint on continental weathering rates under a constant pCO2, and by testing different topography inputs. Secondly, the sensitivity of the Earth's climate to both paleogeography and carbon degassing changes was investigated by coupling the climate and carbon cycle in the GEOCLIM model. Their experiments suggest that even if a progressive improvement in Earth's surface weatherability is taken into account, the new constraints they developed cannot explain the intense cooling over the Mid- to Late Ordovician, even if early Ordovician high temperatures can be replicated within error margins. They also determined, using GEOCLIM in an inverse modeling approach, that the theoretical degassing required to reach the early Ordovician temperatures inferred from proxy data is three to five times greater than current levels. Furthermore, the solid Earth degassing must be lowered to current levels in only 30 to 40 Myrs in order to reproduce the ensuing Ordovician cooling. They concluded that, if accepting the veracity of the high early Ordovician temperatures, alternative sources but also sinks of carbon must be considered to explain the climatic shift over the period.

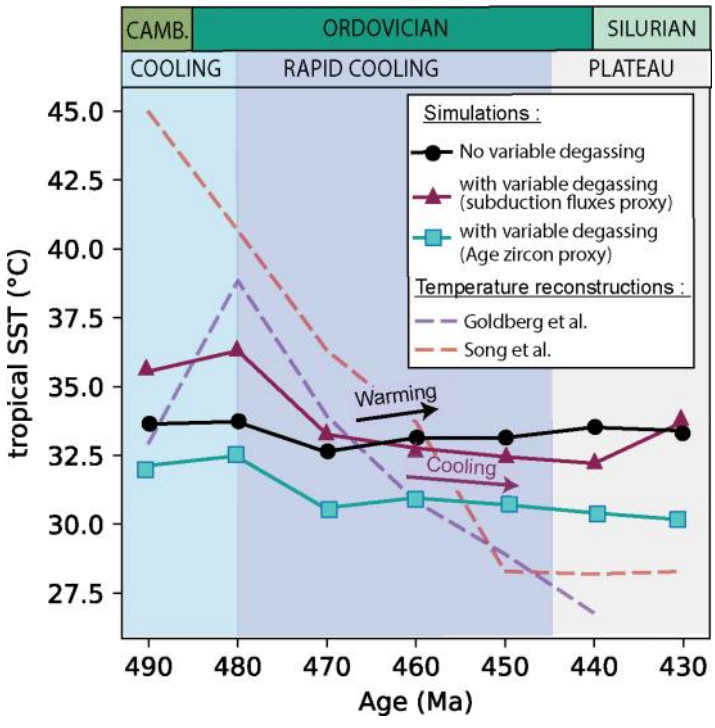

Figure 3.5. *Modelling simulations from GEOCLIM with no degassing (black) highlighting the paleogeographic effect alone and with variable degassing from subduction fluxes proxy (purple) and age zircon distribution proxy (turquoise). The simulations are plotted against temperature reconstructions from Goldberg et al. (2021) and Song et al. (2019).*

Scandinavian Caledonides: Tectonostratigraphy revised.

2022 wraps up results of the NFR FriNat project: 250327/20 on the evolution of the Pre-Caledonian margin of Baltica (awarded in **Torgeir Andersen**). The project has reported ongoing research in the Scandinavian and Scottish Caledonides. Three articles and one book chapter on these topics were published

in 2022. One paper with a detailed account of how a regional transtensional regime controls the structural and sedimentological architecture of Devonian Basins in Western Norway is currently in press. A new study started in 2022, involving field, geochemical and mineralogical work with focus on the listwanite-forming processes from ultramafic rocks of the Highland Border Complex in Scotland is currently being completed.

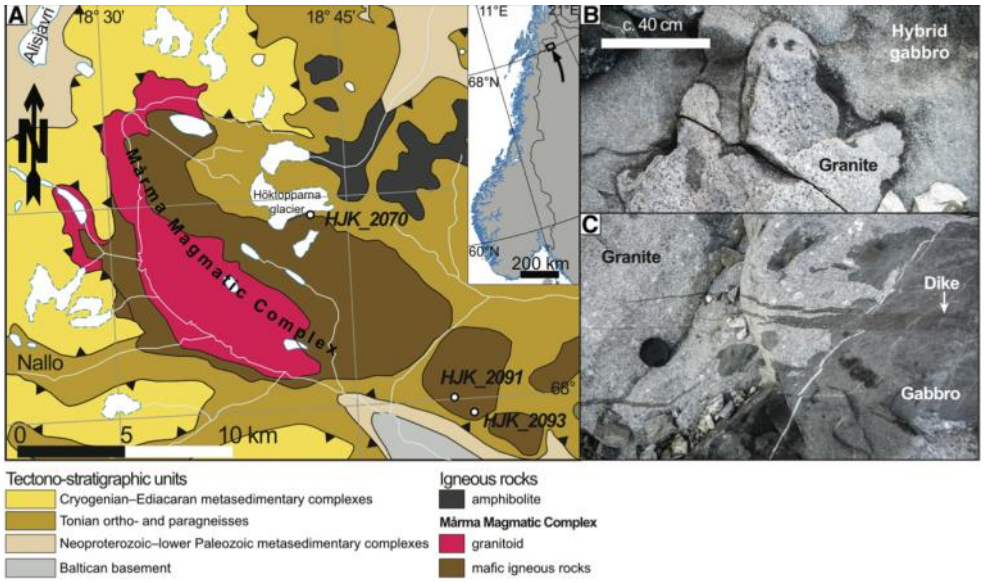

Figure 3.6. *Map of the Pre-Caledonian magma-rich margin of Baltica in the Mårma igneous complex (831 ± 0.33 Ma), NW Sweden. B and C show magma-mixing of felsic and mafic components, truncated by a ~600 Ma dyke of the Scandinavian dyke swarm. HJK-numbers refer to to U/Pb dated zircons samples.*

The effect of Magma Poor and Magma Rich rifted margins on Continental Collision Dynamics.

Different types of rifted margin are generated during the oceanic basin opening phase of the Wilson cycle. Magma-poor margins are often characterized by little syn-rift magmatism and a long continent-ocean transition zone composed of highly stretched and thinned continental lithosphere. On the other hand, magma-rich margins present high volumes of mafic intrusive and extrusive rocks and a possibly strong and dense lower crustal body. **Valeria Turino** (former master student at CEED), **Valentina Magni, Johannes Jakob** (former team member now at NGU), and **Hans Jørgen Kjøll** (former team member now at GEO) investigated how these different types of margins behave during subduction and how they affect the dynamics of continental collision. Their results show that taking into account the presence of a rifted margin in numerical models can considerably delay slab break-off up to 60 Myr after collision, which is more than previously found in numerical studies. Moreover, they find that magma-poor margins are more prone to accrete to the overriding plate and be preserved than magma-rich ones that, instead, subduct more easily. This explains why it is more common to find in the geologic records remnants of magma-poor margins in old suture than those of magma-rich ones. This study highlights how the dynamics of different phases of the Wilson cycle can influence each other.

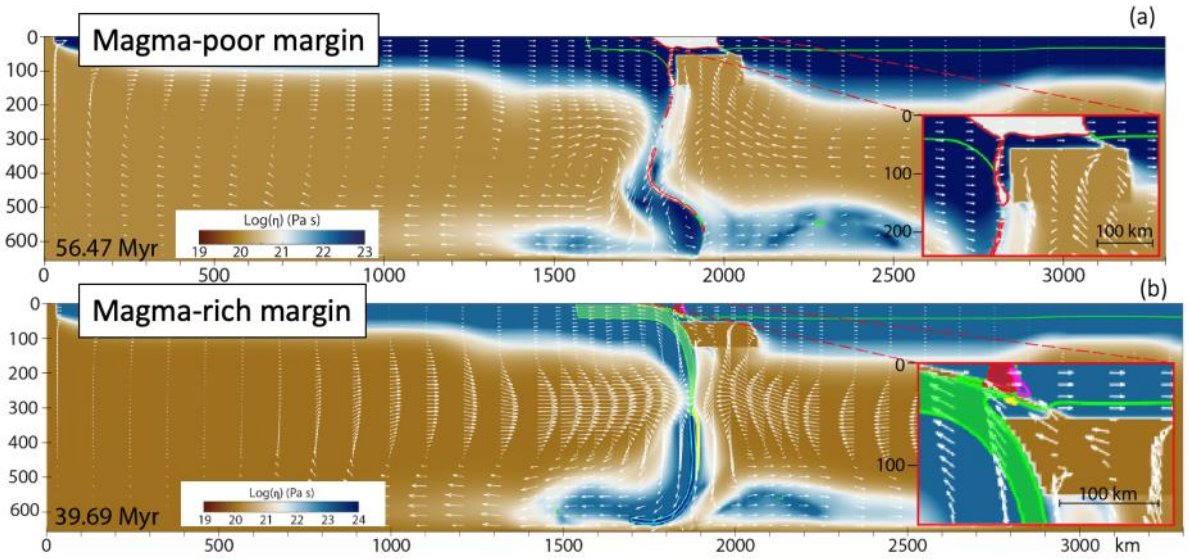

Figure 3.7. *Numerical model of continental collision with a (a) magma-poor and (b) magma-rich margin. A larger volume of margin material is accreted in the magma-poor margin case (a; grey color) compared to the magma-rich margin case (b; red and magenta colors).*

Coupling between mantle anomalies and surface magmatism.

Asbjørn Breivik's highlight from this year takes us to the Gakkel Ridge in the Eurasian Basin has the slowest seafloor spreading worldwide. The western Gakkel Ridge (3°W–85°E; 14–11 mm/a) alternate between magmatic and sparsely magmatic zones, while the eastern Gakkel Ridge (85–126°E; 11–6 mm/a) appears to be dominated by magmatic zones despite ultraslow spreading. Little is known about the seafloor spreading conditions in the past along the entire ridge. Here, the team exploited the residual bathymetry and basement roughness to assess the crustal accretion process of the Gakkel Ridge over time using 23 published multichannel seismic reflection profiles. Full seafloor spreading rates were found to be initially faster (20-24 mm/a) up to ~45 Ma, and residual bathymetry for the older crust is deeper than the world average in the entire Eurasian Basin. There is a sharp transition to 300-400 m shallower residual bathymetry for younger seafloor in the eastern Eurasian Basin. The crustal roughness versus spreading rate of the western basin is on the global trend, while that of the eastern is significantly below. Both low roughness and shallow residual bathymetry of the eastern Eurasian Basin is close to that of normal oceanic crust for spreading rates above 20 mm/a, despite the ultraslow spreading. We interpret this as increased magmatic production of the eastern Gakkel Ridge since ~45 Ma. A recent mantle tomography model shows a low-velocity S-wave anomaly underneath, predicting partial melting in the mantle. Uplift recorded by the sedimentary pattern adjacent to the Lomonosov Ridge indicate that this anomaly started to affect the area at ~45 Ma.

References (full publication list in respective section)

Abdelmalak, M. M., Gac, S., Faleide, J. I., Shephard, G. E., Tsikalas, F., Polteau, S., D., Z., and Torsvik, T., 2023, Quantification and restoration of the pre-drift extension across the NE Atlantic conjugate margins during the mid-Permian-early Cenozoic multi-rifting phases: TECTONICS, v. 42, no. 1, p. e2022TC007386.

Andersen T. B, Jakob J., Kjøll H.J. and Tegner Chr. Vestiges of the Pre-Caledonian margin of Baltica in the Scandinavian Caledonides: Overview, Revision & control on structure of the Mountain Belt. https://www.mdpi.com/2076-3263/12/2/57

Corfu F. and Andersen T.B. A hyperextension assemblage, imbricated in Archean - Paleoproterozoic crust, at the base of the Kalak Nappe Complex in the northern Scandinavian Caledonides *Jl.G.S. London*, https://doi.org/10.1144/jgs2021-140

Jakob J., Andersen T.B., Mohn G., Kjøll H-J. and Beyssac O (2022). A revised tectonostratigraphic scheme for the Scandinavian Caledonides and its implications for our understanding of the Scandian Orogeny GSA Special Paper Volume 554: New Developments in the Appalachian-Caledonian-Variscan Orogen

Jakob J., Kjøll H-J. and Andersen T.B. A (2022) Fossil Magma-rich Rifted Margin in the Scandinavian Caledonides. Chapter 8 In book (Ed. G. Peron Pinvidic) Continental Rifted Margins 2, pp. 185-202, ISBN: 9481789450620. Preprint

Marcilly, C. M., Maffre, P., Le Hir, G., Pohl, A., Fluteau, F., Goddéris, Y., ... & Torsvik, T. H. (2022). Understanding the early Paleozoic carbon cycle balance and climate change from modelling.*Earth and Planetary Science Letters*,*594*, 117717.

Osmundsen P.T., Svendby A.K., Braathen A., Bakke B.A. and Andersen T.B. (2022) Fault growth and orthogonal shortening in trans-tensional supra-detachment basins: Insight from the "Old Red" of Western Norway. In Press: Basin Research.

Shephard, G. What's lurking on top of the below. CAGE Blog (UiT). 2nd September 2022 https://cage.uit.no/2022/09/02/whats-lurking-on-top-of-the-below/

Tan P., & Breivik, A. J. (2022). *Formation of the igneous Logi Ridge, NE Atlantic.* JGR. S. Earth 127, e2021JB023891. https://doi.org/10.1029/2021JB023891

Tan, Breivik, Ding, Zhang, Niu, Li. *Magma budget of the Gakkel Ridge though time, Eurasian Basin, Arctic Ocean*. Submitted JGR

Turino V., Magni V., Jakob J., and Kjøll H.J. (in prep.). The effect of Magma Poor and Magma Rich rifted margins on Continental Collision Dynamics

View of the RV Helmer Hanssen during a teaching-research cruise to the Barents Sea with Adriano Mazzini sampling an oil slick from a zodiac. Photo by: Grace E. Shephard.

Students and lecturers from the UNIS "Arctic Tectonics and Volcanism course" sponsored by NOR-R-AM2 funds on the helicopter deck of the Polarsyssel of the Svalbard Governor. Photo by: Grace E. Shephard.

4. Earth's Crises: LIPs, mass extinctions and environmental changes

In the Earth Crises group we study volcanically driven effects on the climate system and the biosphere, focusing on large igneous provinces (LIPs). The Earth Crises mission is to investigate the role of volcanism in general, and sediment-derived gases in particular, on the history of life on Earth. Here we present a selection of the results, updates, and activities from 2022 focusing on the following highlights: 1) The relationship between Arctic volcanism and carbon cycle changes, 2) Active carbon degassing systems, 3) Volcanic degassing estimates from inclusion studies, 4) IODP Expedition 396 drilling offshore Norway, 5) Volcanic proxies in the sedimentary record, 6) metamorphism and the mercury cycle, and 7) the CLIPT Lab. In addition, we have contributed to papers on a wide range of topics such as planetary geology, iron and manganese cycling in the oceans, digital outcrops models, and the relationship between melt contamination and zircon formation in basaltic igneous rocks.

Highlights from the Earth Crises group

1. Volcanism and carbon cycle perturbations in the High Arctic during the Late Jurassic – Early Cretaceous

There were several large igneous provinces (LIPs) that punctuated the second half of the Mesozoic. The vast scale of these LIPs means that they must have significantly altered global climate and carbon cycle dynamics. Yet, due to difficulties in dating the geological record, and data gaps in some key regions (e.g. the poles), it has been difficult to understand the magnitude and duration of such effects, and to determine how much of the carbon cycle and climate changes observed were caused by the volcanism, or could have arisen due to other factors (e.g. changing paleogeography, solar cycles etc.). Therefore, Madeleine Vickers and Morgan Jones, in collaboration with scientists across both Europe and North America, undertook a detailed geochemical study of sedimentary successions from both Svalbard and Arctic Canada to examine the timing and evidence of volcanic and carbon cycle changes across the latest Jurassic and most of the Early Cretaceous (c. 150 - 115 million years ago). We find evidence that a pulse of volcanism from the High Arctic LIP could have triggered global climate changes resulting an event known as the Ocean Anoxic Event 1a (Fig. 1), which saw dramatic variations in global carbon cycling. Other key climatic perturbations, such as the Weissert Event, and regional Volgian Isotopic Carbon Excursion (VOICE) have a less clear link to LIP volcanism in our high latitude record (Fig. 1).

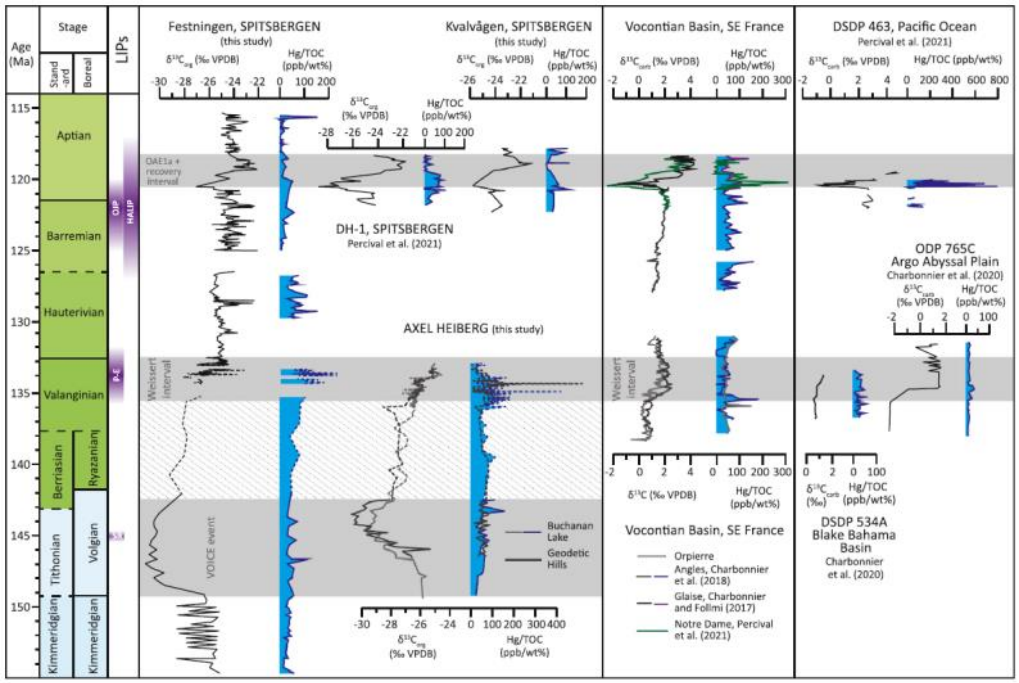

Figure 4.1. *Comparison of Upper Jurassic to Lower Cretaceous Hg/TOC records (excluding data where TOC was <0.2%) from the Boreal Realm (this study) to those from the Tethyan Realm, plotted against approximate time (See Vickers et al., 2023).*

Elevated Hg/TOC, which is a proxy for volcanic activity, is elevated during both Cretaceous carbon isotope perturbations, associated with major global climate and environmental change: namely, the Weissert Event and Ocean Anoxic Event 1a (OAE1a). Interestingly, no change in the Hg/TOC volcanic proxy was observed across the regional, Late Jurassic-aged VOICE event, suggesting that whilst the two global carbon cycle perturbations are linked to major volcanic activity, this smaller scale event was not.

2. Active Earth degassing systems

In the framework of the ERC-LUSI LAB project (PI Adriano Mazzini) we continued our studies on the Indonesian Lusi eruption and fluid migration in Java Island. A new study compared seismic reflection data from ancient (offshore mid-Norway) and the modern Porong and Lusi hydrothermal venting systems investigating geometries and development mechanisms during and after the eruption phases (Fig. 2). Modern hydrothermal venting systems, like the Lusi eruption, are therefore relevant analogues to understand ancient systems (Manton et al., 2022). We also expanded our research on a regional scale, conducting active tomography studies and showing that low angle faults, promoted by the compressional regime in the region, are used by magma and hydrothermal fluids for northward migration (Lupi et al., 2022). This model links the magmatic domain to the northern sedimentary provinces explaining the presence of enigmatic and isolated igneous and hybrid systems piercing the basin tens of kilometers away from the main volcanic arcs (Fig. 2). One example is the Kalang Anyar mud volcano (originally active offshore) currently seeping fluids with deep-sourced mantle-derived component (Mazzini et al., 2023).

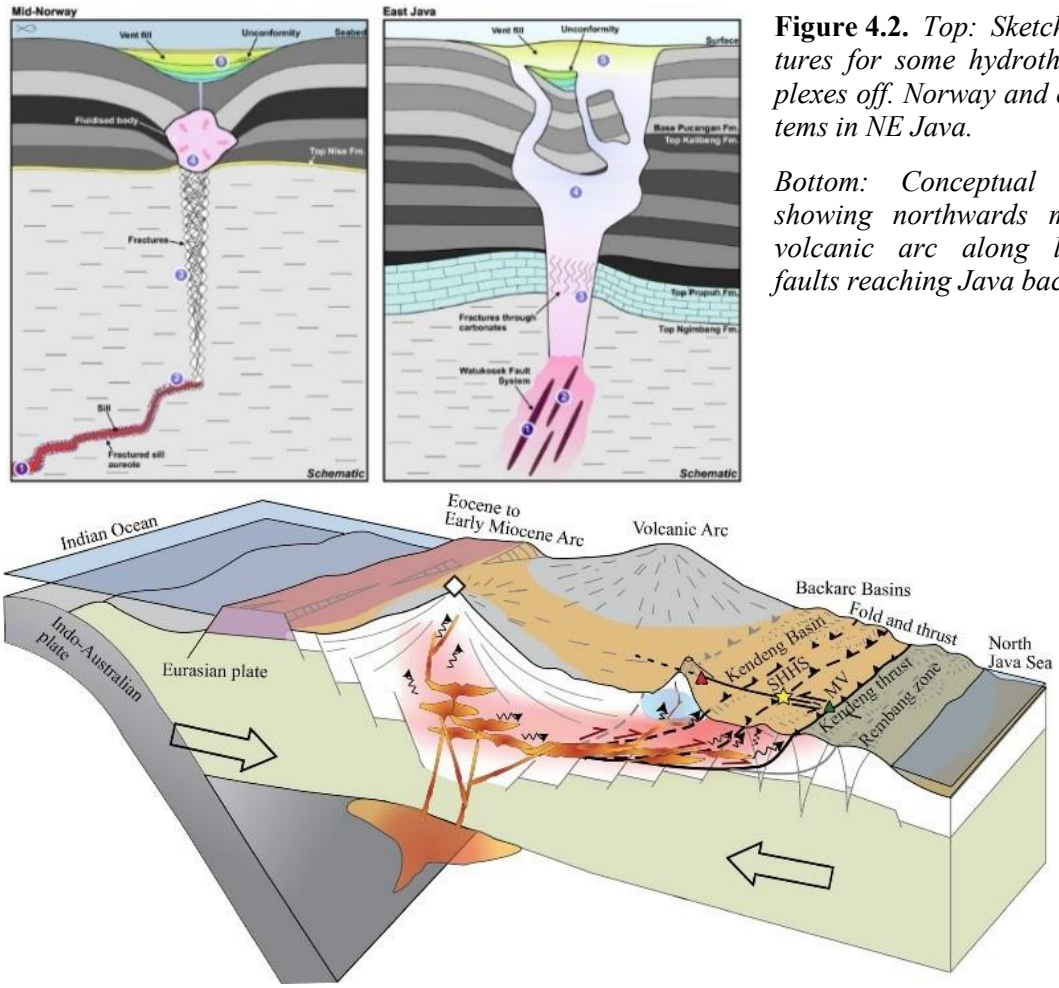

Figure 4.2. *Top: Sketches with key features for some hydrothermal vent complexes off. Norway and eruptive vent systems in NE Java.*

Bottom: Conceptual tectonic model showing northwards migration of the volcanic arc along low-angle thrust faults reaching Java back-arc basin.

HOTMUD project (PI A. Mazzini) field activities continue. In Lake Baikal we conducted an active seismic survey through numerous mud volcanoes and produced a large geochemical gas database from many degassing sites scattered in the lake. During the 2022 Azerbaijan Summer School, attended by nearly 50 international participants, we investigated the creeping mechanisms along mud breccia flows. CEED student Aliénor Labes successfully defended her MSc thesis studying a multidisciplinary database collected from several Azerbaijani mud volcanoes. During the CAGE22-6/Training Through Research-22 expedition we surveyed the Norwegian Barents Sea investigating oil slick emission spots and extensive gas leakage from the seafloor associated to eroded structures within glacimarine landforms and depositional systems. We identified areas of focused fluid discharge within Sentralbanken High (Hopendjupet), Storbanken High, and Kong Karls Platform (Serov et al., 2022). We also used new geophysical data from eastern Storbanken (central Barents Sea) to reconstruct the flow of marine-based ice dome during the final stages of ice-sheet decay (Montelli et al., 2023). New tomography data from the Dead Sea Fault region propose that protracted extensional motion caused crustal thinning and the emplacement of magmatic bodies in the crust (Haddad et al., 2023). SENECA project activities in Antarctica continue and for the first time we report evidence of carbon emissions from the currently thawing permafrost in the dry Valleys region (Ruggiero et al., 2023).

3. Volatile investigation via melt and fluid inclusions in natural and experimental samples

Melt and fluid inclusions offer an extraordinary opportunity to reconstruct the volatile budget evolution in magmas. After defending his PhD thesis about the carbon cycle in the end-Triassic Central Atlantic Magmatic Province (CAMP), Manfredo Capriolo joined CEED in 2021 with MAPLES (MAgma PLays with sEdimentary rockS) project, led by Sara Callegaro. The investigation of inclusions in effusive and intrusive rock samples from the CAMP allowed to reconstruct the volcanic and thermogenic emissions of this LIP, and to assess their impact on the end-Triassic crisis. Starting from the volcanic CO_2 emissions constrained by melt inclusions within CAMP lava flows, we modelled carbon cycle perturbations linked to the main volcanic phase of the CAMP using the CARMER biogeochemical box model. We demonstrated that rapid and pulsed degassing of exclusively volcanic CO_2 from the CAMP, on a similar scale to current anthropogenic emissions, severely affected the end-Triassic climate and environment at a global scale (Capriolo et al., 2022).

Expanding the study of inclusions to other LIPs, Manfredo Capriolo and Sara Callegaro worked with external collaborators on the reconstruction of the magma plumbing system of LIPs with the case studies of CAMP and Deccan Traps, combining Synchrotron Light X-ray microtomography, confocal Raman microspectroscopy, SIMS and EMP analyses (Fig.3). This is the first time that LIPs melt inclusions are targeted by Synchrotron Light X-ray microtomography. The manuscript is in preparation and will be submitted soon. Moreover, we started working on the degassing history of the Siberian Traps and on the magma–sediment interaction in specific areas of the Oslo Rift (e.g., Bile Island).

Within the framework of magma-sediment interaction studies, Callegaro, Capriolo and Svensen also participated to an experimental petrology study aimed at characterizing the process of shale assimilation in basaltic rocks (HALIP case study; Deegan et al., 2022). A follow-up study in progress uses a similar approach for investigating basalt-carbonate interaction.

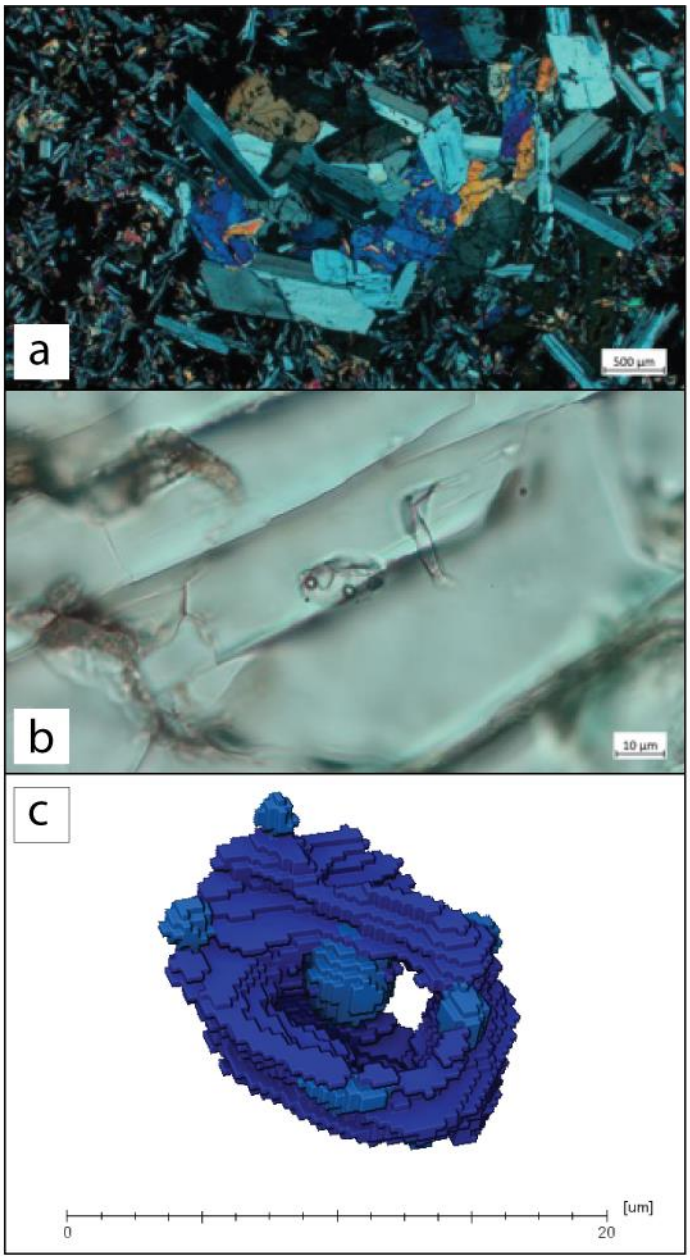

Figure 4.3. *Getting closer and closer. a) CAMP sample NS12 (Nova Scotia, Canada) is scouted for melt inclusions in crystal clots by optical microscopy (2.5×, crossed polarized light); b) a multi-bubble melt inclusion is targeted for Raman spectroscopy and in-situ geochemical investigations (100×, parallel polarized light); c) the multi-bubble melt inclusion is targeted by Synchrotron Light X-ray microtopography that allows its 3D reconstruction and calculation of the bubble/inclusion ratio. Note the scale difference between panels.*

4. Successful IODP drilling on the Møre and Vøring margins

LIPs often coincide with environmental crises such as global warming and mass extinctions, which has led to the hypothesis that LIPs are the cause of these disturbances. However, this relationship is hampered by a shortage of sedimentary sequences proximal to LIPs that preserve numerous volcanic and climatic proxies. The North Atlantic Igneous Province (NAIP) is an ideal case study as it was one of the largest LIPs in the Cenozoic, and numerous exposures around the Northeast Atlantic preserve igneous and sedimentary sequences across the Paleocene Eocene Thermal Maximum (PETM). Collecting high resolution core across this interval

will be able to constrain NAIP activity in both a geochronological and paleoclimate timeframe.

Figure 4.4. *M.L. Vickers, H. Svensen and S. Planke sampling the IODP Exp 396 cores in Bremen, Germany, April 2022.*

The EC team have led two international drilling applications to collect high quality cores of volcanic rocks and sediments across the PETM interval. The highly successful International Ocean Discovery Program (IODP) Expedition 396 recovered more than 2 km of cores from 20 boreholes in the Norwegian Sea in August-October 2021. Sverre Planke (co-chief) and Morgan Jones (geochemist) were shipboard scientists, while Henrik Svensen, Ella Stokke, and Madeleine Vickers provided shore-based support (Fig. 4; Planke et al., 2021; 2022).

A total of 21 boreholes were drilled at 10 sites in five different geological settings on the Vøring and Møre volcanic margin offshore mid-Norway to study the opening of the Northeast Atlantic Ocean c. 56 million years ago. The boreholes sampled a multitude of igneous and sedimentary settings ranging from lava flow fields to hydrothermal vent complexes, along with thick successions of upper Paleocene and lower Eocene strata. A comprehensive suite of wireline logs was collected in eight boreholes. The main goals of the expedition were to provide constraints for geodynamic models to test different hypotheses that can explain the rapid emplacement of Large igneous provinces (LIPs) and the hypothesis that the associated Paleocene-Eocene Thermal Maximum (PETM) was caused by hydrothermal release of carbon in response to magmatic intrusions. Successful drilling, combined with high core recovery of target intervals, should allow us to achieve these goals during post cruise work (Planke et al.,

2022). We subsequently acquired high-resolution seismic reflection data across four of the Vøring Margin in 2022 (Bünz et al., 2022).

5. Volcanic proxies in the sedimentary record

There is often a temporal correlation between the emplacement of LIPs and climatic disturbances in the geological record, suggesting a possible causal relationship. One such example is the peak activity of the North Atlantic Igneous Province (NAIP) coinciding with the Paleocene –Eocene Thermal Maximum (PETM) around 56 million years ago. However, corroborating a causal relationship is hampered by a scarcity of expanded sedimentary records that contain both climatic and volcanic proxies. One locality hosting such a record is Fur Island in Denmark, where an expanded pre- to post-PETM succession containing hundreds of NAIP ash layers is exceptionally well preserved. Morgan Jones, along with Ella Stokke, Madeleine Vickers, Henrik Svensen, and Sverre Planke, worked on the capstone paper to the Ashlantic young research talent project. We compiled a range of environmental proxies, including mercury (Hg) anomalies, paleotemperature proxies, and lithium (Li) and osmium (Os) isotopes, to trace NAIP activity, hydrological changes, weathering, and seawater connectivity across this interval.

Volcanic proxies suggest that NAIP activity was elevated before the PETM and appears to have peaked during the body of the $\delta^{13}C$ excursion, but decreased considerably during the PETM recovery. This suggests that the acme in NAIP activity, dominated by flood basalt volcanism and thermogenic degassing from contact metamorphism, was likely confined to just ~200 kyr (ca. 56.0–55.8 Ma; Fig. 4). The hundreds of thick basaltic ashes in the post-PETM strata likely represent a change from effusive to explosive activity, rather than an increase in NAIP activity. Detrital $\delta^{7}Li$ values and clay abundances suggest that volcanic ash production increased basaltic reactive surface area, likely enhancing silicate weathering and atmospheric carbon sequestration in the early Eocene. Signals in lipid biomarkers and Os isotopes, traditionally used to trace paleotemperature and weathering changes, were used to track seaway connectivity. These proxies indicate that the North Sea was rapidly cut off from the North Atlantic in under 12 kyr during the PETM recovery due to NAIP thermal uplift. Our findings reinforce the hypothesis that the emplacement of the NAIP had a profound and complex impact on Paleocene–Eocene climate, both directly through volcanic and thermogenic degassing, and indirectly by driving regional uplift and changing seaway connectivity. These results are submitted to the open access journal *Climate of the Past* and are available in preprint form on *EGUsphere* (Jones et al., 2023).

.

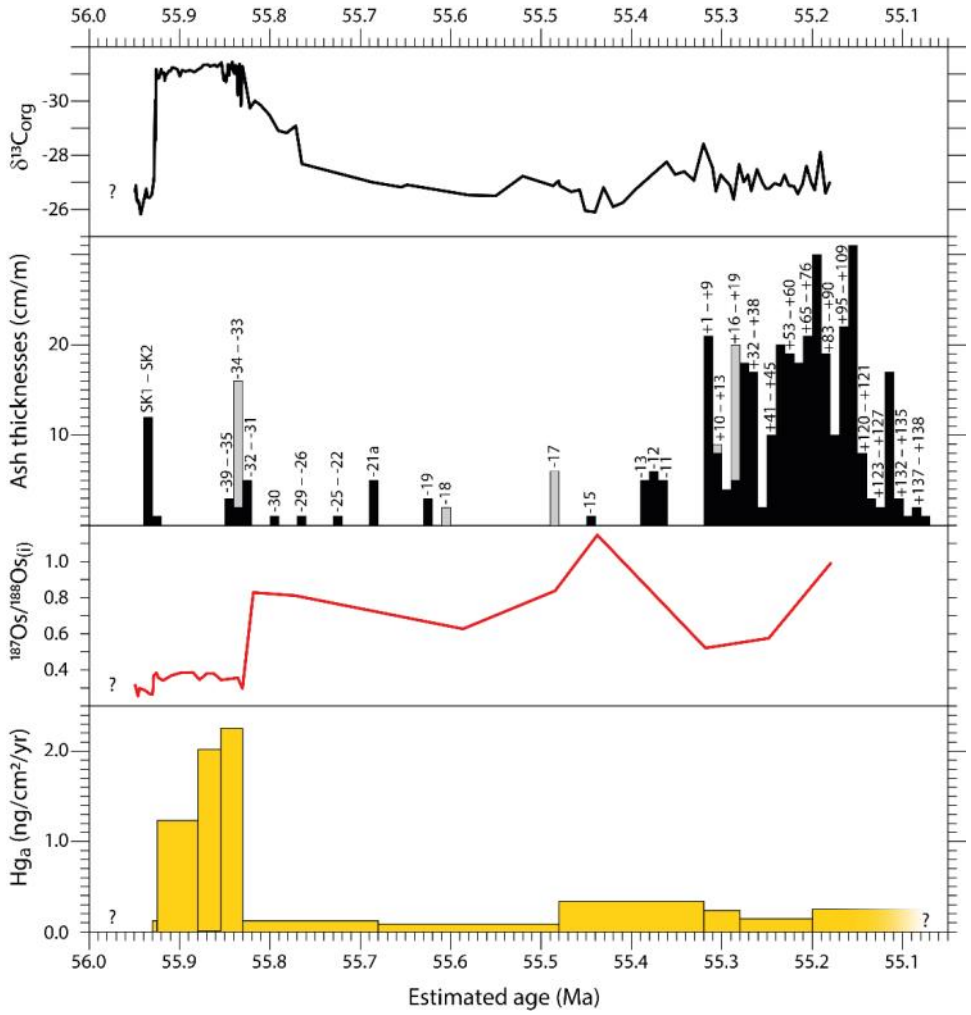

Figure 4.5. *Volcanic proxies through Paleogene sediments in Fur, Denmark, normalized to their estimated depositional age based on a new age model (after Jones et al., 2023). Ash thicknesses as shown as a total percentage of ash per meter of sediment. Black bars denote basaltic ashes and the grey bars denote felsic ashes.* $^{187}Os/^{188}Os$ *isotopes are normalized to initial values* (Os_i) *at 56 Ma. Estimated Hg accumulation rates* (Hg_a) *are subdivided into specific intervals, and show pronounced Hg deposition during the body of the PETM.*

Masters student Karlo Lisica completed his Masters project on the geochemistry and geochronology of Lundy Island in the British Isles, a potential source volcano for some of the ash layers preserved in Denmark. His results showed a close temporal and chemical overlap between Lundy intrusive rocks and ash layer -33 in Denmark. Together with Morgan Jones, Lars Augland, Dougal Jerram, and co-authors, this work has now been converted into a manuscript and is currently in review in the diamond open access journal *Volcanica*.

6. Contact metamorphism of shale and the release of mercury

Elevated mercury (Hg) in sedimentary strata are a widely used tracer for assessing the relationships between LIP activity and global environmental change. A key unknown is the extent to which Hg was sourced from magma versus contact metamorphic sedimentary rocks. We have investigated Hg behavior during contact metamorphism of shales by using examples from several LIPs (Karoo LIP, the High Arctic LIP, and the Skagerak-centred LIP) (Svensen et al., 2023). We show loss of 80–99% of the sedimentary Hg in contact aureoles in four case studies. A combination of geochemical data and thermal modelling around a dyke from the High Arctic LIP shows 33% Hg volatilization in the aureole at 265-300 °C (Figure 5). We hy-

pothesize that gaseous Hg is transported out of aureoles during metamorphism, together with CH_4 and CO_2. The mass of Hg mobilized around a large sill (0.3-1.2 Mt Hg when scaled to an aureole volume of 2000 km3) may be more than present day annual volcanic emissions. Given the efficiency of Hg volatilization, the ultimate net Hg/CO_2 ratio should be similar to the ratio between the initial concentrations in the sedimentary rocks, on the order of 6 to 10. Our results strengthen the validity of using Hg as a proxy for LIP activity, but emphasize that significant Hg can be sourced from devolatilization of organic-bound reservoirs in sedimentary basins.

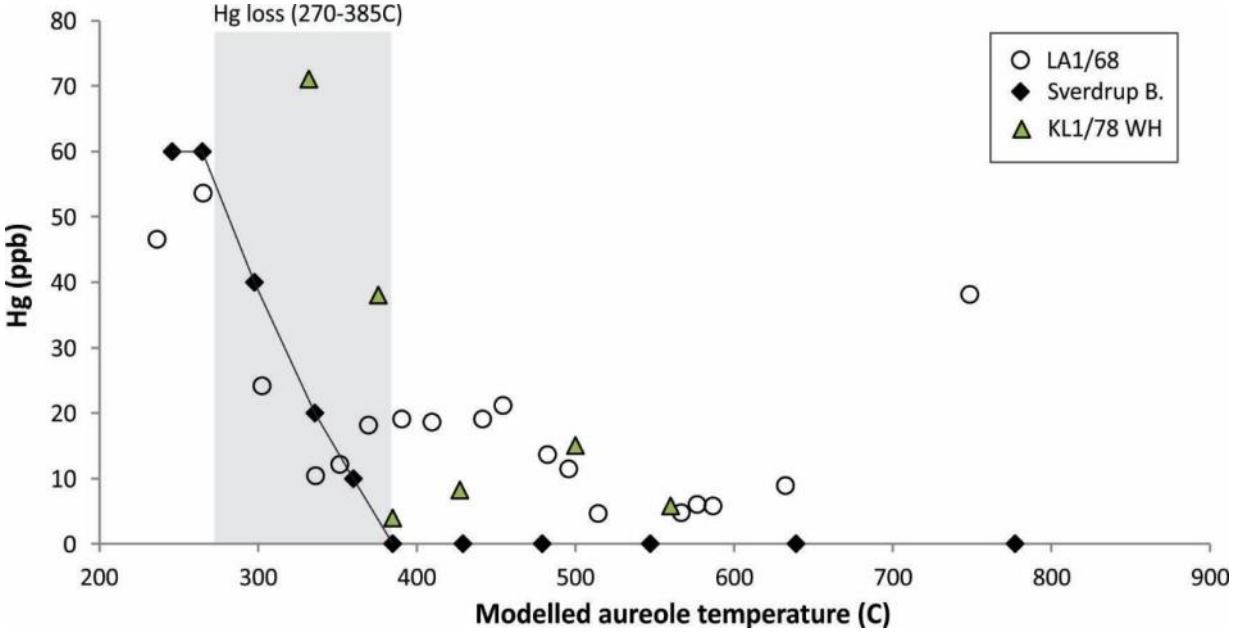

Figure 4.6. *Data and model results from contact aureoles in the Karoo Basin (South Africa) and the Sverdrup Basin (Canada). The mercury content in the aureole plotted against modelled temperature of the aureole, and shows that the Hg is lost during heating. The grey box shows the temperature interval where the Hg rapidly declines from background values. From Svensen et al. (2023).*

7. Farewell to the CLIPT lab!

The end of CEED also means the end of the CLIPT lab, which has provided stable isotope analyses for more than 20 users in CEED and elsewhere within UiO. During its time within CEED (2016-2023), CLIPT lab authors produced 18 peer-reviewed papers, and contributed isotope measurements to many more. With the closing, we say a special goodbye to Bill Hagopian, who is leaving UiO for new adventures. We are grateful for our time serving the UiO community, and proud to have been a valuable member of the CEED endeavor.

References (CEED-affiliated in bold)

Bünz, S., **Planke, S.,** Singhroha, S., Lebedeva-Ivanova, N., Binde, C.M., Akinselure, A.A., Nagpal, U., Wear, J., Holm, T. and Jensen, S.A., 2022. CAGE22-5 Cruise Report: High-resolution 2D and 3D seismic investi gations on the Vøring Margin. CAGE–Centre for Arctic Gas Hydrate, En vironment and Climate Report Series, 10.

Capriolo, M., Mills, B. J. W., Newton, R. J., Dal Corso, J., Dunhill, A. M., Wignall, P.B., and Marzoli, A. (2022). Anthropogenic-scale CO_2 degassing from the Central Atlantic Magmatic Province as a driver of the end-Triassic mass extinction. Global and Planetary Change, 209, 103731, https:// doi.org/10.1016/j.gloplacha.2021.103731.

Deegan, F. M., Bédard, J. H., Grasby, S. E., Dewing, K., Geiger, H., Misiti, V., **Capriolo, M.**, **Callegaro, S.**, **Svensen, H. H.**, Yakymchuk, C., Aradi, L. E., Freda, C., and Troll, V. R. (2022). Magma–Shale Interaction in Large Igneous Provinces: Implications for Climate Warming and Sulfide Genesis. Journal of Petrology, 63, 9, egac094, https:// doi.org/10.1093/petrology/egac094.

Jones M.T., Stokke E.W., Rooney A.D., Frieling J., Pogge von Strandmann P.A.E., Wil son D.J., **Svensen H.H., Planke S.**, Adatte T., Thibault N., **Vickers M.L.**, Mather T.A., Tegner C., Zuchuat V., Schultz B.P. (2023). Tracing North Atlantic volcanism and seaway connectivity across the Paleocene–Eocene Thermal Maximum (PETM). EGUsphere 2023, 1-53. https://doi.org/10.5194/egusphere-2023-36

Lupi, M., De Gori, P., Valoroso, L., Baccheschi, P., Minetto, R., and **Mazzini, A.**, 2022, Northward migration of the Javanese volcanic arc along thrust faults: Earth and Planetary Science Letters, v. 577, p. 117258.

Haddad, A., Chiarabba, C., Lazar, M., **Mazzini, A.**, Polonia, A., Gasperini, L., Lupi, M., 2023. Rifting-Driven Magmatism Along the Dead Sea Conti nental Transform Fault. GRL 50, e2022GL099964.

Manton, B., Müller, P., **Mazzini, A.**, Zastrozhnov, D., **Jerram, D. A.**, Millett, J. M., Schmid, D. W., Berndt, C., Myklebust, R., and **Planke, S.**, 2022, Char acterizing ancient and modern hydrothermal venting systems: Marine Geology, v. 447, p. 106781.

Mazzini, A., Sciarra, A., Lupi, M., Ascough, P., Akhmanov, G., Karyono, K., Husein, A., 2023. Deep Fluids Migration and Submarine Emersion of the Kalang Anyar Mud Volcano (Java, Indonesia): A Multidisciplinary Study. Marine and Petroleum Ge ology 148, 105970.

Montelli, A., Solovyeva, M., Akhmanov, G., **Mazzini, A.**, Piatilova, A., Bakay, E., Dowdeswell, J.A., 2023. The geomorphic record of marine-based ice dome de cay: Final collapse of the Barents Sea ice sheet. Quaternary Science Reviews 303, 107973.

Planke, S., Berndt, C. and Alvarez Zarikian, C.A., 2021. Expedition 396 Scien tific Pro spectus: Mid-Norwegian Continental Margin Magmatism. Sci entific prospectus, 396.

Planke, S., Berndt, C., Alvarez Zarikian, C.A., and the Expedition 396 Scien tists, 2022. Expedition 396 Preliminary Report: Mid-Norwegian Conti nental Margin Magmatism and Paleoclimate Implications. Internation al Ocean Discovery Program. https:// doi.org/10.14379/ iodp.pr.396.2022

Ruggiero, L., Sciarra, A., **Mazzini, A**., Florindo, F., Wilson, G., Tartarello, M.C., Mazzoli, C., Anderson, J.T.H., Romano, V., Worthington, R., Bigi, S., Sassi, R., Ciotoli, G., 2023. Antarctic Permafrost Degassing in Taylor Valley by Extensive Soil Gas Investi gation. Science of The Total Environment 866, 161345.

Serov, P., Patton, H., **Mazzini, A**., Mattingsdal, R., Shephard, G., Cooke, F.A., ..CAGE22-6 / TTR-22 cruise report: GEO-3144/8144 Teaching Cruise: Geologically con trolled hydrocarbon seepage in Hopendjupet and the wider Barents Sea. CAGE–Centre for Arctic Gas Hydrate, Environment and Climate Report Series 10

Svensen, H.H., Jones, M.T., Percival, L.M.E., Grasby, S., Mather, T. (2023) Re lease of mercury during contact metamorphism of shale. In review.

Vickers, M.L., Jelby, M.E., Śliwińska, K.K., Percival, L.M., Wang, F., Sanei, H., Price, G.D., Ullmann, C.V., Grasby, S.E., Reinhardt, L., Mather, T.A., Friel ing, J., Korte, C., Jerrett, R.M., **Jones, M.T.,** Midtkandal, I., and Galloway, J.M. 2023. Volcan ism and carbon cycle perturbations in the High Arctic during the Late Ju rassic– Early Cretaceous. Palaeogeography, Palaeocli matology, Palaeoecology, 613, p.111412.

Svalbard fieldtrip to look for a new drill site, organised by Sverre Planke, March 22. Photo by: Madeleine Vickers.

5. Earth and Beyond: Comparative Planetology

For ten years we had the mission to understand the similarities and differences between Earth and other terrestrial planets with the hypothesis that we can understand the dynamics of Earth and other planets within the same framework, but different parameters.
During these ten years the discovery of explosive numbers of new exoplanets suggested now that things are not necessarily that easy. Physics is the same, but do we understand the chemistry and material properties well enough to actually define the key parameters properly? Our view on determining the style of mantle convection, surface tectonics and volcanism in the system, may be valid for solar system planets, but appear naïve with respect to the multiple possibilities that exoplanets provide.
Nevertheless, without knowing the composition as well as the times and rates, deciphering planetary processes will be difficult. Comparative planetology remains one of the essentials not to get lost in detail and continue keep an eye on the entire system.

The work reported for 2022 comprise a wide range of activities from analysing the populations of discovered small exoplanets, modelling the formation of exoplanetary systems around K dwarf stars for building Earth-like exoplanets using GPU simulations, describing plans for assessing the potential interior structure of exoplanets, studying pathway of Venus‘ evolution through time in which Venus‘ lithosphere can for example be more mobile (like Earth) to begin with and end stagnant (like Mars), but is now in a transitional state. More ‘closely’, we examined the geology of the ExoMars landing site with the help of analogue materials collected for the Planetary Terrestrial Analogues Library. Some of these samples now became Mission Reference Samples. Similarly, remote sensing of Mars and comparison to martian meteorites show that the alteration minerals in nakhlite meteorites and those observed widespread on Mars change the estimates for the volume of magmatic volatiles and martian habitability. Studies of meteorites link extra-terrestrial materials that reached Earth compositionally and dynamically to objects in the solar system, like in the case meteorite Antonin recovered after bolide detection, such as the asteroidal source regions of ordinary chondrites. Boulders that do not fly that far after impact crater formation, rock fragments ejected from the crater cavity could be deposited elsewhere on the surface. Using high-resolution imaging and deep learning allows detecting these boulders and provide important insight into the ejection mechanisms. Last but not least, crater statistics, remote-sensing analysis of the moon and lunar returned samples reveal in combination the revised version of the cratering chronology model that makes the solar system planets’ surfaces older.

Geology of ExoMars Landing Site—Mission Reference Samples from the PTAL collection

The PTAL is the first natural rock (analogue) spectral library that supports geological interpretation of data obtained via remote sensing. It was built with a particular emphasis to include best possible analogues for current and future in-situ martian missions and the main goals of PTAL has been to support the ExoMars mission - the European Space Agency rover that will land at Oxia Planum. The main scientific objectives of the mission are to understand the mineralogy and aqueous evolution of ancient Mars with relevance to habitability.

Oxia Planum is a Noachian plain covered with vast deposits of Fe,Mg- phyllosilicates. In previous years we identified two analogue lithologies, both dominated by trioctahedral Fe,Mg-vermiculite, that showed best spectral analogy to Oxia deposits: Granby Tuff and Otago schists (Krzesinska et al. 2021). Both analogues were suggested to the ExoMars science team

to become Mission Reference Samples. Both were selected for the activity and have been serving various purposes of preparation and training to eventually enhance scientific return of the mission.

We performed detailed in-situ, micron-scale analysis on the Granby Tuff by the ExoMars flight spare instruments: MicrOmega (NIR), RLS (Raman) and completed by sub-micron EDX characterization (Bultel et al. 2022).

Our results allow to address spectral heterogeneity of vermiculite-rich material and to understand exact mineralogy behind specific spectral manifestations. For instance, depth of NIR bands can be linked to illitization of vermiculite and enhanced flatness of spectra to presence of oxidized material, such as Mn- or Fe-oxides (Krzesinska et al. 2022a).

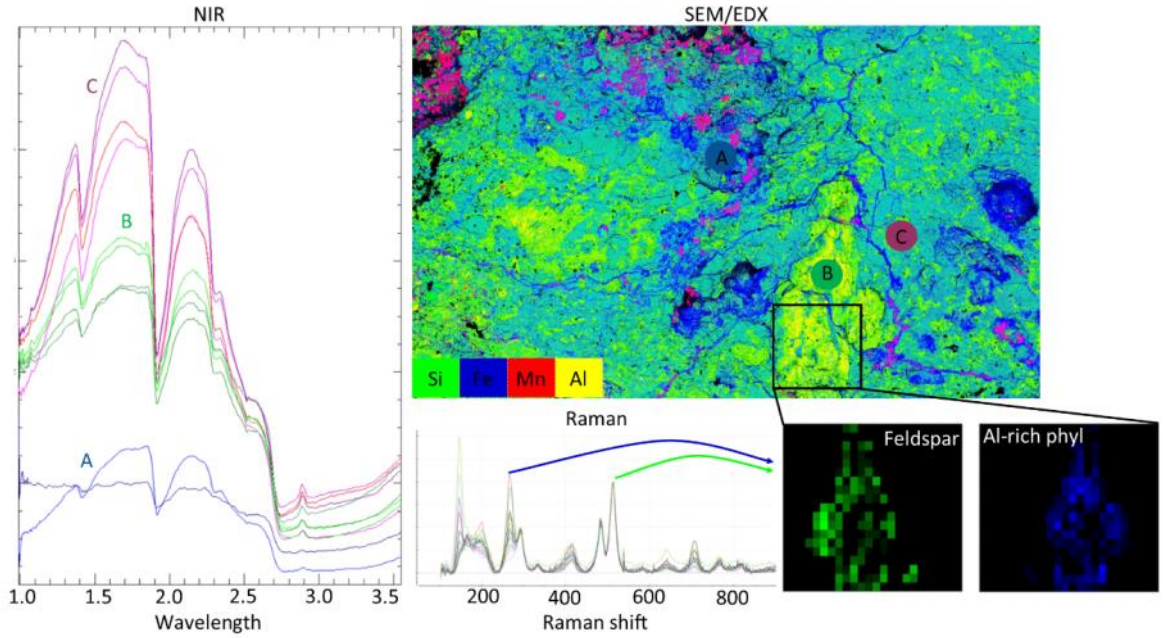

Fig. 5.1. *Multi-technique (NIR, Raman and SEM-EDX) characterisation of Granby Tuff analogue from PTAL collection, for purposes of ExoMars instrument testing and preparing for scientific retrieval about geology of the landing site.*

Alteration minerals in nakhlite martian meteorites - Implications for magmatic volatiles and habitability

Nakhlites are a suite of 20 martian meteorites that crystallized as comagmatic rocks at ~1.3 Ga. and contain relatively abundant (>1 vol%) aqueous alteration minerals: phyllosilicates, carbonates, sulphates and halides. Due to potential implications for martian habitability, it is of high importance to understand source of fluid and mechanisms that led to formation of the alteration minerals in nakhlites.

We analysed the trace elemental compositions of the alteration products in two nakhlites: Nakhla and Lafayette. In Nakhla, Fe,Mg-phyllosilicates and Fe,Mg-carbonates dominate the alteration products. Mn-rich carbonates are present close to edges of olivine grains, at contacts with augite or mesostasis. We observe significant differences in trace elemental compositions of the two groupings of carbonates. Fe,Mg-carbonates do not host any of important trace elements, while Mn-carbonates reveal the presence of Ca, Cu, Zn, Ni, minor La and Ce. Addi-

tionally, clear signals from Cl and Br are detected in association with Mn-rich carbonates. In Lafayette, alteration minerals predominantly occur in olivine and are represented by Fe,Mg-phyllosilicates and carbonates.

Trace elemental composition of alteration minerals in Nakhla and Lafayette reveal a complex aqueous system in the martian subsurface. Distribution of Cl and Br between various alteration minerals and differences in trace elemental composition of two generations of carbonates in Nakhla require further discussion. These features may suggest that: (i) alteration may have occurred in a low fluid:rock environment, where dissolution plays a significant role and the trace elemental budget is strongly influenced by locally dissolved phases, (ii) more than one episode of fluid activity altered the nakhlites in the subsurface, and specifically, Fe,Mg-carbonates formed separately from Mn-rich carbonates in Nakhla, (iii) the altering brine was originally rich in Cl, which affected fractionation of trace elements during fluid percolation and evolution. The Cl content of the fluid may point towards at least some of alteration products in nakhlites forming during the late magmatic stage of evolution, when Cl-rich fluid infiltrated the nakhlite magma chamber (Krzesinska et al., 2022b).

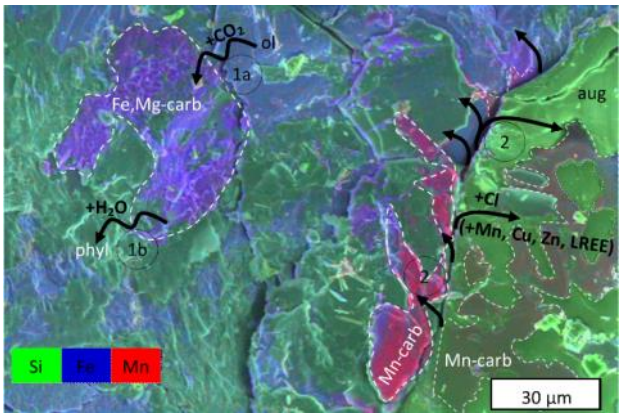

Fig. 5.2. *SEM-EDX image of alteration minerals in Nakhla and proposed scheme of fluid flow to form them, accounting for observed textures and geochemical features.*

Asteroidal source regions of ordinary chondrites – Study of meteorite Antonin recovered after bolide detection

Meteorites that were observed during their passage through atmosphere (fireball) are of particular importance for creating new frontiers in planetary science. This is because pre-atmospheric orbit of the objects can be reconstructed from the fireball trajectory and combined with the laboratory study of the recovered rock. Until now, only ~50 meteorites have been recovered, for which fireball recording exist. Antonin (fall in Poland on 15 July 2021) is one of such rare meteorites.

Antonin was classified by us as L5 chondrite. L chondrites are one of the most common meteorite types that are delivered to Earth, but their source bodies in asteroid belt are not known. The pre-atmospheric, heliocentric orbit of Antonin was reconstructed to show that the meteoroid represented Near Earth Objects (Shrbeny et al., 2022). Probably the meteoroid had long orbit evolution, which must be reflected in collisional history recorded in the rock. We have studied the shock and thermal reprocessing in Antonin to address this question (Shrbeny et al., 2022).

The meteorite must have experienced at least two collisions, one of which had probably place in early time of parent body evolution, when thermal annealing and fluid circulation was pos-

sible after the impact deformation. Products of the annealing are assemblages of troilite and mackinawite and recorders of fluid flow are exceptionally large phosphates. Pb-Pb dating of phosphates is ongoing with an aim to retrieve information on the timing of the event. Second collision was most likely a mild event, resulting in a minor brittle deformation of the rock only. Dating of the gas retention age has been arranged to provide information on time of this collision. The full set of data on collisional history of Antonin has potential to support our understanding of evolution of the parent asteroid, which combined with orbital data on meteoroid can shed new light on plausible source bodies of L chondrites.

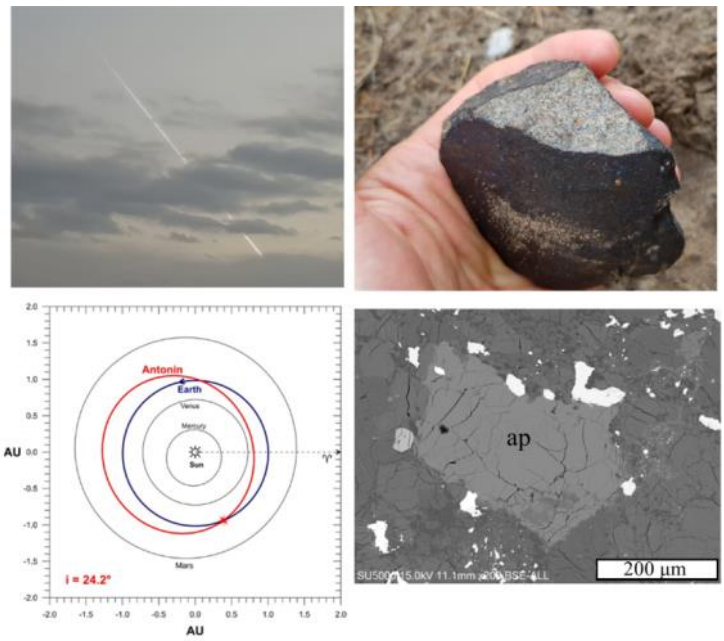

Fig. 5.3. *Top: Observation of fireball related to fall near Antonin, Poland and the recovered meteorite. Bottom: Reconstructed heliocentric orbit of the meteoroid (Shrbeny et al., 2022) and BSE image of phosphate grain (apatite, ap) used to address the collisional evolution of the meteorite parent body*

BOULDERING – Other rock fragments tell about cratering

Craters are very common surface features on many solid planets and moons. During an impact, rock fragments ejected from the crater cavity could be deposited elsewhere on the surface, where they could potentially form secondary craters. Boulders are the only remnants of these ejected materials. Their size and shape, as well as the terrain on which they are found, provide important insight into the ejection mechanisms. BOULDERING project plans to use high-resolution imaging and deep learning to further investigate the size and shape distributions of boulder populations. Project results could boost our understanding of planetary surface evolution.

Achieving the project objectives depend on an algorithm that can automatically detect boulders on planetary surfaces. Therefore, for a large portion of the year (it is a very time-consuming task), was used to manually digitized boulder populations around impact craters on the surfaces of Mars and the Moon. The current outcome comprises large mapping effort of boulder populations around impact craters on Mars and the Moon (approximately 100,000 boulders were mapped), fieldwork at two locations with abundant boulders (rocks) in the Sierra Nevada, California (including manual measurements and drone imagery), and digitizing of boulder populations at the two terrestrial locations (Prieur et al. 2022 a,b).

This provided the required inputs for the algorithm's training. After weeks of work in October/ November 2022 in the training and tuning of model parameters, now a trained algorithm with more than 70% precision exists and recall values in the detection of boulders (see Fig. 1). This is the most crucial milestone in the BOULDERING project. Future work includes improving the performances of the model further and construct a database of boulder populations around multiple impact craters. The database will provide the basis of the data to understand better how factors such as terrain properties influence the ejection mechanisms.

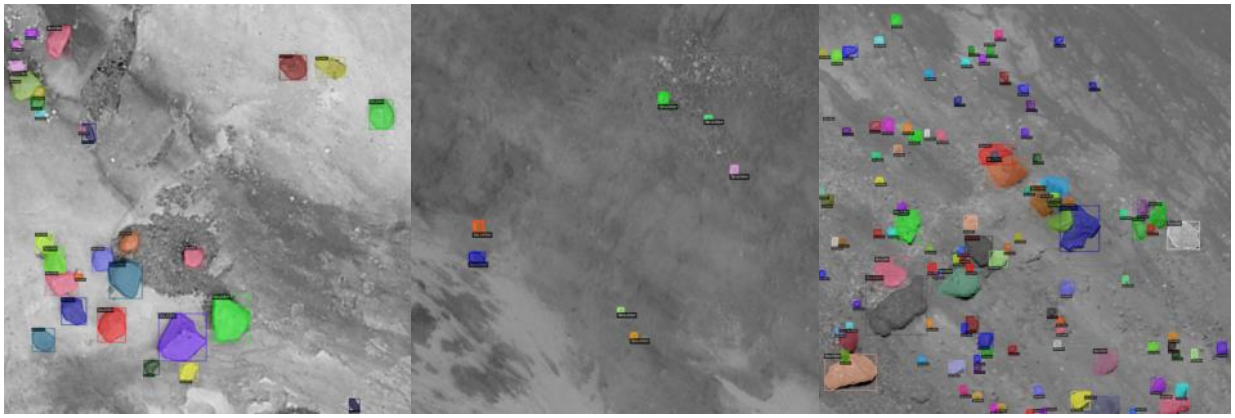

Fig 5.4. *Example of boulder predictions with the newly trained algorithm at a terrestrial location in California (left), and on the surface of the Moon (middle & right).*

Interior dynamics – Venus, Earth, Europa

The research activities during 2022 were mostly part of the *PLATONICS* project (NFR Young Research Talents). After implementation of composite rheology in our models of mantle convection, we specifically addressed the role of dynamic grain-size evolution. We focused on how grain size evolution affects the global tectonic regime of a planet and found that enhanced grain size reduction can reduce the degree of episodicity and favor more continuous lithospheric mobility, such as proposed for the recent Earth's history. To investigate the role of grain size evolution in the divergence of Earth's and Venus' tectonic regime, we further adjusted our numerical setup to account for Venus' conditions, that is higher surface temperature. For yield strengths that yield Earth-like behavior at low surface temperatures, an increase in surface temperature does not lead to an episodic regime, but rather to a regime with sluggish drips and relatively poor localization of deformation. Thus, Venus is either not in an episodic regime or a different cause than surface temperature must be put forward for explaining the tectonic divergence of Earth and Venus.

Further work on Venus involved a comprehensive review on Venus' mantle evolution and dynamics (Rolf et al. 2022), which sets the framework to be fed by future data. This work also defined a number of science questions related to Venus' deep interior that may be resolved with future data from the upcoming missions to this planet. We have started to investigate one of these aspects, the largely uncertain core size and its role in shaping the evolution of the mantle. Preliminarily, substantial changes in core radius alter the history of cooling and volcanism and can in cases lead to different tectonic regimes at present-day.

To transfer our framework to icy satellites, we updated our model with additional deformation mechanisms that are thought to be relevant within planetary ice shells (basal slip, grain boundary sliding). Applying this framework to Europa shows that deformation is indeed dominated

by these two mechanisms. This predicts an immobile layer at the top of Europa's convecting ice shell whose thickness is governed by grain size and the degree of tidal heating. An immobile layer is at odds with Europa's presumably young surface. In our models, surface mobilization can only be achieved by additional plastic deformation, with strong impact on the thermal structure of the entire ice shell.

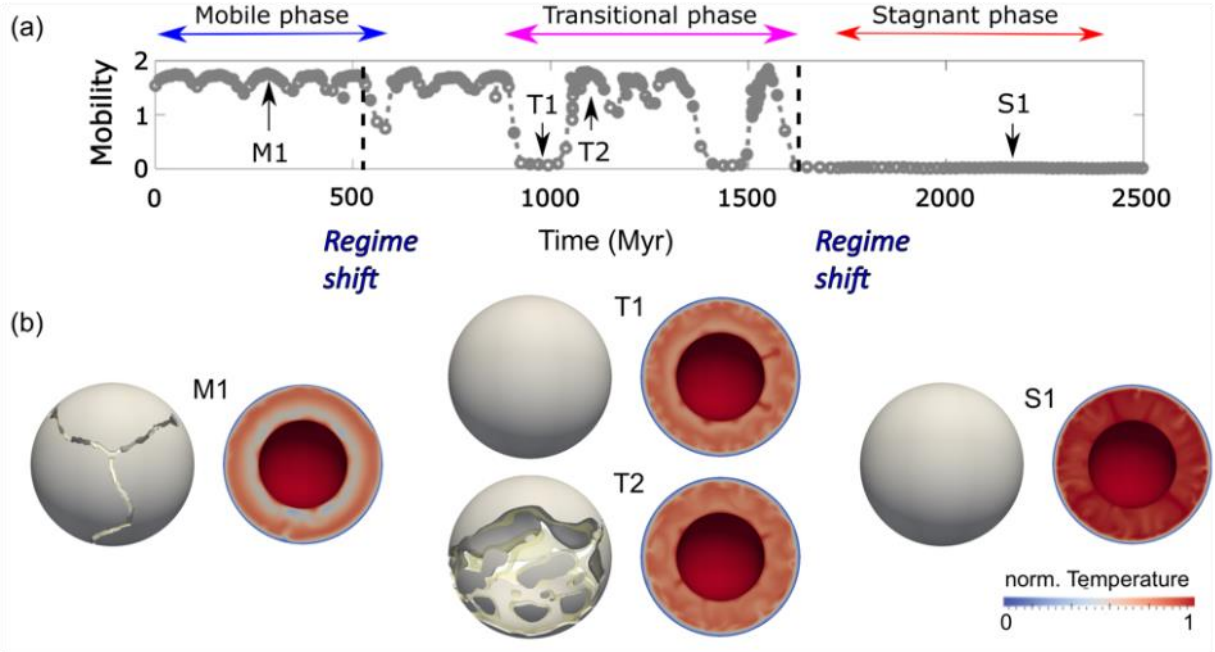

Fig. 5.5. *Illustration of ONE possible pathway of Venus' evolution through time, taken from [4]. Panel (a) shows the temporal evolution of surface mobility, panel (b) shows model cuts of viscosity and temperature for three respective times as indicated. According to this scenario, Venus' lithosphere was more mobile (like Earth) in a previous epoch and will be stagnant in the future (like Mars), but is now in a transitional state. Such a scenario – as well as many others – remains a valid possibility given the sparse, currently available data from Venus.*

Building Earth-like exoplanets: GPU simulations of late-stage terrestrial planet formation around K dwarf stars

We ran a large number of numerical N-body simulations of planet formation via planetesimal accretion around K dwarf stars (stars a bit less massive than the Sun and of particular interest in the search for extra-terrestrial life). The simulations were conducted mostly on the Norwegian supercomputer Betzy operated by Sigma2 and simulated 20 Myr of evolution to allow us to study dynamical evolution of the systems as well as their final characteristics and architectures. The main goal was to reproduce the known population of exoplanets orbiting this type of stars, specifically mostly close-in super-Earths (presumably rocky exoplanets of several Earth masses located very close to their host star). We explored the effects that various initial conditions and configurations of our models have on the final stage of planetary accretion around two stars with different masses. The final architectures and long-term stability of the systems are shown in Figure 5.6. Type I orbital migration is still a challenge for this type of simulations as it leads to a rapid mass loss during the early stage of planet formation. We managed to reproduce the observed population by implementing a cavity (a region of zero net torque on a planet acting as a planetary trap) around the host star to prevent the excessive mass loss. A paper is ready to be submitted (Hatalova et al.).

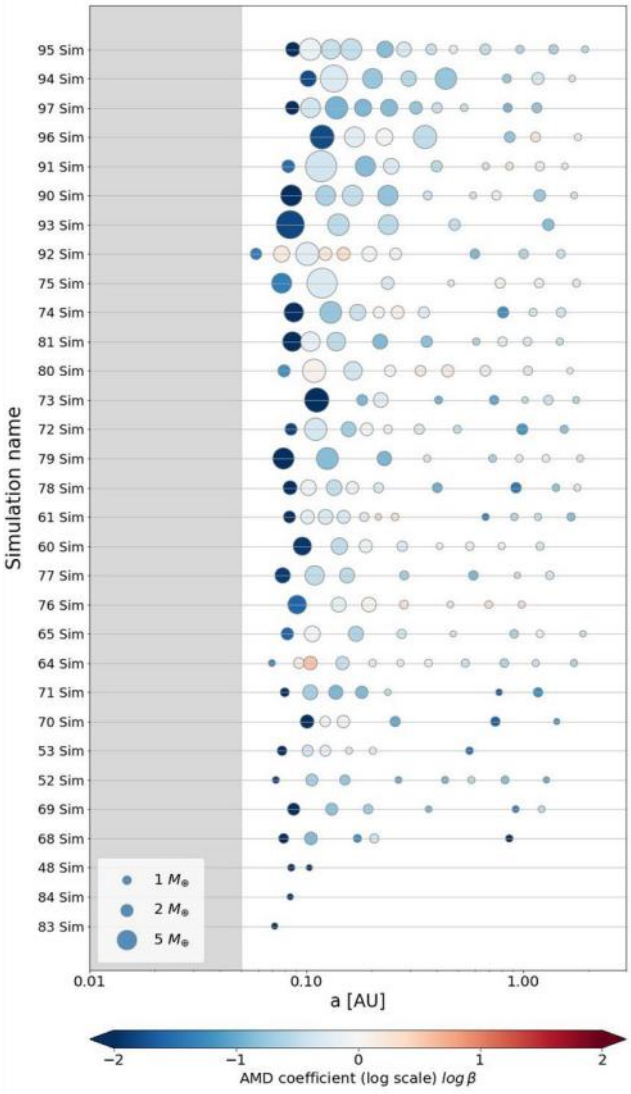

Fig. 5.6. *Simulated systems after 20 Myr of evolution. Each planet is represented by a circle, whose size is proportional to the mass of the planet and colour indicates its long-term stability.*

How rocky are the discovered small exoplanets?

The rocky exoplanet population of known exoplanets follows the Earth-like composition (i.e., layered structure with iron-nickel core and silicate mantle) up to a mass cut-off at 32 Earth masses. Due to high instellation for most of the terrestrial exoplanets, it is unlikely that the ones with large sizes have ice-rich cores. The potentially volatile-rich population presents a much larger dispersion that could reflect an even larger diversity in composition among such planets. The intense irradiance could be a reason why such a variety has been seen in the volatile-rich exoplanets due to their sensitivity to incident flux. Although Neptune and Uranus seemingly belong to this group by mass and radius, we cannot rely on our knowledge of their structure, because similar planets in the exoplanet population are much hotter. It is nevertheless possible that some volatile-rich planets made it to the inner parts of their systems via migration. In the density-mass diagram (see Fig. 5.7), the densities vary more for volatile-rich than for the rocky population. A given density corresponds to a narrower range of radii than mass. The slope for the M-R relation curve for volatile-rich planets grow faster than a curve for homogeneously dense sphere, and for terrestrial planets is close to expected for incompressible interiors. At first glance, it may seem that a steeper M-R relation for this population might fit better. But careful consideration of the position of the rocky population could lead to

an idea that planets seem to cluster along colour-coded equation-of-state curves for different interior structures (Mamonova 2022). Analogously, it could be also true for the volatile-rich population.

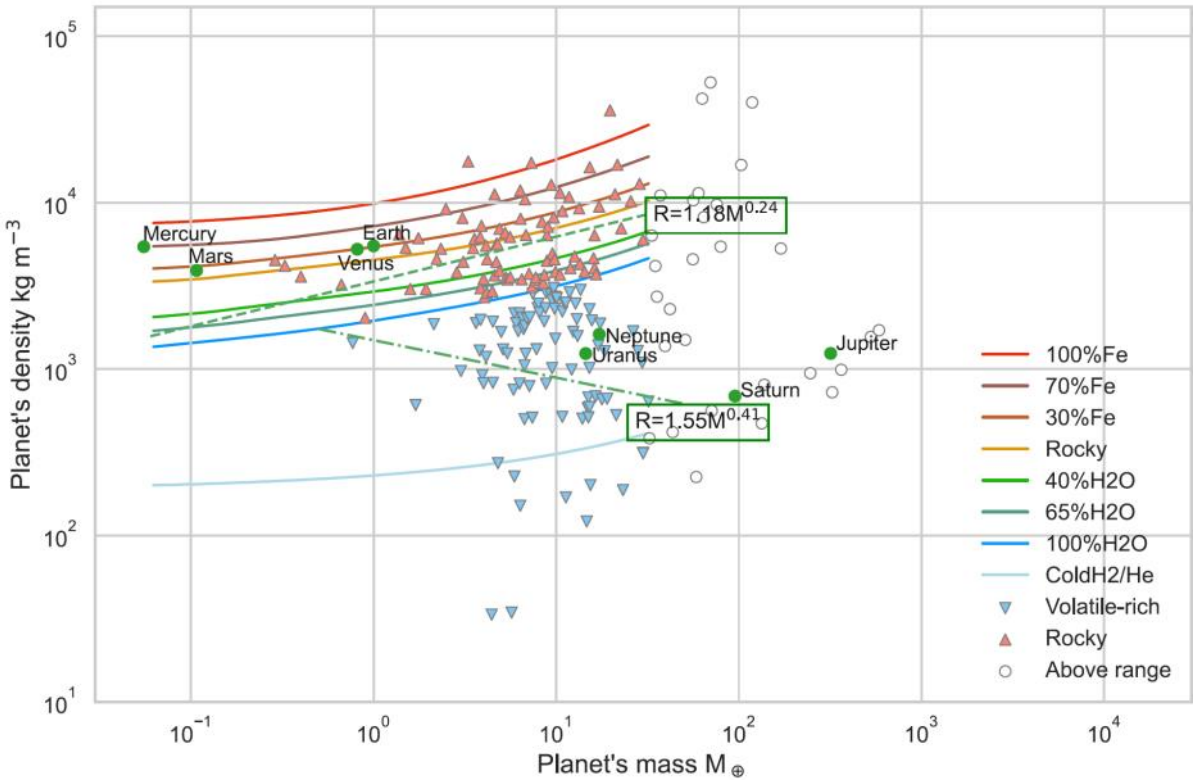

Fig. 5.7. *The mass-density diagram of this study sample. The red and blue triangles correspond to rocky and volatile-rich planets, respectively. The white circles represent the planets, excluded when calculating the M-R relation. The green dash-dotted and dashed curves represent fitted M-R relation for volatile-rich and rocky planets separated by the 100%H2O curve, respectively. The coloured interior curves are from Zeng et al. (2016). The solar system planets (green dots) were added for comparison.*

Lunar Time Travels – Introduction to a Revised Cratering Chronology Model

Lunar cratering-chronology models are to provide temporal constraints globally by linking crater densities with isotope geochemistry. Such a chrono-stratigraphy uses crater statistics by deriving size-resolved and area-normalised crater frequencies, and it is one of the few tools to globally assess times and rates of the geological evolution of the respective planetary body (Wu et al. 2022). Since the Apollo and Luna missions, plenty of new information has arisen, such as global spectral mapping, improvement in dating of samples and mapping of geological units as well as crater statistics. Recently, the sample return of the Chang'E 5 mission added a new calibration point. Therefore, the existing lunar cratering-chronology models need revision to account for these developments.

We prepared a self-consistent, revised, lunar cratering-chronology model that accounts for the above updates. Unprecedentedly, we use the spectral information at the actual landing sites and the spectral and mineral data of the samples to define the outline of the counting units. Thus, we uniquely describe count areas that concomitantly define the samples selectable for the calibration age. The calibration of the impactor flux before 3.9 Ga remains challenging.

The heterogeneous nature of breccia samples challenges the definition of homogeneous units and suitable reference samples to establish appropriate sample-unit links. The 'Late Heavy Bombardment' concept captures rather the last large basin formation event, Orientale (Werner et al. 2022), as a marker horizon, instead of the subsequent formation of several basins in a short time period. Compared to previous models, the new calibration pairs (frequency vs. age) suggest a monotonically decaying and, more importantly, lower throughout projectile flux. This lower flux is NOT the result of a systematic shift related to the derivation of the crater frequencies, but relates to different outlines of counting units and modern sample ages. Applying the new model to crater counts across the Moon suggests much older surfaces (by at least by 200 million years) than any of the current cratering-chronology models. Transferring this model to other solid-surface planetary bodies implies the ageing of these surfaces, too.

References

Bultel, B., A.M. Krzesinska, M. Veneranda, D. Loizeau, C. Pilorget, V. Hamm, L. Lourit, G. Lequertier, J.-P. Bibring, **S. C. Werner** (2022) Micro-scale characterization of vermiculite -rich sample from Granby Tuff, an analogue to Oxia Planum clays. *EGU General Assembly Conference Abstracts*, EGU22-11272

Helled, R., **S. Werner,** C. Dorn, T. Guillot, M. Ikoma, Y. Ito, M. Kama, T. Lichtenberg, Y. Miguel, O. Shorttle, P. J. Tackley, D. Valencia, A. Vazan (2022) Ariel Planetary Interiors White Paper, *Experimental Astronomy,* 53:323-356, doi: 10.1007/s10686-021-09739-3.

Krzesinska, A.M., B. Bultel, S.C. Werner (2022a) Analogues for Martian crustal and aqueous processes: Lessons learnt from mineralogy and geochemistry of rocks in the PTAL collection. *EGU General Assembly Conference Abstracts*, EGU22-12286

Krzesinska, A.M., P.F. Schofield, K. Geraki, J.F.W. Mosselmans, J.R. Michalski (2022b) Trace Elemental Composition of Alteration Minerals in Nakhlites—Source and Nature of Aqueous Fluids. LPI Contributions 2695, 6191

Krzesińska, A.M., B. Bultel, D. Loizeau, D. Craw, R. April, F. Poulet, **S.C. Werner** (2021). Mineralogical and Spectral (Near-Infrared) Characterization of Fe-Rich Vermiculite-Bearing Terrestrial Deposits and Constraints for Mineralogy of Oxia Planum, ExoMars 2022 Landing Site, *Astrobiology* 21 (8), 997-1016.

Loizeau, D., C. Pilorget, F. Poulet, C. Lantz, J.-P. Bibring, V. Hamm, C. Royer, **H. Dypvik, A. M. Krzesinska,** F. Rull, **S.C. Werner** (2022) Planetary Terrestrial Analogues Library Project: 3. Characterization of Samples With MicrOmega *Astrobiology* 22, 263–292. doi:10.1089/ast.2020.2420263

Mamonova, E. (2022) Qualitative and quantitative study of known exoplanets and exoplanetary systems. *Master Thesis.* https://www.duo.uio.no/handle/10852/95719.

Prieur, N.C., L. Rubanenko, Z. Xiao, H. Kerner, **S.C. Werner** and M.G.A. Lapôtre. (2022a) A large training dataset of boulder sizes and shapes as a first step towards the automated detection of rock fragments on planetary surfaces. *Lunar and Planetary Science Conference* (LPSC) 2022 #1835.

Prieur, N.C., B. Amaro, E. Gonzalez, L. Rubanenko, Z. Xiao, H. Kerner, **S.C. Werner** and M.G.A. Lapôtre. (2022b) Deep Learning for Boulder Detection on Planetary Surfaces. *American Geophysical Union* (AGU) 2022 #P23A-02.

Rolf, T., Weller, M., Gülcher, A., Byrne, P., O'Rourke, J.G., Herrick, R., Bjonnes, E., Davaille, A., Ghail, R., Gillmann, C., Plesa, A.-C., Smrekar, S. (2022). Dynamics and Evolution of Venus' Mantle Through Time, *Space Sci. Rev.,* 218, 70 (doi:10.1007/s11214-022-00937-9)

Shrbený, L., **Krzesińska, A.M.,** Borovička, J., Spurný, P., Tymiński, Z., Kmieciak, K. (2022) Analysis of the daylight fireball of July 15, 2021, leading to a meteorite fall and findnear

Antonin, Poland, and a description of the recovered chondrite. *Meteoritics & Planetary Science* 57, 2108–2126 (doi: 10.1111/maps.13929)

Werner. S.C., Bultel, B., Rolf, T., Assis-Fernandes, V. (2022), Orientale ejecta at the Apollo 14 landing site implies a 200-million-year stratigraphic time-shift on the Moon, *Planet. Sci. Journal,* 3, 65, (doi:10.3847/PSJ/ac54a6)

Wu, B., Wang, Y., **Werner, S.C., Prieur, N.C.,** Xiao, Z. (2022) A Global Analysis of Crater Depth/Diameter Ratios on the Moon, *Geophysical Research Letters*, 49(20), e2022GL100886

Visit to the meteorite exhibition at the Natural History Museum in Oslo for a practical session during the DEEP course 'Mineralogy of Planetary Surfaces and Biosignatures'. Photo credit: Simon Anghel.

6. Earth Laboratory

The Earth Laboratory Team focuses on research in paleomagnetism and its applications to paleogeographic reconstructions, plate tectonics, and the behavior of the Earth's magnetic field in the geological past.

Overview

In 2022, the Earth Laboratory Team continued to contribute to further the overall goals of CEED by conducting research in paleomagnetism and plate reconstructions, probing into the history of the Earth's magnetic field in deep geologic past, and developing novel methodologies for the analysis of paleomagnetic data. Over this year, our researchers published fourteen contributions in peer-reviewed journals, submitted seven more manuscripts for publication (currently under review), and conducted four fieldwork expeditions for collecting materials for the future paleomagnetic work. In August-September 2022, our team organized and hosted the 9th meeting of the Nordic Paleomagnetism Workshops Series (a series of international paleomagnetic workshops that dates back to the 1980's), which brought together more than 40 leading experts in paleomagnetism from Europe, the United States, Australia and China to produce an update of the global paleomagnetic database and work on unresolved issues of paleomagnetism in the Phanerozoic, Paleozoic and Precambrian. The team was also successful in securing funding for continuing our work after the end of CEED tenure. **Mathew Domeier** was awarded a five-year Consolidator Grant by the European Research Council (ERC) for the 'EPIC' project, which aims at unravelling the enigmatic behavior of the geomagnetic field in observed paleomagnetic record of Ediacaran time (~540 to 600 million years ago) and its possible links to climatic, geochemical and biologic changes that were unfolding on Earth's surface at the same time. **Annique van der Boon** won a Young Research Talent grant from the Research Council of Norway (NFR) to investigate anomalous behavior of the Earth's magnetic field in the Devonian-Carboniferous. Here we present a selection of our results from 2022 and brief summaries of the 'EPIC' and 'PANDA' projects.

Precambrian paleogeography of Baltica and Rodinia

The ~1140-900-million-year-old mountain range in southwestern Norway, known as the Sveconorwegian orogen (SNO), is traditionally viewed as a continuation of the Grenville orogen in eastern North America (Laurentia) formed due to collision with the Amazonia continental block during the assembly of the Rodinia supercontinent (Figure 6.1a). However, recent studies have challenged this view, suggesting that the two orogens, albeit overlapping temporally, were formed in different tectonic settings. Slagstad et al. (2020) argued that the observed geological record and timing of tectonic and magmatic events across the SNO do not support a continental collision scenario, but can be readily explained by tectonic processes at or behind an active continental arc, whereby the SNO was constructed by reamalgamation of crustal blocks that had been fragmented from the southwestern margin of Fennoscandia at earlier time. The presence of an active arc along the western Baltica margin during the 1140-940 Ma interval presents a challenge for nearly all models of Rodinia assembly, which commonly assume that the Grenville and Sveconorwegian belts were conjugate features, and hence seek to juxtapose Laurentia and Baltica at that time (as, for example, in Figure 6.1a). Independent assessment of the position of Baltica with respect to other Rodinia blocks relying on paleomagnetism has been so far largely hindered by the scarcity of reliable paleomagnetic poles for the most critical time interval between ~1100 and 900 Ma. In our new study led by **Evgeniy Kulakov** (Kulakov et al., 2022), we collected paleomagnetic data and $^{40}Ar/^{39}Ar$ age dates from metaigneous rocks of the SNO in southern Nor-

way. Rock-magnetic and geochronological analyses indicated that the sampled rocks have retained magnetizations that were imparted during distinct orogenic events. This allowed us to define three new paleomagnetic poles for Baltica that correspond to the magnetization ages of ~1090 Ma, 1000 Ma, and 900 Ma (Figure 6.1b). The oldest pole constrains the paleogeographic position of Baltica at intermediate latitudes at 1090 Ma, whereas coeval paleomagnetic data from North America suggest a nearly equatorial paleolatitude of the eastern Laurentian margin (Figure 6.1c). Thus, the connection between the Grenville and Sveconorwegian belts in the early Rodinia assembly is not supported. At younger times, the reconstructed positions of Baltica and Laurentia show smaller latitudinal discrepancies, but do not lend support to a close fit that would juxtapose the Grenville and Sveconorwegian orogens in the core of Rodinia either (e.g., Figure 6.1c). Overall, we find no geologic or paleomagnetic evidence for a close Baltica-Laurentia connection during the assembly of Rodinia. Our new data and paleogeographic reconstructions are consistent with the tectonic model that attributes the origin of the SNO to the reaccretion of fragmented continental margin behind an active arc (Slagstad et al., 2020), which raises a question: is it possible that Baltica has never been a part of Rodinia?

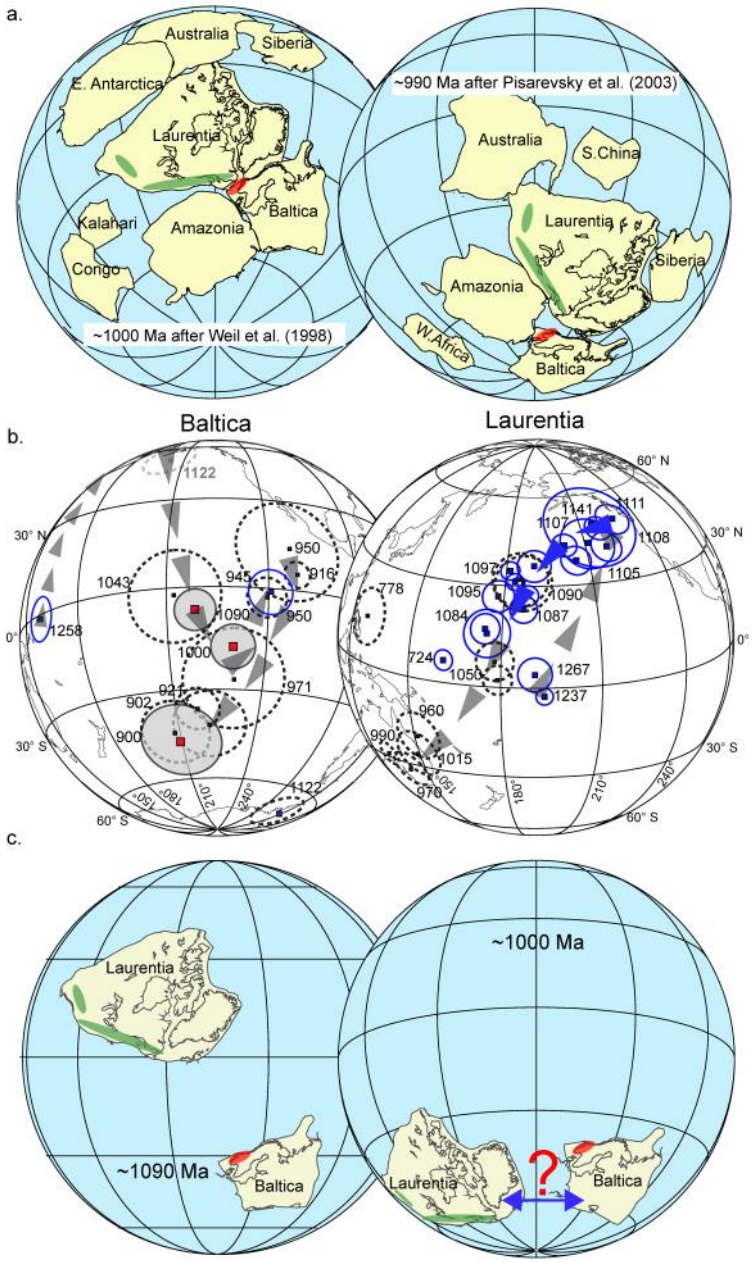

Figure 6.1. *(a) Two paleogeographic models illustrating a typical fit of Rodinia assembly at ~1 Ga; the shaded areas are the SNO (red) and the Grenville orogeny (green). (b) Paleomagnetic poles for Baltica and Laurentia. Red poles with gray-shaded 95% uncertainty circles are the new poles from southern Norway (Kulakov et al., 2022); the remaining poles are from the compilation of Evans et al. (2021). (c) Paleogeographic reconstructions of Baltica and Laurentia at 1090 and 1000 Ma; note that relative longitudes are arbitrary in these reconstructions.*

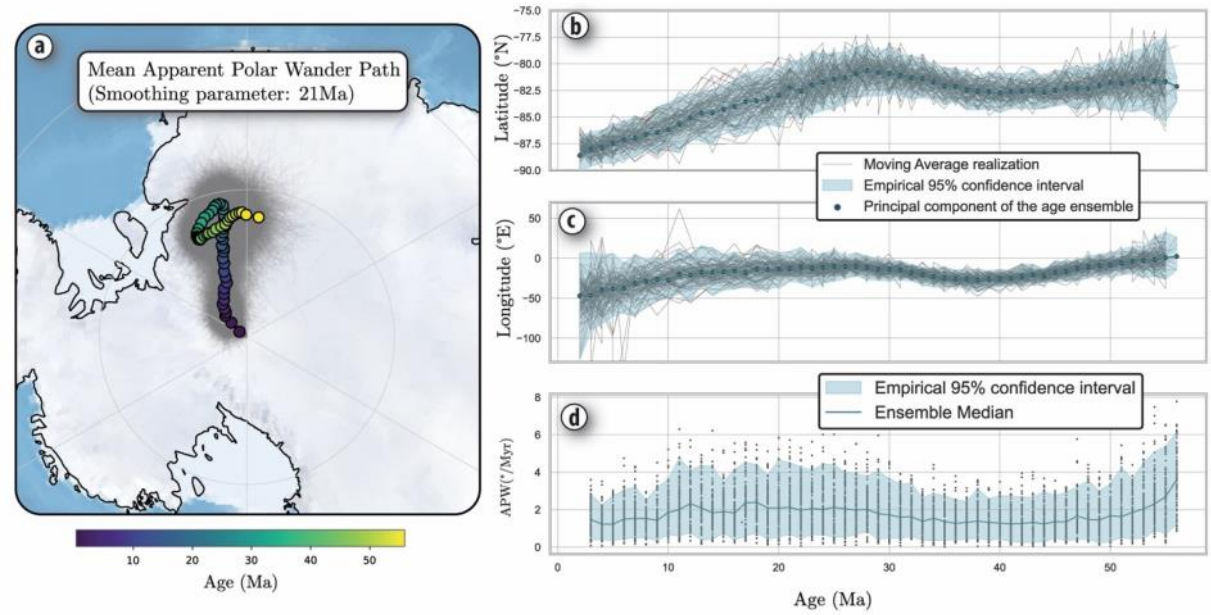

Figure 6.2. *(a) A high-resolution APWP (1 Myr time steps) for Cenozoic North America built from VGPs. (b-d) Decomposition of the APWP into different time series: (b) latitude, (c) longitude, and (d) rate of apparent polar wander (APW). The grey lines show the ensemble moving window averages, while light-color areas show the 95% confidence intervals.*

Uncertainty of polar wander paths: A case study of Cenozoic North America

Records of Earth's ancient magnetic field preserved in rocks provide valuable information for understanding past tectonic plate motions. These paleomagnetic records are collected from individual rock samples and subsequently grouped to develop global-scale paths called apparent polar wander paths (APWPs). APWPs represent the time-dependent position of Earth's spin axis relative to different blocks of lithosphere, providing us with a foundation for understanding the Earth's paleogeography. However, the conventional methods for analyzing and grouping paleomagnetic data are limited in the way they propagate and quantify uncertainties, and the consequences of these limitations are not known. In a new study led by **Leandro Gallo** (Gallo et al., in prep), we addressed these limitations through the introduction of new methodology, which was applied to a large paleomagnetic dataset from North America for the past 60 million years, representing one of the richest archives of paleomagnetic data in space and time.

Paleomagnetic studies typically report data at the level of sampling sites, but when APWPs are constructed, it has been standard practice to collapse site-level data into summary statistics describing locality- or study-level paleomagnetic poles, whereby a wealth of site-level information is lost. In our Cenozoic dataset for North America, we have preserved this information by compiling individual site-level paleomagnetic directions, virtual geomagnetic poles (VGPs), magnetization ages, and uncertainties associated with these values. Furthermore, we have supplemented each site-level entry with relevant metadata that enable filtering the dataset by a variety of criteria (e.g., the number of samples, within-site scatter). Due to the uncertainty associated with each input datum, it is crucial to develop a confidence metric on the estimated APWP, a problem referred to as forward uncertainty quantification (i.e., uncertainty propagation).

Yet, conventional approaches either entirely lack propagation of site-level uncertainty, or employ ad-hoc assumptions about probability distribution functions for underlying data that may be inadequate to model them. Crucially, it has been largely unexplored whether these shortcomings introduce bias in APWPs and/or distort their reported uncertainties (e.g., Vaes et al., 2022). In our study, we incorporated site-level uncertainties by employing Monte Carlo analysis for the site-mean directions and associated ages coupled with weighted bootstrap resampling of the site-level dataset. This provided us with a means to propagate uncertainties from the site level into the APWP by simultaneously resampling both the dataset and directions. Using this approach, we defined a high-resolution APWP for North America for the Cenozoic at 1 Myr time steps (Figure 6.2). Our results demonstrate that even in the presence of substantial noise, polar wandering can be assessed with unprecedented temporal and spatial resolution, while data uncertainties can be rigorously propagated and incorporated into APWP models.

EPIC: Untangling Ediacaran paleomagnetism to contextualize immense global change

This year our group began the ERC-funded project 'EPIC' (Untangling Ediacaran paleomagnetism to contextualize immense global change). The project is led by **Mathew Domeier** and seeks to determine the nature of dramatic changes seen in records of Earth's geomagnetic field between about 600 and 540 million years ago. These changes imply that something highly unusual was occurring either in the solid Earth and/or Earth's core, at the same time that immense climatic, geochemical and biologic changes were unfolding on Earth's surface. Four alternative hypotheses have been proposed to explain the enigmatic Ediacaran paleomagnetic data: 1) the tectonic plates were moving especially fast, 2) many of the paleomagnetic data have been corrupted, 3) the solid Earth tipped rapidly in response to mass distribution changes ('true polar wander'), and 4) the geomagnetic field was behaving abnormally (Figure 6.3). Each of these hypotheses has far-reaching implications for the Earth sciences. Our work through the EPIC project aims to directly test these alternative hypotheses through the collection of new observational and experimental data from Ediacaran sections around the globe. To this end, we have conducted two fieldwork expeditions this summer and fall in northern Norway (Varanger Peninsula) and in Paraguay, and we continued to advance ongoing paleomagnetic investigations of the Egersund dikes and Ediacaran rocks from Newfoundland.

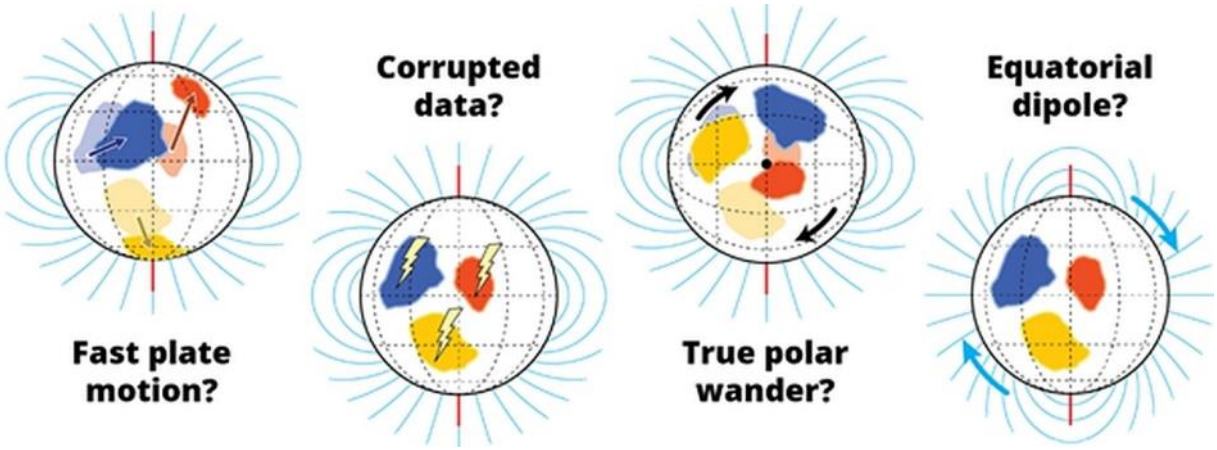

Figure 6.3. *Alternative processes proposed to explain the enigmatic paleomagnetic data from the Ediacaran Period.*

PANDA: Investigating anomalous behaviour of Earth's magnetic field in the middle Paleozoic

In the middle Paleozoic (~440-340 million years ago), life on land emerged, the first plants and forests developed, and many biotic crises took place. Geoscience research relies on paleogeographic reconstructions of the continents, which are based on paleomagnetism. However, the middle Paleozoic forms a conspicuous gap in our knowledge of Earth's magnetic field. The exact limits of this gap have not been established yet, but there is a striking scarcity of high-quality, unambiguous paleomagnetic data for around 100 million years in the Carboniferous and Devonian (Figure 6.4), hindering our understanding of the deep interior of our planet. Importantly, the absence of high quality paleomagnetic data in this time prevents the understanding of the behaviour of Earth's magnetic field in this key interval for Earth evolution, and hampers the use of paleomagnetism as a tool for dating and correlation. A recurring observation in middle Paleozoic paleomagnetism is that magnetizations are often weak, below sensitivity limits of traditional magnetometers, making them effectively unmeasurable with standard techniques. NFR-funded project PANDA led by **Annique van der Boon** will investigate promising sedimentary and igneous rocks from the late Silurian to early Carboniferous with new high precision techniques. Advances in magnetometer technology in the last few years increased the sensitivity of equipment, which now allows measurements of samples that were previously unmeasurable. PANDA will use the newly developed Quantum Diamond Microscope, to map magnetizations of minerals inside rocks in unprecedented detail. Altogether, PANDA will elucidate the behaviour of Earth's magnetic field, show whether it was anomalous, and if so, for how long this

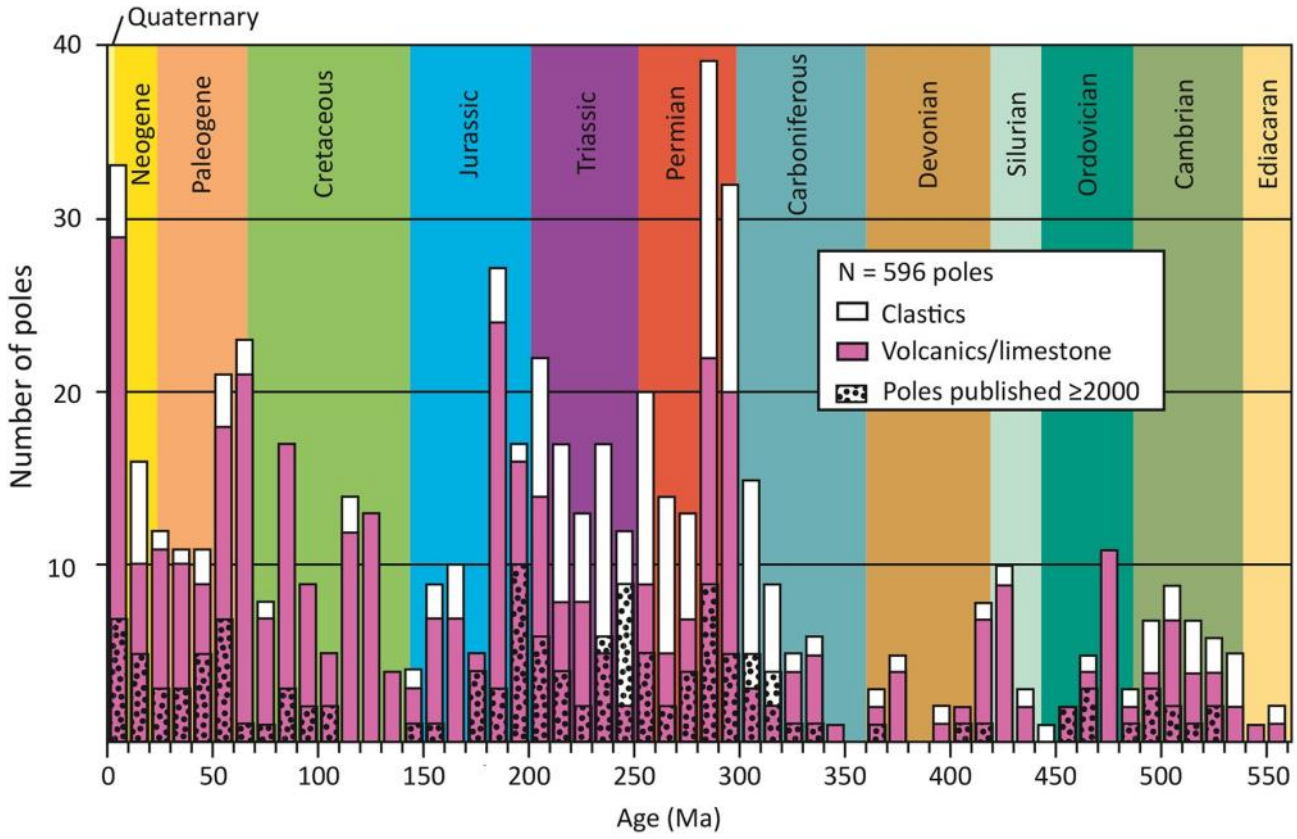

Figure 6.4. *Paleomagnetic data coverage for the Phanerozoic. Bars show the number of paleomagnetic poles in 10-Myr-wide age bins in global paleomagnetic compilation of Torsvik et al. (2012) that meet their minimum reliability criteria. The number of poles published after the year 2000 are shown by dotted bars. Note the striking scarcity of data for the ~340-440 Ma interval. After van der Boon et al. (2022).*

National Geomagnetic Laboratory

The Earth Laboratory team runs and manages a Norwegian national geomagnetic laboratory (the Ivar Giæver Geomagnetic Laboratory, www.iggl.no); a summary of research project that used the laboratory facilities in 2022 is presented in Table 6.1.

Table 6.1. *Research projects that used the geomagnetic laboratory in 2022 (CEED members in* ***bold****).*

*Magnetostratigraphy of Devonian sedimentary rocks of Svalbard (**Annique van der Boon**)*
*Paleomagnetism and rock magnetism of the Egersund dikes (**Yi Xue, Mathew Domeier, Petter Silkoset, Evgeniy Kulakov**)*
*Paleomagnetic and rock magnetic measurements of Middle Devonian sediments from Mimerdalen, Svalbard (**Annique van der Boon, Mathew Domeier**)*
*Ediacaran field behavior and tectonics from the Avalonia zone of eastern Newfoundland, Canada (**Mathew Domeier**, Boris Robert, GFZ Potsdam)*
*Ediacaran paleointensity study of Egersund dikes, Norway (**Yi Xue, Mathew Domeier**)*
Identifying Magnetic Phases in Additively Manufactured High-Entropy Alloy FeCoNi-AlxMnx (Alexander Amble Larsen, Department of Physics, UiO)
Magnetic properties of high-entropy ferromagnetic alloys (Anthoulina Poulina, Department of Physics, UiO)

References

Evans, D. A. D., Pesonen, L. J., Eglington, B. M., et al. (2021). An expanding list of reliable paleomagnetic poles for Precambrian tectonic reconstructions, in Ancient Supercontinents and the Paleogeography of the Earth (L. J. Pesonen, J. Salminen et al., eds.), Elsevier, pp. 605-639, https://doi.org/10.1016/B978-0-12-818533-9.00007-2.

Kulakov, E. V., T. Slagstad, M. Ganerod, T. H. Torsvik (2022). Paleomagnetism and 40Ar/39Ar geochronology of Meso-Neoproterozoic rocks from southwest Norway. Implications for magnetic remanence ages and the paleogeography of Baltica in a Rodinia supercontinent context. Precambrian research, 379, https://doi.org/10.1016/j.precamres.2022.106695.

Slagstad, T., Marker, M., Roberts, N.M.W., et al. (2020). The Sveconorwegian orogeny – Reamalgamation of the fragmented southwestern margin of Fennoscandia, Precambrian Research, 350, https://doi.org/10.1016/j.precamres.2020.105877.

Torsvik, T. H., Van der Voo, R., Preeden, U., et al. (2012). Phanerozoic polar wander, palaeogeography and dynamics, Earth-Science Reviews, 114, https://doi.org/10.1016j.earscirev.2012.06.007.

Vaes, B., **Gallo**, **L. C.,** van Hinsbergen, D. J. J. (2022). On Pole Position: Causes of Dispersion of the Paleomagnetic Poles Behind Apparent Polar Wander Paths, Journal of Geophysical Research: Solid Earth, 127, e2022JB023953, https://doi.org/10.1029/2022JB023953.

van der Boon, A., Biggin, A. J., Thallner, D., et al. (2022). A Persistent Non-uniformitarian Paleomagnetic Field in the Devonian? Earth Science Reviews, 231, https://doi.org/10.1016/j.earscirev.2022.104073.

Photos from the field

Drone photo of the EPIC team sampling on the Varanger Peninsula. Photo credit: Leandro Gallo.

Annique van der Boon sampling a Carboniferous dike near Honningsvåg.

Work of the IX meeting of the Nordic Paleomagnetic Workshop Series, Kringlen Gjestegård, Norway, 2022. Photo credit: Pavel Dubrovine.

The Else-Ragnhild Neumann Award

CEED awards every year the Else-Ragnhild Neumann Award for Women in Geosciences. It goes to a woman who through her PhD or postdoctoral work has made a significant contribution to research in Geosciences.

*The committee members for 2022 were Professor **Anny Cazenave**, LEGOS-CNES Toulouse, France, Professor **Claudio Faccenna,** Università Roma TRE and University of Texas at Austin and Head of department **Per Barth Lilje**, Institute of Theoretical Astrophysics, UiO.*

Requirements for nomination

The nominee should reside in Norway at the time of nomination. Women are eligible for the first 7 years following their degree, except in the case of significant interruptions to a research career.

About the award

The Else-Ragnhild Neumann award honors the scientific contribution of Professor Else -Ragnhild Neumann.

*In 1981, she became **the first female professor in Geosciences in Norway**. Neumann worked with the University of Oslo. She is still active and publish about volcanism and links to mantle processes. She studied the Oslo region, the Canary Islands and other volcanic islands, the Siberian Traps and other areas that experienced significant magmatism.*

Her most recent article is: Hyung, E., Sedaghatpour, F., Larsen, B. T., **Neumann, E. R**., Eriksen, Z. T., Petaev, M. I., Jacobsen, S. B. (2023). A Peridotite source for strongly alkalic ultrabasic HIMU lavas of the Oslo Rift, Norway, *Chemical Geology* V. 622.

For 2022, the award had one winner: **Jessica Ann McBeck** from the University of Oslo (UiO). She was recognised at a conference at The Centre for Earth Evolution and Dynamics (CEED), University of Oslo, on 7.12.2022.

Jessica Ann McBeck was recognized for *having a most impressive publication record. Her combination of using numerical modelling, laboratory experiments and utilisation of field data to get better forecasting of earthquakes is most interesting.* The international committee for the Else-Ragnhild Neumann Award for Women in Geosciences concluded that Jessica McBeck's scientific work deserves recognition because of her original work combining numerical modelling, laboratory experiments and utilisation of field data to get better forecasting of earthquakes.

The winner was nominated by **François Renard,** Director of the Njord Centre, UiO**, Bjørn Jamtveit**, Vice-Dean for Research, Faculty of Mathematics and Natural Sciences, UiO, and **Anders Malthe-Sørenssen**, Professor of Physics, UiO.

Else-Ragnhild Neumann Award Logo designed by: ***Fabio Crameri.***

Jessica McBeck is a researcher at the Njord Centre, and the Department of Geosciences, at the University of Oslo. She studies fracture network coalescence and strain localization in both experiments and numerical models. The long-term goal of her work is to identify the evolving characteristics of fracture networks and strain fields that may help forecast the timing of the next large earthquake.

Jessica Ann McBeck, the winner of the 2022 Else-Ragnhild Neumann Award.

Photo: CEED/UiO.

The prize winner has received national and international recognition, she was recognized as an outstanding reviewer for her contributions to peer review at Communications Earth & Environment and she will also receive the Arne Richter Award for Outstanding Early Career Scientists from the European Geosciences Union in 2023.

Selected, recent publications:

McBeck, J., & Renard, F. (2022). Deriving three-dimensional properties of fracture networks from two-dimensional observations in rocks approaching failure under triaxial compression: Implications for fluid flow. *Water Resources Research*, 58, e2022WR032783.

McBeck, J. A., Ben-Zion, Y., Zhou, X., & Renard, F. (2022). Precursory off-fault deformation in restraining and releasing step overs: Insights from discrete element method models. *Journal of Geophysical Research: Solid Earth*, 127, e2022JB024326.

McBeck, J. (2022) Predicting the Timing of Catastrophic Failure During Triaxial Compression: Insights from Discrete Element Method Simulations. *Pure Appl. Geophys.* 179, 3625–3645.

F. Van Stappen, J., **McBeck, J.A.**, Cordonnier, B. *et al.* (2022) 4D Synchrotron X-ray Imaging of Grain Scale Deformation Mechanisms in a Seismogenic Gas Reservoir Sandstone During Axial Compaction. *Rock Mech Rock Eng* 55, 4697–4715.

Outreach highlights

Image 1: *After 7 years of closure. the newly re-opened wing of Natural History Museum at Tøyen in Oslo was a highlight for Norway, Oslo and the UiO (geo)science communities. Several CEED researchers gave their input for the exhibitions and were in attendance for the opening day on 6th May 2022. Entrance for UiO employees and a guest is free. Photo by: Grace Shephard.*

As we entered the final year as a Centre of Excellence, CEED's outreach efforts still continued across digital and in-person platforms. In 2022 we noted a large number of followers joining our social media channels, a function of the pandemic, which we tried to maintain this past calendar year. As in previous years there has been a mix of both individual and group-driven outreach initiatives which we highlight below. While it is unclear if some of the CEED social media channels will be converted into the new SFF PHAB's channels (we anticipate a similar follower profile), our legacy CEED content should remain available online for a little while longer.

As the CEED coordinator for Outreach, I would like to thank all of the colleagues and collaborators for your contributions to CEED outreach and science communication over the past decade. Even if not undertaken under the "CEED" logo, your science communication initiatives are appreciated. I have been really impressed and inspired by you, and am grateful that so many of you took the time to engage with a wider audience whether it through sending a photo, resharing a post, writing a blog entry, writing a book or giving a talk. I hope you will in turn be inspired to continue these initiatives in your future roles; communicating our research, activities and experiences to the wider public is an important service and legacy for us all, and it is also an opportunity for us to reflect in turn on our role as scientists.

CEED's main avenues of outreach for this past year include the CEED website, CEED Blog, social media channels (Facebook, Instagram, Twitter, YouTube), Department of Geosciences website, GEOOnsdag at the UiO Science Library, and UiO news outlets including Ti-

tan.uio.no. In the Norwegian media, the main avenues included forskning.no and geoforskning.no Many individual projects also have social media accounts (especially several of the NFR Young Researcher Talent awardees e.g. ANIMA, MAPLES, ASHLANTIC and POLARIS projects).

Photo 1: *"The Wilson Cycle" series was a highlight for CEED Outreach in 2022. The four-part series were filmed in western Norway and released on the CEED YouTube channel. Photo: Screenshots from YouTube.*

Selected highlights of outreach events from 2022 include:

- The hotly anticipated Wilson Cycle series (photo 1) was released over summer 2022 and collectively have been viewed over 7000 times. The four-part series delved into the Wilson Cycle, one of the most fundamental concepts in geology. It explains the process of orogeny, which related to the formation of the world's large-scale mountain belts by a series geological events. The series was coordinated by Torgeir Anderson with Dougal Jerram as the narrator, and featured a number of CEED researchers and collaborators.
- Postdoctoral researcher and recent NFR awardee Annique van der Boon won the "Det usynlige skjoldet fra jordens indre"- a Norwegian language public blog article competition organized by geoforskning.no. As winner of the competition, her article was featured in Aftenposten (image 2).
- The Norwegian GoNorth Initiative to the Arctic Ocean (Eurasia Basin, offshore Barents margin) was featured highly in Norwegian media. Onboard the new iceclass vessel R/V Kronsprins Haakon were CEED scientists Alexander Minakov and Juan Camilo Meza-Cala (project leader Jan Inge Faleide).
- Razvan Caracas's Moon Impact exhibition continued its travelling tour to several new locations throughout 2022.
- Henrik Svensen released a new book called "Et land av stein – Bergartene some har formet Norge".
- Trond Torsvik gave a highly attended talk for GeoOnsdag at the University's Science Library on "Planetær beboelighet" (Planetary Habitability).
- Earth's deep "blobs" (or everyone's favourite acronym LLSVP - Large Low-Shear Wave Velocity Provinces) featured a few times in large-scale media in 2022. Including comments from Bernhard Steinberger and Björn Heyn in BBC and Forskning.no articles.
- Kate Selway and Clint Conrad continued their fieldwork on the Greenland icesheet as related to the NFR-funded MAGPIE project. Kate documented her experiences in a video blog and several articles (photo 2).

- Agata Krzesińska gave a talk about meteorites at the Norwegian chapter of Pint of Science - Polish edition.
- Both Agi Kiraly and Grace Shephard were finalists in the EGU 22 Photo competition in Vienna. Unfortuantely, neither were the winners but will try again with snaps for the next EGU.
- Grace Shephard and former CEED researcher Fabio Crameri received funding from the iEarth SFU in Norway and developed a course on how to "Create and Share Better Science Graphics." An aim was to increase the number and type of figures on the s-Ink.org open science graphics repository.

Image 2: *Postdoctoral researcher and recent NFR awardee Annique van der Boon won a Norwegian language public blog competition organized by geoforskning.no. As winner of the competition, her article "Det usynlige skjoldet fra jordens indre" was featured in Aftenposten Photo: Annique van der Boon/Aftenposten.*

Some statistics from social media and outreach in 2022:

The CEED Blog – 14 blog articles published

Facebook - 1256 followers, 64 individual posts

Twitter - 1502 followers, 70 original tweets

Instagram – 241 followers, 24 posts

YouTube – 342 subscribers, 4 videos

Photo 2: *Kate Selway (right, facing camera) on the Greenland Icesheet as part of the MAGPIE project. Kate and the team travelled over 4200 km on the snow scooters over 42 days.*

Image 3: *CEED's last post as a Centre of Excellence on Social Media.*

CEED Outreach team members:

Grace Shephard (Coordinator), Trine Sannesmoen (CEED webpage), Gunn Kristin Tjoflot (GEO), Valentina Magni (CEED Instagram).

The Norwegian Research School for Dynamics and Evolution of Earth and Planets *(DEEP) is a National Research School in Geosciences, funded by the Research Council of Norway for the period 2016-23. It is hosted by CEED and lead by Professor* ***Stephanie C. Werner****, with* ***Sara A. Nettum*** *and* ***Sofie H. Ryen*** *as the Administrative coordinators in 2022. DEEP aims to educate solid earth and planetary scientists in a holistic way, placing the Earth's structure and evolution in a comparative planetology perspective. DEEP gathers Norwegian PhD students and researchers within geophysics, mineralogy, geochemistry and comparative planetology.*

How do I know how I am doing? (22–24.03)

This course is held by Claus Jebsen and Maja Vikan.

The everyday as a PhD candidate can be overwhelming. Doing a PhD is a great personal investment. It can be stressful handling deadlines, critical reviews and refusals, large scale projects and the feeling that it is all on our own shoulders. And how do you even know how you are doing? This course aims to build resilience, self-understanding and how to utilize feedback in a fruitful way.

There were 16 participants for the course: 15 PhD candidates, 3 of which were from CEED.

GEO-DEEP9400 Solid Earth—Fluid Earth Interactions (2-6.05)

Course responsible: Carmen Gaina and Adriano Mazzini.

Featured lecturers: Adriano Mazzini, Carmen Gaina, Clint Conrad, Grigorii G. Akhmanov, Hans Jørgen Kjøll, Henrik Svensen, Karen Mair, Karin Andreassen, Matteo Lupi, Morgan Jones, Olivier Galland, Petr Brož, Reidar Trønnes, Sverre Planke, Valerie Maupin, Valentina Magni.

This intensive PhD course (5 ECTS) addresses topics like material recycling across the geospheres and how mantle dynamics, volcanism, plate tectonics influences long-term, global environmental and climatic changes.

There were 15 participants for the course: 15 PhD candidates, 1 of which were from CEED.

GEO-DEEP9508 Artificial Intelligence, Data Science and Geographic Information Systems (GIS) (20-24.06)

Course responsible: Stephanie Werner.

Featured lecturers: Gabriela Spakman.

This intensive course (5 ECTS) explores state-of-the art principles, methods, and techniques related to applications of artificial intelligence and data science in relation to Earth and planetary remote sensing data processing. The course intends to train the participants in open science and towards integrated solutions of data science and Geographic Information Systems (GIS). In this way the participant can give a new dimension to their research by adding the spatial component to their data and be able to process, analyse, combine, and visualise the data in time and space. The aim of this specific course is to familiarise the participants with the possibilities of applying AI (Artificial Intelligence) to data with a spatial component making use of Esri software (in this case ArcGIS Pro).

There were 10 participants for this course: 9 PhD candidates and 1 other. 1 of the PhD candidates and 1 of the other participants were from CEED.

Writing with results (19.09-08.11)

This course is held by Mathew Stiller-Reeve.

At several stages during PhD studies, PhD candidates will have periods with lots of writing. Many struggle with writing efficiently and do not feel competent about their writing skills. In this course, participants work through the whole writing process together. The course covers some of the basics of clear and concise writing, as well as how to apply these skills directly to the texts being written. This course includes discussions, brainstorming, planning, writing, and editing. We also develop forums for peer-to-peer reflection and collaboration. By the end of the course, the candidates will hopefully have a research article ready for submission.

There were 7 participants: 7 PhD candidates.

GEO-DEEP9100 Planetary Physics and Global Tectonics (3–7.10)

Course responsible: Stephanie Werner.

Featured lecturers: Maëlis Arnould, Annique van der Boon, Razvan Caracas, Fabio Crameri, Björn Heyn, Ágnes Király, Valentina Magni, Alexander Minakov and Tobias Rolf.

This intensive course (5 ECTS) will give an introduction to the physics and tectonic processes that govern the properties and evolution of the Earth and other planets. This includes how the Earth and planets in the Solar System form, and how this compares to other planetary systems.

There were 4 participants for this course: 2 PhD candidates and 2 master students. The two PhD candidates were from CEED.

GEO-DEEP9509 Interactions between star-planet couples (from Sun-Earth to Star-Exoplanet) (21-25.11)

Course responsible: Stephanie Werner.

Featured lecturers: Annique van der Boon, Ramon Brasser, Jane Luu, Chloé Marcilly, Atul Mohan, Trond Torsvik, Sven Wedemeyer, and Stephanie Werner.

In this course, we will bridge topics from the realm of astrophysics and geosciences. We intend to train participants in the fundamental workings of stars, the Sun, planets and exoplanets. The course aims at familiarising with current state-of-the-art models of the different objects and models that prescribe their interactions (e.g. solar wind, flares, stellar activities onto bodies with and without a magnetic field) and how these compare with spacecraft and telescope observations. We will also address on which timescales solar activity modulates the climate on Earth and at which timescales planetary activity or human action dominate.

There were 7 participants for this course: 6 PhD candidates and 1 other. 2 of the PhD candidates were from CEED.

Table 1. Teaching by CEED staff at UiO

DEEP courses and CEED members are given in **bold,** courses arranged by CEED outside UiO are in grey

Course code & name	Semester	ECTS	Course responsible
GEO1000 Klima og bærekraft: Naturlige prosesser og menneskets påvirkning	Autumn 22	10	T. Berntsen, **T.H. Torsvik**
GEO1100 Jordens utvikling	Autumn 22	10	**H.H. Svensen,** T. Berntsen, K.S. Lilleøren, A. Bryn
GEO2140 Solid Earth Geophysics	Spring 22	10	**A.J. Breivik**
GEO2300 Physical processes in the geosciences	Autumn 22	10	J. Lacasce, **V. Maupin**, A. L. Sjur, A. van Hove
GEO3000 Bachelor-oppgave i geologi	Spring 22	10	K.S. Lilleøren, **H.H. Svensen**
GEO-AST3410/4410 Planetology	Autumn 22	10	**S.C. Werner,** V. Hansteen
GEO4120 Near-Surface Geophysics	Autumn 22	10	**A. Breivik/** K. Muller, A. Alexander, T. Eiken
GEO4218 Basin Formation and Development	Autumn 22	10	**J. I. Faleide,** J. Jahren, F. Tsikalas, **S. Gac**
GEO4240 Seismic Interpretation	Spring 22	10	**J.I. Faleide,** I.A. Anell, M. Hassaan
GEO4360 Field methods in hydrogeology	Spring 22	5	A. Sundal, A. Popp, P. Aagard, H. Hellevang, L. -A. Erstad, C. Sena, **A. Breivik**
GEO4630/9630 Geodynamics	Autumn 22	10	**C. Conrad**
GEO4840/9840 Tectonics	Spring 22	10	L. Menegon, O. Galland, **G. Shephard,** H. J. Kjøll, **M. M. Domeier**
GEO-DEEP9400 Solid Earth—Fluid Earth Interactions	Spring 22	5	**A. Mazzini, C. Gaina, C. Conrad, H. H. Svensen, M. T. Jones, R. Trønnes, S. Planke, V. Maupin, V. Magni**
GEO-DEEP9508 Artificial Intelligence, Data Science and Geographic Information Systems (GIS)	Spring 22	5	**S. Werner**

Table 1 cont.
Teaching by CEED staff at UiO

GEO-DEEP9100 Planetary Physics and Global Tectonics	Autumn 22	5	**A. van der Boon, R. Caracas, B. Heyn, Á, Király, V. Magni, A. Minakov, T. Rolf**
GEO-DEEP9509 Interactions between star-planet couples (from Sun-Earth to Star-Exoplanet)	Autumn 22	5	**A. van der Boon, J. Luu, C. Marcilly, T. H. Torsvik, S. Werner**

Florence Ramirez defended her PhD in November 2022.
Photo by: Ágí Kíraly.

PhD student projects (**bold**: finished in 2022 and for CEED members)

Name	Topic	Supervisors	Funding
Anzulović, Ana	Modelling impact of melts on mantle diffusion and viscosity with geodynamic implications.	**R. Caracas**	EU
Ballo, Eirik	Reconstructing climatic, environmental and societal dynamics in Scandinavia in the Iron- and Viking-Age (RECESS).	**H. Svensen,** M. Bajard**,** Makke	UiO
Beloša, Lea	The Role of Fracture Zones in Geodynamic Processes. * Co-supervisors: **A. Breivik, R. Trønnes, A. Mazzini,** and **S. Callegaro**	Main supervisor **C. Gaina,** see *	UiO
Hatalova, Petra	Building Earth-like exoplanets	**S. Werner**, R. Brasser	UiO
Jerkins, Annie E. (Norsar)	Improved understanding of Seismicity in the North Sea.	V. Oye, **V. Maupin,** L. Ottemøller, F. Halpaap	
Marcilly, Chloé F.M.	**Modelling of the atmospheric CO2 and O2 levels during the Phanerozoic.**	**T. H. Torsvik, H. Svensen, M. Jones, T. Heimdal**	UiO
Meza Cala, Juan C.	Tectonic and geodynamic evolution of the SW Eurasia Basin. *Co-supervisors: **A. Minakov**, **G. Shephard** and **C. Gaina**.	Main supervisor **J. I. Faleide**, see*	RCN
Ramirez, Florence	**Constraining the mantle viscosity of Greenland with geophysical observations.**	**C. Conrad**, K. Selway	SFF
Wang, Yijun	Evolution of anisotropic viscosity in the upper mantle and its effect on subduction	**A. Kiraly, C. Conrad**	RCN
Weerdesteijn, Maaike	3D glacial isostatic adjustment modeling for Greenland.	**C. Conrad**, K. Selway	RCN
Xue, Yi	Paleointensity and paleomagnetic investigations of the Ediacaran geomagnetic field.	**M. Domeier, L. C. Gallo**	ERC

Dr Philos project

Name	Topic
Halvorsen, Erik	Paleomagnetic and magnetic fabric studies of Early Cretaceous sills from Central Svalbard: unraveling Early Cretaceous paleopole and suggested Cenozoic remagnetization in addition to divergent magnetic fabric.

Master student projects with one or more supervisors at CEED

Bold: finished in 2022

Name	Topic	CEED-supervisor(s)
Bondevik, Lars Harstad	**Fault interpretation in high-resolution P-cable seismic data - Hoop Fault Complex**	S. Planke
Eliassen, Gard L.	Structural evolution of the Sele High and Ling Depression	J. I. Faleide
Herrem, Amailie S.	**Influence of salt and regional tectonics on the structural and sedimentary basin development, Tiddlybanken Basin, southeastern Norwegian Barents Sea.**	J. I. Faleide
Labes, Aliénor M. P.	**Morphologies and gas emissions from the Gobstan-Shamakhy mud volcano province, Azerbaijan**	A. Mazzini
Lundahl, Jenny N. B.	**Modelling of acoustic wave propagation in the ocean in the presence of a laterally varying ice layer**	V. Maupin
Mamenova, Elena	**Qualitative and quantitative study of known exoplanets and exoplanetary systems**	S. Werner
Wang, Helene	**Mapping heterogeneous water storage within the Earth's mantle**	C. P. Conrad, M. Domeier, G. E. Shephard, V. Magni

International cooperation

Country	Activity	Person(s) involved (CEED members in bold)
Australia	STEM pen pal for children	**G. Shephard**, V. Chang, Cardiac Research Institute
Australia, Spain, USA	Uncertainties in paleobio-geographic reconstructions	**M. Domeier**
Australia, France, Germany, Netherlands; USA	Building paleomagnetic apparent polar wander paths with site-level data	**L. Gallo, M. Domeier, A. van der Boon, G. Shephard, A. Kiraly**
Canada	Devonian anoxia	**A. van der Boon**, P. Kabanov
Canada	Geochemistry of Cretaceous sediments from the Arctic	**M. Vickers**, J. Galloway
Canada	Supercontinents and mantle dynamics	**G. Shephard**, P. Heron
Canada	Science eduction and outreach, teaching in prisons	**G.Shephard**, P. Heron
Canada	Sulfur in clinopyroxenes - experimental petrology and applications	**S. Callegaro**, D. R. Baker
Canada, USA, Russia	NOR-R-AM2 project; A Norwegian-Russian-North American collaboration in Arctic research and collaboration	**C. Gaina**, **G. Shephard**, **M. Jones**, K. Senger, O. Anfinson, B. Coakley, **J. I. Faleide**, D. Stockli and others
China	Paleomagnetism of the North and South Qiangtang terranes	**M. Domeier**
Denmark	Supervising project of Bo Pagh Schultz on ikaite and glendonites	**M. Vickers**, B. P. Schultz
Denmark	Re-analysing biomarker extracts ofr temperature reconstructions	**M. Vickers**, K. Sliwinska
Finland	Svalbard HALIP	G. Shephard, K. Senger, A. Sartell, C. Beier
Finland	Sulfur in clinopyroxenes - the Karoo LIP	**S. Callegaro**, A. Luttinen
France	Lunar Crater Record and Spectral Analysis	B. Bultel, **S. Werner**
Germany	Middle Devonian rocks of Germany	**A. van der Boon**, P. Königshof

Germany	Investigating ash and glendonite formation	**M. Vickers**, J. Longman, D. Evans
Hungary	Investigation of melt and fluid inclusions by confocal Raman microspectroscopy and microthermometry	**M. Capriolo**, L.E. Aradi, Cs. Szabó
Hungary	Planet formation	R. Brasser, **P. Hatalova, S. Werner**
India	Venus interior surface interaction	S. Uppalapati, **T. Rolf, S. Werner**
Iran	Geochemistry and petrology of volcanic rocks in Iran	**A. van der Boon**, M. Honarmand
Italy	Large Igneous Provinces petrogenetic processes (CAMP and Deccan Traps)	**S. Callegaro, M. Capriolo**, A. Marzoli
Japan	Crater Records on Icy Moons	E. Wong, R. Brasser, **S. Werner**
Netherlands	Micromagnetic and paleointensity measurements of Devonian igneous rocks	**A. van der Boon**, L. de Groot, R. de Boer
Netherlands	Geochemistry and petrology of volcanic rocks in Iran	**A. van der Boon**, P. Mason
Netherlands	Biomarkers from glendonite -bearing strata of IODP exp 396 cores	**M. Vickers**, A. Sluijs, F. Peterse
Netherlands	Paleomagnetic data-analysis	**L. Gallo**, B. Vaes, D. van Hinsbergen
Poland	Supervision of PhD project on cosmogenic nuclides in meteorites	**A**. **Krzesinska**, Z. Tyminski, E. Iller
Sweden	Oxygen and sulphur isotope geochemistry	**S. Callegaro, M. Capriolo,** F. M. Deegan, R. Merle, M. J. Whitehouse
Sweden	Contact metamorphism around Siberian Traps sills	**S. Callegaro, H. H. Svensen**, F. M. Deegan
Switzerland	Clumped isotope thermometry of glendonites	**M. Vickers**, S. Bernasconi
Switzerland	Science communication and outreach, graphics and presenting	**G. Shephard**, F. Crameri
UK	Minor and trace element geochemistry of glendonites	**M. Vickers**, C. Ullmann

International cooperation

Country	Activity	Person(s) involved (CEED members in bold)
UK	Synthesys Project: Alteration mineralogy of the Chassigny martian meteorite as an indicator of source and geochemical properties of subsurface fluids within the martian crust	**A. Krzesinska**, P. Schofield
USA	Investigating Oligocene/ Neogene glendonites from Alaska	**M. Vickers**, J. Counts
USA	Ti-in-quartz geothermobarometry and cathodoluminescence	**M. Capriolo**, M. Ackerson
USA	Integrating anisotropic viscosity calculations into ASPECT	**A.Kiraly**, R. Gassmoeller, J. Dannberg, M. Fraters, L. Hansen
USA	An optimization method for paleomagnetic Euler pole analysis	**L. Gallo, M. Domeier**
USA	The onset of cometary activity	**J. Luu**, D. Jewitt
USA	Destruction of small bodies in the solar system	**J. Luu**, D. Jewitt

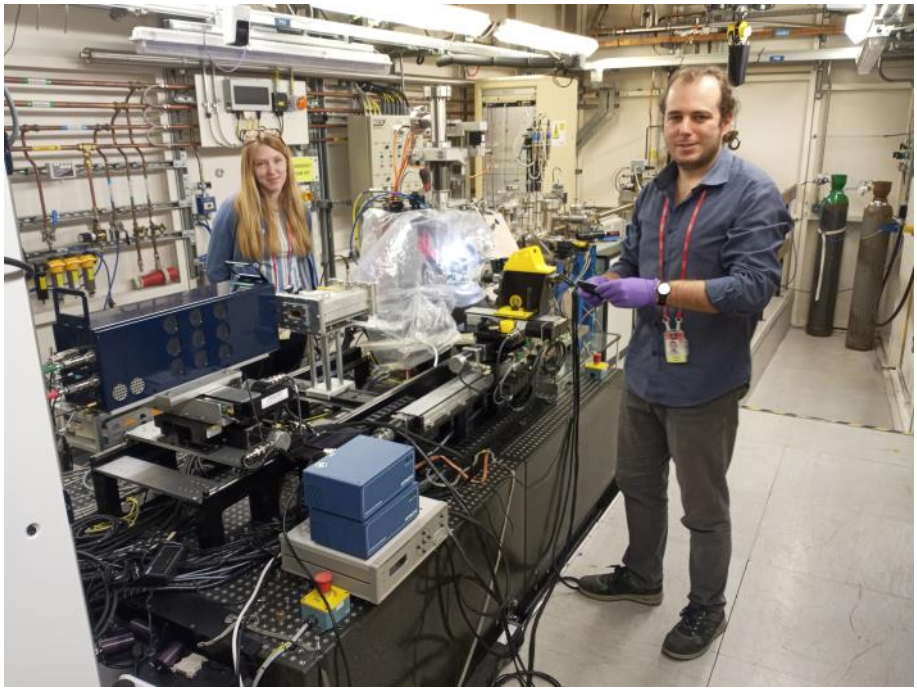

Sample change in the experimental hutch of beamline I18 at Diamond Synchrotron Light Source (UK). The experimental session (April 2022) was led by Sara Callegaro (CEED) and aimed to investigate augite crystals from Large Igneous Provinces by Synchrotron X-ray fluorescence. Raven Polk (McGill University) and Manfredo Capriolo (CEED) are standing in the picture.

EGU sessions by CEED members	
MAL46: SSP Division Outstanding ECS Award Lecture by Yin Lu	Convener: M. De Batist | Co-conveners: H. Weissert, A. Fantasia, **M. Vickers**
SSP1.1: Open session on stratigraphy, sedimentology and palaeontology.	Convener: S. Lokier | Co-conveners: **M. Vickers**, A. FantasiaECS, G. A. Douillet
SSP2.4: Polar climate and environmental change throughout geological time	Convener: **M. Vickers** | Co-convener: K. K. Sliwinska
GD8.2 North Atlantic and Arctic connections: Evolution, structure and landscapes	Convener: A. Smyrak-Sikora | Co-conveners: **G. E. Shephard,** R. Steffen, O. Anfinson
PS4.5 Mars Science and Exploration	Convener: B. Bultel | Co-conveners: **A. Krzesinska**, A. Piccialli, J. Flahaut, X. Long
GD5.2: Subduction dynamics, volatiles and melts: Investigations from surface to deep mantle	Convener: **Á. Király**ECS | Co-conveners: O. H. Göğüş, T. Gerya, J. van Hunen
TS9.1 Analogue and numerical modelling of tectonic processes	Convener: F. Zwaan | Co-conveners: **V. Magni**, M. RudolfECS, **Á. Király**ECS, F. Corbi
TS 7.4 Merged Sessions: "A trans-disciplinary view of the Tethyan realm through space and time: subduction and collisional zones from the Mediterranean to southeast Asia" and "The Arabian Plate and its surroundings – past and present"	Convener: D. GürerECS | Co-conveners: A. Scharf, **Á. Király**ECS, C. Piromallo, A. ParsonsECS, F. Mattern

AGU sessions by CEED members	
DI53A: Advances in Mantle Convection and Planetary Evolution	Convener: X. Bao | Co-Conveners: K.A. O'Farrell, B.J. Foley, D. Degen, J. Dannberg, **T. Rolf**, M. Rudolph, S. Ghelichkhan

Conferences organized by CEED

Date	Title and organizers (bold: organizers from CEED)
1.3.	The 9th CEED birthday symposium: Earth and Life Evolution (**T.H. Torsvik, N.M. Thorud, T. Sannesmoen)**
31.07-06.08	Nordic paleomagnetic workshop **(T. H. Torsvik)**
13.11-19.11	Earth's History, Dynamics and Planetary Habitability **(T.H. Torsvik, S. Werner, V. Magni, A. Kiraly, M.T. Jones, T. Sannesmoen)**
7.12-9.12	The Christmas Symposium **(T. Sannesmoen)**
28.02.23	All Things must pass: CEED Closure **(T. H. Torsvik, T. Sannesmoen)**

Illustration made for the 9th birthday symposium by: Grace Shephard.

Workshops, lab work, research stay outside UiO		
10-21.01	Research stay, optical microscopy and sample preparation, University of Padova, Italy.	M. Capriolo
21.01-04.02	Research stay, confocal Raman microspectroscopy, University of Budapest, Hungary.	M. Capriolo
2-28.03	Clumped isotope measurements and lab work , ETH Zürich, Switzerland.	M. Vickers
3.4-28.8	Research stay, FTIR analysis of volcanic ash, University of Iceland.	E. W. Stokke

Workshops, lab work, research stay outside UiO		
8-11.4 and 22-26.9	Synchrotron work, Diamond Light Source, UK.	S. Callegaro, M. Capriolo
20-28.4	Core sampling party for IODP EXP396, MARUM, Bremen, Germany.	S. Planke, M. Vickers, H. H. Svensen, D. Jerram
9.5-8.6	Research stay, SEM/EDX analysis, Natural History Museum London, England.	A. Krzesinska
15-24.5	ASPECT Hackathon, Cody, Wyoming, USA.	Á. Király, Y. Wang, M. Weerdesteijn
21.6-28.6	Paleomagnetic measurements and lab work, Fort Hoofddijk paleomagnetic laboratory, the Netherlands.	Organizer: A. van der Boon
27-29.6 and 29-31.8	Research stay, SIMS analysis and sample preparation, National Museum of Natural History, Stockholm, Sweden.	M. Capriolo
15-19.8	Core logging and sampling (IODP 396), MARUM, Bremen, Germany.	M. Vickers, E. Dowding
5-9.9	Understanding Oxygen fugacity in Geoscience school, University of Trieste, Italy.	M. Capriolo
15.9	IGV Research Seminar, Stockholm University, Sweden.	Speaker: M. Vickers
25-30.9	ICDP 2022 Training Course, Geozentrum KTB, Windischeschenbach, Germany.	M. Vickers
3-14.10 and 31.10-11.11	Organic biomarker extraction and analysis, University of Utrecht, the Netherlands.	Organizer: M. Vickers
18-21.10	SVALCLIME ECORD-ICDP MagellanPlus workshop, UNIS Svalbard. *Speakers: S. Planke, M. Jones, M. Vickers, A. van der Boon. Other participants: L. Gallo, G. Shephard.	Organizers*: S. Planke, M. Jones.
21-23.11	NorthGreen- ECORD-ICDP MagellanPlus workshop, Copenhagen, Denmark.	Speaker: G. Shephard. Other participants: M. Vickers
23-28.11	Synchrotron work, Paul Scherrer Institute, Switzerland.	M. Vickers

Field work in Europe		
1-3.5	Sampling in Northern Denmark: Paleogene sediments hosting glendonites.	M. Vickers
2-8.5	Highland border Complex in Scotland, UK: Alteration of highland border peridotites.	T. B. Andersen, H. Austrheim
5.8	Sampling of molten lava, Meradalir, Iceland: Training in volcanology.	E. W. Stokke
19-29.10	Paleomagnetic fieldwork in the Orkney islands, UK: Paleozoic plate tectonic reconstructions and paleointensity.	M. Domeier, A. van der Boon
Field work in Norway		
29.03-03.04	Fieldwork in Svalbard	S. Planke, M. Vickers
30.05-15.06	Paleomagnetic fieldwork in northern Norway: Ediacaran paleomagnetism of the Varanger peninsula	M. Domeier, L. Gallo
21.07-24.07	Paleomagnetic fieldwork in Honningsvåg	T. H. Torsvik, S. Werner, A. van der Boon
Summer	Fieldwork in the Oslo Rift are (e.g. Gran)	H. H. Svensen, S. Callegaro, M. Capriolo, H. J. Kjøll, S. Planke

Fieldwork outside Europe		
April-June	Magnetotellurics Fieldwork in Greenland: MAGPIE Fieldwork on the Greenland Ice Sheet.	C. Conrad, K. Selway
28.11-14.12	Paleomagnetic fieldwork in Paraguay: Ediacaran paleomagnetism	M. Domeier, L. Gallo

Project funding in 2022

UiO project #	Projects, project leader	Total funding in 2022
100050001	123272 Centre for Earth Evolution and Dynamics, Gaina (2013-23),	22 114
100061001	246929/F20 Clim-VoTe, ISP-Geofag, Niscancioglu (2015-20)	51
100083001	249040/F60 DEEP Research school, Werner (2016-23)	2 324
100264001	276032 Platonics, Rolf (2018-22)	1 224
100345001	288449 Magpie, Conrad (2019-23)	3 967
100521001	301096 Maples, Callegaro (2020-23)	2 648
100566001	309477 Nor-R-Am II, Gaina (Intpart 2020-23)	1 235
100145101	314742/F20 Anima, Kiraly. (2021-25)	1 602
100688101	322421/E40 Strain Partitioning and Decoupling in Hornsund during the Ellesmerian and Eurekan orogenies, Koehl. (2021)	21
102596101	328697/E40 Research in Svalbard: An APECS workshop, Shephard. (2021-22)	46
102880101	326238/F20 Polaris, Shephard. (2021-25)	11
102820101	325567/F20 HIDDEN, Caracas. (2021-25)	1 993
103080101	325984/F20 DYPOLE, Faleide. (2021-25)	1 398
690591	RO-NO-2019-0428 Baja Mare, Gaina (EØS, with Romania 2020-23)	1 885
690604	456924 Poles together, Augland (EØS with Poland 2020-23)	1 129
102545101	101025975 Tango, Gallo. (MSCA 2021-2023)	1 138
102824101	101030364 Bouldering, Prieur. (MSCA 2021-2023)	983
102822101	101024218 Icecap. Vickers. (MSCA 2021-2023)	1000
103888101	101043844 ERC EPIC Horizon, Domeier (2022-2027)	644
UiO funding	Strategy grant (2013-22) in kkr	2 000
UiO funding	UiO contribution (Egenandel)	28 119

** in kkr*

Invited guest lectures at CEED

1. Burning shales, acid ponds, and toxic waters—the long term impact of Cretaceous volcanism on the Canadian Arctic. Jan. 27, 2022, 13:15-14:00, Zoom, by Stephen E. Grasby from Geological Survey of Canada. Hosted by Henrik Svensen.
2. Deciphering Supercontinent Cycles and Global Geodynamics: Paleomagnetic data from the Grand Canyon. Feb. 17, 2022, 13:15-14:00, Zoom, by Athena Eyster from the John Hopkins University. Hosted by Clint Conrad.
3. Planetary lava tubes exploration and the DAEDALUS mission concept. Feb. 24, 2022, 13:15-14:00, Zoom, by Riccardo Pozzobon from University of Padova. Hosted by Sara Callegaro.
4. Perturbation of the deep-Earth carbon cycle in response to the Cambrian Explosion. Mar. 3, 2022, 13:15-14:00, Aud. 3, by Andrea Giuliani from ETH, Zurich. Hosted by Reidar Trønnes.
5. Seismic geomorphology and stratigraphy of volcanoes buried in sedimentary basins and their impact on geoenergy exploration. Mar. 10, 2022, 13:15-14:00, Aud. 3, by Alan Bischoff from the Geological Survey of Finland. Hosted by Sverre Planke.
6. Unlocking seasonal climate records from modern and fossil tree-rings. Mar. 24, 2022, 13:15-14:00, Aud. 3, by William Lukens from James Madison University. Hosted by Anne Hope Jahren.
7. Lost continents and preserved primordial reservoirs: A history both ancient and deep. Mar. 31, 2022, 17:15-18:00, Zoom, by Matthew Jackson from the University of California, Santa Barbara. Hosted by Reidar Trønnes.
8. The chalk of NW Europe: from the birth of the chalk to the end of an era. Apr. 7, 2022, 13:15-14:00, Aud. 3/Zoom, by Nicolas Thibault from the University of Copenhagen. Hosted by Madeleine Vickers.
9. Explosive submarine eruptions. Apr. 21, 2022, 13:15-14:00, Aud. 3, by Michael Manga from UC Berkeley. Hosted by Adriano Mazzini.
10. Analogue modelling of inversion tectonics: investigating the role of multiple extensional basins in foreland fold-and-thrust belts. Apr. 28, 2022, 13:15-14:00, Aud. 3, by Nicolas Molnar from RWTH Aachen University. Hosted by Ágnes Király.
11. How are mountains and basins formed by lithosphere dynamics in the southeast Carpathians? May 5, 2022, 13:15-14:00, Aud. 3, by Oğuz Göğüş from Istanbul University. Hosted by Ágnes Király.
12. The DART Mission and Planetary Defense: A Crash Course. May 12, 2022, 13:15-14:00, Aud. 3, by Andy Rivkin from Nasa/JPL. Hosted by Anne Hope Jahren.
13. Vulcan's Secret: what volcanic compositions tell us about upper mantle dynamics. May 19, 2022, 13:15-14:00, Aud. 3, by Marthe Klöcking from Georg-August University, Göttingen. Hosted by Alexander Minakov.
14. A Dynamic Lithosphere-Asthenosphere Boundary beneath Middle Atlantic Ridge. June 2, 2022, 13:15-14:00, Aud. 3, by Shunguo Wang from NTNU. Hosted by Clint Conrad.
15. On survival and destruction of cratons. Sep. 8, 2022, 13:15-14:00, Aud.3, by Jyotirmoy Paul from the University of Bayreuth. Hosted by Clint Conrad.
16. Micromagnetic Tomography for Paleomagnetism and Rock-Magnetism. Sep. 15, 2022, 13:15-14:00, Aud. 3, by Lennart de Groot from Utrecht University. Hosted by Mat Domeier.

17. Christopher Hansteen and the search for a magnetic pole in Siberia. Sep. 30, 2022, Aud. 3, by Vidar Enebakk from the Norwegian National Committees for Research Ethics. Hosted by Annique van der Boon.
18. Carbon release & sequestration during extreme global climatic change events in Earth history. Oct. 6, 2022, 13:15-14:00, Aud. 3, by Weimu Xu from the University College of Dublin. Hosted by Morgan Jones.
19. Ending the Early Eocene Hothouse and the role of the Arctic Azolla phenomenon. Oct. 20, 2022, 13:15-14:00, Aud. 3, by Henk Brinkhus from Utrecht University. Hosted by Henrik Svensen.
20. Using Sulfur Cycle Proxies to Understand Mass Extinction Events. Oct. 27, 2022, 13:15-14:00, Aud. 3, by Robert Newton from University of Leeds. Hosted by Manfredo Capriolo.
21. The anomalous geomagnetic field at the Ediacaran-Cambrian transition—how much do we really know? Nov. 3, 2022, 15:15-16:00, Aud. 3, by Daniele Thalner from University of Florida. Hosted by Annique van der Boon.
22. Making the Ocean Floor: Two-phase dynamics of mantle melting and formation of oceanic lithosphere. Nov. 10, 2022, 13:15-14:00, Aud. 3, by Adina Püsök from the University of Oxford. Hosted by Valentina Magni.
23. Building mountainous islands in South-East Asia: a multi-faceted climate cooling process. Dec. 1, 2022, 13:15-14:00, Aud. 3, by Pierre Maffre from the University of California, Berkeley. Hosted by Chloé Markussen Marcilly.
24. Rapid shifting of a deep magmatic source at Fagradalsfjall volcano, Iceland. Dec. 2, 2022, 15:15-16:00, Aud. 3, by Alberto Caracciolo from the University of Iceland. Hosted by Ella Wulfsberg Stokke.

The Wilson lecture is an annual public lecture within the fields of Geosciences, arranged by CEED. The lecture for 2022 was unfortunately cancelled.

Scientific publications *: young CEED scientist as first author: 14

1. **Abdelmalak, Mohamed Mansour**; **Gac, Sebastien**; **Faleide, Jan Inge**; **Shephard, Grace**; Tsikalas, Filippos; Polteau, Stephane; Zastrozhnov, Dmitry; **Torsvik, Trond Helge**. Quantification and Restoration of the Pre-Drift Extension Across the NE Atlantic Conjugate Margins During the Mid-Permian-Early Cenozoic Multi-Rifting Phases. Tectonics 2022 ;Volum 42.(1) UiO IFE
2. **Andersen, Torgeir Bjørge**; Jakob, Johannes; Kjøll, Hans Jørgen; Tegner, Christian. Vestiges in the Pre-Caledonian Passive Margin of Baltica in the Scandinavian Caledonides: Overview, Revisions and Control on the Structure of the Mountain Belt. Geosciences 2022 ;Volum 12.(57) NGU UiO
3. Anfinson, Owen A.; Odlum, Margo L.; Piepjohn, Karsten; Poulaki, Eirini M.; **Shephard, Grace**; Stockli, Daniel F.; Levang, Devin; Jensen, Maria; Pavlovskaia, Elena. Provenance Analysis of the Andrée Land Basin and Implications for the Paleogeography of Svalbard in the Devonian. Tectonics 2022 ;Volum 41.(11) UNIS UiO
4. Antunes, Verónica; Planès, Thomas; Obermann, Anne; Panzera, Francesco; D'Amico, Sebastiano; **Mazzini, Adriano**; Sciarra, Alessandra; Ricci, Tullio; Lupi, Matteo. Insights into the dynamics of the Nirano Mud Volcano through seismic characterization of drumbeat signals and V/H analysis. Journal of Volcanology and Geothermal Research 2022 ;Volum 431. UiO
5. Bajard, Manon Juliette Andree; **Ballo, Eirik Gottschalk**; Høeg, Helge Irgens; Bakke, Jostein; Støren, Eivind Wilhelm Nagel; Loftsgarden, Kjetil; Iversen, Frode; **Hagopian, William Martin**; **Jahren, Anne Hope Florine**; **Svensen, Henrik Hovland**; **Krüger, Kirstin**. Climate adaptation of pre-Viking societies. Quaternary Science Reviews 2022 ;Volum 278. UiO UiB
6. Baker, Don R; **Callegaro, Sara**; De Min, Angelo; Whitehouse, Martin J.; Marzoli, Andrea. Fluorine Partitioning between Quadrilateral Clinopyroxenes and Melt. Am. Mineral. 2022, 107, 167–177, doi:10.2138/am-2021-7868.
7. Banjan, Mathilde; Christian, Crouzet; Pierre, Sabatier; Hervé, Jomard; Bajard, Manon Juliette Andree; Francois, Demory; Anne-Lise, Develle; Jean-Philippe, Jenny; Bernard, Fanget; Emmanuel, Malet; Findling, Nathaniel; Philippe, Alain; Julien, Didier; Vincent, Bichet; Sylvain, Clapot; Erwan, Messager. Did the Younger Dryas to Holocene climate transition favour high seismicity rates in the north-western Alps?. Sedimentology 2022 ;Volum 70.(2) s.538-568 UiO
8. Baziotis, Ioannis; Xydous, Stamatios; Papoutsa, Angeliki; Hu, Jinping; Ma, Chi; Klemme, Stephan; Berndt, Jasper; Ferrière, Ludovic; **Caracas, Razvan**; Asimow, Paul D.. Jadeite and related species in shocked meteorites: Limitations on inference of shock conditions. American Mineralogist 2022 ;Volum 107.(10) s.1868-1877 UiO
9. Bellwald, Benjamin; Stokke, Henrik Henriksen; Winsborrow, Monica; **Planke, Sverre**; Sættem, Joar; Lebedeva-Ivanova, Nina; Hafeez, Amer; Kurjanski, Bartosz; Myklebust, Reidun Alice; Polteau, Stephane. Structural and fluid-migration control on hill-hole pair formation: Evidence from high-resolution 3D seismic data from the SW Barents Sea. Geomorphology 2022 ;Volum 420. IFE UiO UiT
10. Blischke, Anett; Brandsdóttir, Bryndís; Stoker, Martyn S.; **Gaina, Carmen**; Erlendsson, Ögmundur; Tegner, Christian Maughan; Halldórsson, Sæmundur A.; Helgadóttir, Helga M.; Gautason, Bjarni; **Planke, Sverre**; Koppers, Anthony A. P.; Hopper, John R.. Seismic Volcanostratigraphy: The Key to Resolving the Jan Mayen Microcontinent and Iceland Plateau Rift Evolution. Geochemistry Geophysics Geosystems 2022 ;Volum 23. (4) UiO
11. Bono, R.K.; Paterson, G.A.; **van der Boon, A.**; Engbers, Y.A.; Michael Grappone, J.; Handford, B.; Hawkins, L.M.A.; Lloyd, S.J.; Sprain, C.J.; Thallner, D.; et al. The PINT Database: A Definitive Compilation of Absolute Palaeomagnetic Intensity Determinations since 4 Billion Years Ago. Geophys. J. Int. 2022, 229, 522–545, doi:10.1093/gji/ggab490.

12. Boscaini, Andrea; **Callegaro, Sara**; Sun, Yadong; Marzoli, Andrea. Late Permian to Late Triassic Large Igneous Provinces: Timing, Eruptive Style and Paleoenvironmental Perturbations. Frontiers in Earth Science 2022 ;Volum 10. UiO
13. Boscaini, Andrea; Marzoli, A; Bertrand, Hervé; Chiaradia, Massimo; Jourdan, Fred; Faccenda, Manuele; Meyzen, Christine M; **Callegaro, Sara**; Serrano Duràn, Lina Maria. Cratonic keels controlled the emplacement of the Central Atlantic Magmatic Province (CAMP). Earth and Planetary Science Letters 2022 ;Volum 584. UiO
14. Brož, P., Oehler, D., **Mazzini, A**., Hauber, E., Komatsu, G., Etiope, G., and Cuřín, V.: An overview of sedimentary volcanism on Mars, EGUsphere [preprint], https://doi.org/10.5194/egusphere-2022-1458, 2023
15. Brož, P.; Hauber, E.; Conway, S.J.; Luzzi, E.; **Mazzini, Adriano**; Noblet, A.; Jaroš, J.; Fawdon, P.; Markonis, Y.. New evidence for sedimentary volcanism on Chryse Planitia, Mars. Icarus (New York, N.Y. 1962) 2022 ;Volum 382. UiO
16. Bulut, N; Thybo, H; **Maupin, Valerie**. Highly heterogeneous upper-mantle structure in Fennoscandia from finite-frequency P-body-wave tomography. Geophysical Journal International 2022 ;Volum 230.(2) s.1197-1214 UiO
17. Bögels, T.F.J.; **Caracas, Razvan**. Critical point and supercritical regime of MgO. Physical review B (PRB) 2022 ;Volum 105.(6) UiO
18. Caballero, J.A.; González-Álvarez, E.; Brady, M.; Trifonov, T.; Ellis, T.G.; Dorn, C.; Cifuentes, C.; Molaverdikhani, K.; Bean, J.L.; Boyajian, T.; Rodríguez, E.; Sanz-Forcada, J.; Zapatero Osorio, Osorio; Abia, C.; Amado, P.J.; Anugu, N.; Béjar, V.J.S.; Davies, C.L.; Dreizler, S.; Dubois, F.; Ennis, J.; Espinoza, N.; Farrington, C.D.; López, A. García; Gardner, T.; Hatzes, A.P.; Henning, Th.; Herrero, E.; Herrero-Cisneros, E.; Kaminski, A.; Kasper, D.; Klement, R.; Kraus, S.; Labdon, A.; Lanthermann, C.; Le Bouquin, Bouquin; González, M. J. Lópej; Luque, R.; Mann, A.W.; Marfil, E.; Monnier, J.D.; Montes, D.; Morales, J.C.; Pallé, E.; Pedraz, S.; Quirrenbach, A.; Reffert, S.; Reiners, A.; Ribas, I.; Rodríguez-López, C.; Schaefer, G.; Schweitzer, A.; Seifahrt, A.; Setterholm, B.R.; **Shan, Yutong**; Shulyak, D.; Solano, E.; Sreenivas, K.R.; Stefánsson, G.; Stürmer, J.; Tabernero, H.M.; Tal-Or, L.; Ten Brummelaar, Brummelaar; Vanaverbeke, S.; Von Braun, Braun; Youngblood, A.; Zechmeister, M.. A detailed analysis of the Gl 486 planetary system. Astronomy and Astrophysics (A & A) 2022 ;Volum 665. UiO
19. ***Capriolo, Manfredo**; Mills, Benjamin J.W.; Newton, Robert J.; Dal Corso, Jacopo; Dunhill, Alexander M.; Wignall, Paul B.; Marzoli, Andrea. Anthropogenic-scale CO2 degassing from the Central Atlantic Magmatic Province as a driver of the end-Triassic mass extinction. Global and Planetary Change 2022 ;Volum 209. UiO
20. ***Cordoba, Antonio Manjon Cabeza**; Ballmer, Maxim D.. The role of edge-driven convection in the generation ofvolcanism - Part 2: Interaction with mantle plumes, applied to the Canary Islands. Solid Earth (SE) 2022 ;Volum 13.(10) s.1585-1605 UiO
21. **Corfu, Fernando**; **Andersen, Torgeir Bjørge**. A hyperextension assemblage, imbricated in Archean– Paleoproterozoic crust, at the base of the Kalak Nappe Complex in the northern Scandinavian Caledonides. Journal of the Geological Society 2022 ;Volum 179.(4) UiO
22. Corseri, Romain; **Planke, Sverre**; Gelius, Leiv Jacob; **Faleide, Jan Inge**; Senger, Kim; **Abdelmalak, Mohamed Mansour**. Magnetotelluric image of a hyper-extended and serpentinized rift system. Earth and Planetary Science Letters 2022 ;Volum 602. UiO UNIS
23. Cramwinckel, M.J.; van der Ploeg, R.; van Helmond, N.A.G.M.; Waarlo, N.; Agnini, C.; Bijl, P.K.; **van der Boon, A**.; Brinkhuis, H.; Frieling, J.; Krijgsman, W.; et al. Deoxygenation and Organic Carbon Sequestration in the Tethyan Realm Associated with the Middle Eocene Climatic Optimum. GSA Bull. 2022, doi:10.1130/B36280.1.

24. Dal Corso, Jacopo; Song, Haijun; **Callegaro, Sara**; Chu, Daoliang; Sun, Yadong; Hilton, Jason; Grasby, Stephen E.; Joachimski, Michael; Wignall, Paul B.. Environmental crises at the Permian–Triassic mass extinction. Nature Reviews Earth & Environment 2022 ;Volum 3. s.197-214 UiO
25. ***Davis, Anne**; Solomatova, Natalia V.; Campbell, Andrew; **Caracas, Razvan**. The speciation and coordination of a deep Earth carbonate-silicate-metal melt. Journal of Geophysical Research (JGR): Solid Earth 2022 ;Volum 127.(3) UiO
26. Deegan, Frances M.; Bédard, Jean H.; Grasby, Stephen E.; Dewing, Keith; Geiger, Harri; Misiti, Valeria; **Capriolo, Manfredo**; **Callegaro, Sara**; **Svensen, Henrik Hovland**; Yachimchuk, Chris; Aradi, László E.; Freda, Carmela; Troll, Valentin R. Magma–Shale Interaction in Large Igneous Provinces: Implications for Climate Warming and Sulfide Genesis. Journal of Petrology 2022 ;Volum 63.(9) s.1-10 UiO
27. Drewitt, J.W.E.; Walter, M.J.; **Brodholt, J.P**.; Muir, J.M.R.; Lord, O.T. Hydrous Silicate Melts and the Deep Mantle H2O Cycle. Earth Planet. Sci. Lett. 2022, 581, 117408, doi:10.1016/j.epsl.2022.117408.
28. Ezad, I.S.; Dobson, D.P.; Thomson, A.R.; Jennings, E.S.; Hunt, S.A.; **Brodholt, J.P**. Kelyphite Textures Experimentally Reproduced through Garnet Breakdown in the Presence of a Melt Phase. J. Petrol. 2022, 63, doi:10.1093/petrology/egac110.
29. Ezad, I.S.; Einsle, J.F.; Dobson, D.P.; Hunt, S.A.; Thomson, A.R.; **Brodholt, J.P.** Improving Grain Size Analysis Using Computer Vision Techniques and Implications for Grain Growth Kinetics. Am. Mineral. 2022, 107, 262–273, doi:10.2138/am-2021-7797.
30. Frank, Thomas; Åkesson, Henning; Fleurian, Basile de; Morlighem, M.; **Nisancioglu, Kerim Hestnes**. Geometric controls of tidewater glacier dynamics. The Cryosphere 2022 ;Volum 16.(2) s.581-601 UiO UiB
31. Fu, Hairuo; Jacobsen, Stein B.; Larsen, Bjørn Tore; Eriksen, Zachary T.. Ca-isotopes as a robust tracer of magmatic differentiation. Earth and Planetary Science Letters 2022 ;Volum 594. UiO
32. ***Gallo, Leandro Cesar**; Sapienza, Facundo; **Domeier, Mathew Michael**. An optimization method for paleomagnetic Euler pole analysis. Computers & Geosciences 2022 ;Volum 166. UiO
33. Gaynor, Sean P.; **Svensen, Henrik Hovland**; Polteau, Stephane; Schaltegger, Urs. Local melt contamination and global climate impact: Dating the emplacement of Karoo LIP sills into organic-rich shale. Earth and Planetary Science Letters 2022 ;Volum 579. UiO IFE
34. Gupta, S.; Schmidt, C.; Böttner, C.; Rüpke, L.; Hartz, Ebbe Hvidegård. Spontaneously Exsolved Free Gas During Major Storms as an Ephemeral Gas Source for Pockmark Formation. Geochemistry Geophysics Geosystems 2022 ;Volum 23.(8) UiO
35. He, Zhiyu; Rödel, Melanie; Lütgert, Julian; Bergermann, Armin; Bethkenhagen, Mandy; Chekrygina, Deniza; Cowan, Thomas E.; Descamps, Adrien; French, Martin; Galtier, Eric; Gleason, Arianna E.; Glenn, Griffin D.; Glenzer, Siegfried H.; Inubushi, Yuichi; Hartley, Nicholas J.; **Hernandez, Jean-Alexis**; Heuser, Benjamin; Humphries, Oliver S.; Kamimura, Nobuki; Katagiri, Kento; Khaghani, Dimitri; Lee, Hae Ja; McBride, Emma E.; Miyanishi, Kohei; Nagler, Bob; Ofori-Okai, Benjamin; Ozaki, Norimasa; Pandolfi, Silvia; Qu, Chongbing; Ranjan, Divyanshu; Redmer, Ronald; Schoenwaelder, Christopher; Schuster, Anja K.; Stevenson, Michael G.; Sueda, Keiichi; Togashi, Tadashi; Vinci, Tommaso; Voigt, Katja; Vorberger, Jan; Yabashi, Makina; Yabuuchi, Toshinori; Zinta, Lisa M.V.; Ravasio, Alessandra; Kraus, Dominik. Diamond formation kinetics in shock-compressed C-H-O samples recorded by small-angle x-ray scattering and x-ray diffraction. Science Advances 2022 ;Volum 8.(35) UiO
36. ***Hernandez, Jean-Alexis**; **Caracas, Razvan**; Labrosse, Stéphane. Stability of high-

temperature salty ice suggests electrolyte permeability in water-rich exoplanet icy mantles. Nature Communications 2022 ;Volum 13. UiO

37. ***Hernandez, Jean-Alexis; Mohn, Chris Erik**; Guren, Marthe Grønlie; Baron, Marzena Anna; Trønnes, Reidar G. Ab Initio Atomistic Simulations of Ca-Perovskite Melting. Geophysical Research Letters 2022 ;Volum 49.(20) UiO
38. ***Heyn, Björn Holger**; **Conrad, Clinton Phillips**. On the Relation Between Basal Erosion of the Lithosphere and Surface Heat Flux for Continental Plume Tracks. Geophysical Research Letters 2022 ;Volum 49.(7) UiO
39. Huang, D.; **Brodholt, J.P**.; Sossi, P.; Li, Y.; Murakami, M. Nitrogen Speciation in Silicate Melts at Mantle Conditions From Ab Initio Simulations. Geophys. Res. Lett. 2022, 49, doi:10.1029/2021GL095546.
40. Huang, D.; Murakami, M.; **Brodholt, J.P**.; McCammon, C.; Petitgirard, S. Structural Evolution in a Pyrolitic Magma Ocean under Mantle Conditions. Earth Planet. Sci. Lett. 2022, 584, 117473, doi:10.1016/j.epsl.2022.117473.
41. Jakob, Johannes; **Andersen, Torgeir Bjørge**; Mohn, Geoffroy; Kjøll, Hans Jørgen; Beyssac, Olivier. Revised tectono-stratigraphic scheme for the Scandinavian Caledonides and its implications for our understanding of the Scandian orogeny. I:New Developments in the Appalachian-Caledonian-Variscan Orogen. Geological Society of America 2022 ISBN 978-0-8137-2554-3. s.335-374 NGU UiO
42. Jakob, Johannes; Kjøll, Hans Jørgen; **Andersen, Torgeir Bjørge**. A Fossil Magma-rich Rifted Margin in the Scandinavian Caledonides. I: Continental Rifted Margins 2: Case examples. ISTE 2022 ISBN 9781789450620. s.185-202 NGU UiO
43. **Jerram, Dougal Alexander**; Caddick, Mark. The Field Description of Metamorphic Rocks. Wiley-Blackwell 2022 (ISBN 9781118618752) UiO
44. **Jones, Morgan Thomas**. Seismic Characteristics of the Largest Measured Subglacial Flood from the Eastern Skaftá cauldron, Iceland. Earth Surface Dynamics 2022 UiO
45. Kim, Y.; Jewitt, D.; **Luu, J**.; Li, J.; Mutchler, M. Comet 108P/Ciffreo: The Blob. Astron. J. 2023, 165, 150, doi:10.3847/1538-3881/acba07.
46. ***Koehl, Jean-Baptiste P**.; Bergh, Steffen Gunnar; Sylvester, Arthur G.. Tectonic evolution of the Indio Hills segment of the San Andreas fault in southern California, southwestern USA. Solid Earth (SE) 2022 ;Volum 13.(8) s.1169-1190 UiT UiO
47. ***Koehl, Jean-Baptiste Philippe**; Magee, Craig; Anell, Ingrid. Impact of Timanian thrust systems on the late Neoproterozoic–Phanerozoic tectonic evolution of the Barents Sea and Svalbard. Solid Earth (SE) 2022 ;Volum 13.(1) s.85-115 UiT UiO
48. Kolyukhin, Dmitriy; **Minakov, Alexander**. Simulation of Gaussian random field in a ball. Monte Carlo Methods and Applications 2022 ;Volum 28.(1) s.85-95 UiO
49. **Kulakov, Evgeniy**; Slagstad, Trond; Ganerød, Morgan; **Torsvik, Trond Helge**. Paleomagnetism and 40Ar/39Ar geochronology of Meso-Neoproterozoic rocks from southwest Norway. Implications for magnetic remanence ages and the paleogeography of Baltica in a Rodinia supercontinent context. Precambrian Research 2022 ;Volum 379. NGU UiO
50. **Kulakov, Evgeniy**; **Torsvik, Trond Helge**. Comment on “Paleomagnetism of the Guanyang Devonian sedimentary successions in Guangxi province, South China” by Wu et al. Gondwana Research 2022 ;Volum 107. s.66-72 UiO
51. Li, Yunguo; Guo, Xuan; Voadlo, Lidunka; **Brodholt, John Peter**; Ni, Huaiwei. The effect of water on the outer core transport properties. Physics of the Earth and Planetary Interiors 2022 ;Volum 329-330. UiO
52. Li, Yunguo; Voadlo, Lidunka; Ballentine, Chris; **Brodholt, John Peter**. Primitive noble gases sampled from ocean island basalts cannot be from the Earth’s core. Nature Communications 2022 ;Volum 13. UiO
53. Li, Yunguo; Voadlo, Lidunka; **Brodholt, John Peter**. ElasT: A toolkit for thermoelastic calculations. Computer Physics Communications 2022 ;Volum 273. UiO

54. Loizeau, Damien; Pilorget, Cédric; Poulet, François; Lantz, Cateline; Bibring, Jean-Pierre; Hamm, Vincent; Royer, Clément; Dypvik, Henning; **Krzesinska, Agata Magdalena**; Rull, Fernando; **Werner, Stephanie C**.. Planetary Terrestrial Analogues Library Project: 3. Characterization of Samples with MicrOmega. Astrobiology 2022 ;Volum 22.(3) s.263-292 UiO
55. Longman, Jack; Palmer, Martin R.; Gernon, Thomas M.; Manners, Hayley R.; **Jones, Morgan Thomas**. Subaerial volcanism is a potentially major contributor to oceanic iron and manganese cycles. Communications Earth & Environment 2022 ;Volum 3.(1) UiO
56. Lupi, Matteo; De Gori, Pasquale; Valoroso, Luisa; Baccheschi, Paola; Minetto, Riccardo; **Mazzini, Adriano**. Northward migration of the Javanese volcanic arc along thrust faults. Earth and Planetary Science Letters 2022 ;Volum 577. UiO
57. Luque, R.; Fulton, B.J.; Kunimoto, M.; Amado, P.J.; Gorrini, P.; Dreizler, S.; Hellier, C.; Henry, G.W.; Molaverdikhani, K.; Morello, G.; Peña-Moñino, L.; Pérez-Torres, M.; Pozuelos, F.J.; **Shan, Yutong**; Anglada-Escudé, G.; Béjar, V.J.S.; Bergond, G.; Boyle, A.W.; Caballero, J.A.; Charbonneau, D.; Ciardi, D.R.; Dufoer, S.; Espinoza, N.; Everett, M.; Fischer, D.; Hatzes, A.P.; Henning, Th.; Hesse, K.; Howard, A.W.; Howell, S.B.; Isaacson, H.; Jeffers, S.V.; Jenkins, J.M.; Kane, S.R.; Kemmer, J.; Khalafinejad, S.; Kidwell, R.C.; Kossakowski, D.; Latham, D.W.; Lillo-Box, J.; Lissauer, J.J.; Montes, D.; Orell-Miquel, J.; Pallé, E.; Pollacco, D.; Quirrenbach, A.; Reffert, S.; Reiners, A.; Ribas, I.; Ricker, G.R.; Rogers, L.A.; Sanz-Forcada, J.; Schlecker, M.; Schweitzer, A.; Seager, S.; Shporer, A.; Stassun, K.G.; Stock, S.; Tal-Or, L.; Ting, E.B.; Trifonov, T.; Vanaverbeke, S.; Vanderspek, R.; Villaseñor, J.; Winn, J.N.; Winters, J.G.; Zapatero Osorio, Osorio. The HD 260655 system: Two rocky worlds transiting a bright M dwarf at 10 pc. Astronomy and Astrophysics (A & A) 2022 ;Volum 664. UiO
58. Luspay-Kuti, Adrienn; Mousis, Olivier; Pauzat, Françoise; **Ozgurel, Ozge**; Ellinger, Yves; Lunine, Jonathan I.; Fuselier, Stephen A.; Mandt, Kathleen E.; Trattner, Karlheinz J.; Petrinec, Steven M.. Dual storage and release of molecular oxygen in comet 67P/Churyumov–Gerasimenko. Nature Astronomy 2022 ;Volum 6. s.724-730 UiO
59. Mahmoudi, Shahryar; **Corfu, Fernando**. The composite Triassic–Eocene Poshteh pluton, eastern Iran, an Eo-Cimmerian element south of the main Paleotethys suture. International journal of earth sciences 2022 ;Volum 111.(3) s.969-985 UiO
60. Manton, Ben; Müller, Philipp; **Mazzini, Adriano**; Zastrozhnov, Dmitry; **Jerram, Dougal Alexander**; Millett, John M.; Schmid, Daniel Walter; Berndt, Christian; Myklebust, Reidun Alice; **Planke, Sverre**. Characterizing ancient and modern hydrothermal venting systems. Marine Geology 2022 ;Volum 447. UiB UiO
61. ***Marcilly, Chloe M.**; Maffre, Pierre; Le Hir, Guillaume; Pohl, Alexandre; Fluteau, Frédéric; Godderis, Yves; Donnadieu, Yannick; **Heimdal, Thea Hatlen**; **Torsvik, Trond Helge**. Understanding the early Paleozoic carbon cycle balance and climate change from modelling. Earth and Planetary Science Letters 2022 ;Volum 594. UiO
62. ***Marcilly, Chloe M**.; **Torsvik, Trond Helge**; **Conrad, Clinton Phillips**. Global Phanerozoic sea levels from paleogeographic flooding maps. Gondwana Research 2022 ;Volum 110. s.128-142 UiO
63. Marins, Gabriel M.; Parizek-Silva, Yaro; Millett, John M.; **Jerram, Dougal Alexander**; Rossetti, Lucas M.M.; de Jesus e Souza, Ariany; Planke, Sverre; Bevilaqua, Leandro A.; Carmo, Isabela de O.. Characterization of volcanic reservoirs; insights from the Badejo and Linguado oil field, Campos Basin, Brazil. Marine and Petroleum Geology 2022 ;Volum 146. UiO
64. Mauerberger, Alexandra; Sadeghisorkhani, Hamzeh; **Maupin, Valerie**; Gudmundsson, Ólafur; Tilmann, Frederik. A shear-wave velocity model for the Scandinavian lithosphere from Rayleigh waves and ambient noise - Implications for the origin of the topography of the Scandes mountain range. Tectonophysics 2022 ;Volum 838. UiO

65. **Maupin, Valerie**; Mauerberger, Alexandra; Tilmann, Frederik. The Radial Anisotropy of the Continental Lithosphere From Analysis of Love and Rayleigh Wave Phase Velocities in Fennoscandia. Journal of Geophysical Research (JGR): Solid Earth 2022 ;Volum 127.(10) UiO
66. **Mazzini, A**.; Sciarra, A.; Lupi, M.; Ascough, P.; Akhmanov, G.; Karyono, K.; Husein, A. Deep Fluids Migration and Submarine Emersion of the Kalang Anyar Mud Volcano (Java, Indonesia): A Multidisciplinary Study. Mar. Pet. Geol. 2023, 148, 105970, doi:10.1016/j.marpetgeo.2022.105970
67. **Medvedev, Sergei**; Hartz, Ebbe Hvidegård; Schmid, Daniel Walter; Zakariassen, Erik; Varhaug, Per. Influence of glaciations on North Sea petroleum systems. Geological Society Special Publication 2022 ;Volum 494.(1) s.481-498 UiO
68. Moorkamp, Max; Özaydn, Sinan; **Selway, Katherine**; Jones, Alan G.. Probing the Southern African Lithosphere With Magnetotellurics—Part I: Model Construction. Journal of Geophysical Research (JGR): Solid Earth 2022 ;Volum 127.(3) UiO
69. Müller, Axel; Romer, Rolf L.; **Augland, Lars Eivind**; Zhou, Haoyang; Rosing-Schow, Nanna; Spratt, John; Husdal, Tomas. Two-stage regional rare-element pegmatite formation at Tysfjord, Norway: implications for the timing of late Svecofennian and late Caledonian high-temperature events. International journal of earth sciences 2022 ;Volum 111. s.987-1007 UiO
70. ***Ozgurel, O**.; Duflot, D.; Masella, M.; Réal, F.; Toubin, C. A Molecular Scale Investigation of Organic/Inorganic Ion Selectivity at the Air–Liquid Interface. ACS Earth Sp. Chem. 2022, 6, 1698–1716, doi:10.1021/acsearthspacechem.1c00394
71. Pedro, J.B.; Andersson, Carin; Vettoretti, G.; Voelker, A.H.L.; Waelbroeck, C.; Dokken, Trond Martin; Jensen, Mari Fjalstad; Rasmussen, S.O.; Sessford, Evangeline; Jochum, M.; **Nisancioglu, Kerim Hestnes**. Dansgaard-Oeschger and Heinrich event temperature anomalies in the North Atlantic set by sea ice, frontal position and thermocline structure. Quaternary Science Reviews 2022 ;Volum 289. NORCE UiB UiO
72. **Planke, Sverre**; Berndt, Christian; Alvarez Zarikian, Carlos A.; Agarwal, Amar; Andrews, Graham D.M.; Betlem, Peter; Bhattacharya, Joyeeta; Brinkhuis, Henk; Chatterjee, Sayantani; Christopoulou, Marialena; Clementi, Vincent J.; Ferré, Eric C.; Filina, Irina Y.; Frieling, Joost; Guo, Pengyuan; Harper, Dustin T.; **Jones, Morgan T**; Lambart, Sarah; Longman, Jack; Millett, John M.; Mohn, Geoffroy; Nakaoka, Reina; Scherer, Reed P.; Tegner, Christian Maughan; Varela, Natalia; Wang, Mengyuan; Xu, Weimu; Yager, Stacy L.. Mid-Norwegian Margin Magmatism and Paleoclimate Implications. International Ocean Discovery Program 2022 ;Volum 396. UiO UNIS
73. **Planke, Sverre**; **Jones, Morgan Thomas**. Expedition 396 Preliminary Report: Mid-Norwegian continental margin magmatism and paleoclimate implications. International Ocean Discovery Program 2022 UiO
74. Poulos, Markos; Giaremis, Stefanos; Kioseoglou, Joseph; Arvanitidis, John; Christofilos, Dimitris; Ves, Sotirios; Hehlen, Markus P.; Allan, Neil L.; **Mohn, Chris Erik**; Papagelis, Konstantinos. Lattice dynamics and thermodynamic properties of Y3Al5O12 (YAG). Journal of Physics and Chemistry of Solids 2022 ;Volum 162. UiO
75. ***Ramirez, Florence Dela Cruz**; **Selway, Katherine**; **Conrad, Clinton Phillips**; Lithgow-Bertelloni, C.. Constraining Upper Mantle Viscosity Using Temperature and Water Content Inferred From Seismic and Magnetotelluric Data. Journal of Geophysical Research (JGR): Solid Earth 2022 ;Volum 127.(8) UiO
76. Reiners, A.; Shulyak, D.; Käpylä, P.J.; Ribas, I.; Nagel, E.; Zechmeister, M.; Caballero, J.A.; **Shan, Yutong**; Fuhrmeister, B.; Quirrenbach, A.; Amado, P.J.; Montes, D.; Jeffers, S.V.; Azzaro, M.; Béjar, V.J.S.; Chaturvedi, P.; Henning, Th.; Kürster, M.; Pallé, E.. Magnetism, rotation, and nonthermal emission in cool stars: Average magnetic field measurements in 292 M dwarfs. Astronomy and Astrophysics (A & A) 2022 ;Volum 662. UiO

77. Rezaei-Kahkhaei, Mehdi; **Corfu, Fernando**; Galindo, Carmen; Rahbar, Reza; Ghasemi, Habibollah. Adakite genesis and plate convergent process: Constraints from whole rock and mineral chemistry, Sr, Nd, Pb isotopic compositions and U-Pb ages of the Lakhshak magmatic suite, East Iran. Lithos 2022 ;Volum 426-427. UiO
78. ***Rolf, Tobias**; Weller, Matt; Gülcher, Anna; Byrne, Paul; O'Rourke, Joseph G.; Herrick, Robert; Bjonnes, Evan; Davaille, Anne; Ghail, Richard; Gillman, Cedric; Plesa, Ana-Catalina; Smrekar, Suzanne. Dynamics and Evolution of Venus' Mantle Through Time. Space Science Reviews 2022 ;Volum 218. UiO
79. Ruggiero, L.; Sciarra, A.; **Mazzini, A**.; Florindo, F.; Wilson, G.; Tartarello, M.C.; Mazzoli, C.; Anderson, J.T.H.; Romano, V.; Worthington, R.; et al. Antarctic Permafrost Degassing in Taylor Valley by Extensive Soil Gas Investigation. Sci. Total Environ. 2023, 866, 161345, doi:10.1016/j.scitotenv.2022.161345.
80. Schlecker, M.; Burn, R.; Sabotta, S.; Seifert, A.; Henning, T.; Emsenhuber, A.; Mordasini, C.; Reffert, S.; **Shan, Yutong**; Klahr, H.. RV-detected planets around M dwarfs: Challenges for core accretion models. Astronomy and Astrophysics (A & A) 2022 ;Volum 664. UiO
81. Schliffke, Nicholas; van Hunen, Jeroen; Allen, Mark B.; **Magni, Valentina**; Gueydan, Frédéric. Episodic back-arc spreading centre jumps controlled by transform fault to overriding plate strength ratio. Nature Communications 2022 ;Volum 13. s.1-7 UiO
82. Schmidt, Christopher; Gupta, Shubhangi; Rüpke, Lars; Burwicz-Galerne, Ewa; Hartz, Ebbe Hvidegård. Sedimentation-driven cyclic rebuilding of gas hydrates. Marine and Petroleum Geology 2022 ;Volum 140. UiO
83. **Schweitzer, Johannes**. Die Gründung der Deutschen Geophysikalischen Gesellschaft im Rahmen der internationalen Beziehungen zu Beginn des zwanzigsten Jahrhunderts. In: DGG (ed.) Geophysik im Wandel, 2022, https://dgg-online.de/WordPress_01/wp-content/uploads/2022/08/DGG100_Schweitzer_v4.pdf
84. **Schweitzer, Johannes.** An Unknown Letter of Charles F. Richter about Magnitude Scales and His Relationship to Beno Gutenberg. Seismological Research Letters 2022 ;Volum 93.(1) s.458-464 UiO NORSAR
85. Serov, P.; Patton, H.; **Mazzini, A**.; Mattingsdal, R.; **Shephard, G**.; Cooke, F.A.; Martins de Aguiar, V.C.; Holm, V.D.; Alessandrini, G.; **Meza Cala, J.C**.; et al. CAGE22-6 Cruise Report: GEO-3144/8144 Teaching Cruise: Geologically Controlled Hydrocarbon Seepage in Hopendjupet and the Wider Barents Sea. CAGE – Cent. Arct. Gas Hydrate, Environ. Clim. Rep. Ser. 2022, 10, doi:10.7557/cage.6769
86. Shen, Jun; Yin, Runsheng; Algeo, Thomas J.; **Svensen, Henrik Hovland**; Schoepfer, Shane D.. Mercury evidence for combustion of organic-rich sediments during the end-Triassic crisis. Nature Communications 2022 ;Volum 13. UiO
87. Shrbený, Lukáš; **Krzesinska, Agata Magdalena**; Borovika, Jií; Spurný, Pavel; Tymiski, Zbigniew; Kmieciak, Kryspin. Analysis of the daylight fireball of July 15, 2021, leading to a meteorite fall and find near Antonin, Poland, and a description of the recovered chondrite. Meteoritics and Planetary Science 2022 ;Volum 57.(12) s.2108-2126 UiO
88. Slagstad, Trond; Henderson, Iain Henry Campbell; Roberts, Nick MW; **Kulakov, Evgeniy**; Ganerød, Morgan; Kirkland, Christopher L.; Dalslåen, Bjørgunn Heggem; Creaser, Robert A; Coint, Nolwenn. Anorthosite formation and emplacement coupled with differential tectonic exhumation of ultrahigh-temperature rocks in a Sveconorwegian continental back-arc setting. Precambrian Research 2022 ;Volum 376. NGU UiO
89. Solomatova, Natalia V.; **Caracas, Razvan**; Bindi, Luca; Asimow, Paul D.. Ab initio study of the structure and relative stability of MgSiO4H2polymorphs at high pressures and temperatures. American Mineralogist 2022 ;Volum 107.(5) s.781-789 UiO
90. **Steinberger, Bernhard**. Comment on "Will Earth's next supercontinent assemble through the closure of the Pacific Ocean?". National Science Review 2022 ;Volum 9. UiO
91. **Steinberger, Bernhard**; Steinberger, Alisha. Mantle plumes and their interactions. I:

Dynamics of Plate Tectonics and Mantle Convection. Elsevier 2022 ISBN 9780323857338. UiO

92. Straume, Eivind Olavson; Nummelin, Aleksi Henrynpoika; **Gaina, Carmen**; **Nisancioglu, Kerim Hestnes**. Climate transition at the Eocene-Oligocene influenced by bathymetric changes to the Atlantic-Arctic oceanic gateways. Proceedings of the National Academy of Sciences of the United States of America 2022 ;Volum 119.(17) UiO NORCE UiB
93. **Svensen, Henrik Hovland**. Et land av stein. Bergartene som har formet Norge. Kagge Forlag AS 2022 (ISBN 9788248929901) 311 s. UiO
94. **Trønnes, Reidar G**; **Mohn, Chris Erik**; Grømer, Bendik; Hernandez, Jean-Alexis; Guren, MG; Baron, Marzena Anna. Dense, residual davemaoite in the lowermost mantle: implications for ULVZs and LLSVPs. Abstr. Conf. on Earth's History, Dynamics and Planetary Habitability, Sundvollen, Norway, Nov. 13-19. www.nhm.uio.no/english/about/organization/research□collections/people/rtronnes/4/other/Sundvollen-abstr-RGT.pdf. Conf. on Earth's History, Dynamics and Planetary Habitability, Sundvollen, Norway, Nov. 13-19 2022 UiO
95. Tsikalas, Filippos; **Meza Cala, Juan Camilo**; **Abdelmalak, Mohamed Mansour**; **Faleide, Jan Inge**; Brekke, Harald. Lofoten Composite Tectono-Sedimentary Element, Norwegian Rifted Margin, Norwegian Sea. Geological Society of London Memoirs 2022 ;Volum 57. UiO
96. Uenzelmann-Neben, Gabriele; Bohaty, Steven M.; Childress, Laurel B.; Archontikis, Odysseas A.; Batenburg, Sietske J.; Bijl, Peter K.; Burkett, Ashley M.; Chanda, Pratyusha; Coenen, Jason J.; Dallanave, Edoardo; Davidson, Peter C.; Doiron, Kelsey E.; Geldmacher, Jörg; Gürer, Derya; Haynes, Shannon J.; Herrle, Jens O.; Ichiyama, Yuji; Jana, Debadrita; Jones, Matthew M.; Kato, Chie; Kulhanek, Denise K.; Li, Juan; Liu, Jia; McManus, James; Yakutchik, Maryalice; Cawthra, Hayley C.; **Minakov, Alexander**; Penman, Donald E.; Sprain, Courtney J.; Tessin, Allyson C.; Wagner, Thomas; Westerhold, Thomas. Agulhas Plateau Cretaceous Climate: drilling the Agulhas Plateau and Transkei Basin to reconstruct the Cretaceous–Paleogene tectonic and climatic evolution of the Southern Ocean basin. International Ocean Discovery Program 2022 ;Volum 392. UiO
97. Vaes, Bram; **Gallo, Leandro Cesar**; Van Hinsbergen, Douwe. On Pole Position: Causes of Dispersion of the Paleomagnetic Poles Behind Apparent Polar Wander Paths. Journal of Geophysical Research (JGR): Solid Earth 2022 ;Volum 127.(4) UiO
98. ***van der Boon, A**.; Biggin, A.J.; Paterson, G.A.; Kavanagh, J.L. Magnetic to the Core – Communicating Palaeomagnetism with Hands-on Activities. Geosci. Commun. 2022, 5, 55–66, doi:10.5194/gc-5-55-2022
99. ***van der Boon, Annique**; Biggin, Andrew J.; Thallner, Daniele; Hounslow, Mark; Bono, Richard; Nawrocki, Jerzy; Wójcik, K; Paszkowski, Mariusz; Königshof, Peter; de Backer, Tim; Kabanov, Pavel; Gouwy, Sofie; VandenBerg, Richard; da Silva, Anne-Christine. A Persistent Non-uniformitarian Paleomagnetic Field in the Devonian?. Earth-Science Reviews 2022 ;Volum 231. UiO
100. Van Zelst, Iris; Crameri, Fabio; Pusok, Adina E.; Glerum, Anne; Dannberg, Juliane; Thieulot, Cedric. 101 geodynamic modelling: How to design, interpret, and communicate numerical studies of the solid Earth. Solid Earth (SE) 2022 ;Volum 13.(3) s.583-637 UiO
101. ***Vickers, Madeleine Larissa**; Hougård, Iben W.; Alsen, Peter; Ullmann, Clemens V.; Jelby, Mads Engholm; Bedington, Michael; Korte, Christoph. Middle to Late Jurassic palaeoclimatic and palaeoceanographic trends in the Euro-Boreal region: Geochemical insights from East Greenland belemnites. Palaeogeography, Palaeoclimatology, Palaeoecology 2022 ;Volum 597. UiO
102. ***Vickers, Madeleine Larissa**; Vickers, Martin; Rickaby, Rosalind E.M.; Wu, Han; Bernasconi, Stefano M.; Ullmann, Clemens V.; Bohrmann, Gerhard; Spielhagen, Robert F.; Kassens, Heidemarie; Pagh Schultz, Bo; Alwmark, Carl; Thibault, Nicolas; Korte,

Christoph. The ikaite to calcite transformation: Implications for palaeoclimate studies. Geochimica et Cosmochimica Acta 2022 ;Volum 334. s.201-216 UiO

103. Vidishcheva, O; Akhmanov, G.; Kislitsyna, E.; **Mazzini, Adriano**; Mal'tseva, A.; Poludetkina, E.; Bakay, E.; Man'ko, I.; Korost, D.; Khlystov, Oleg. Variations in molecular and isotopes composition of seepage gases in the north-western and south-eastern parts of Lake Baikal. Georesursy 2022 ;Volum 24.(2) s.209-216 UiO
104. ***Weerdesteijn, Maaike Francine Maria**; **Conrad, Clinton Phillips**; Naliboff, John B.. Solid Earth Uplift Due To Contemporary Ice Melt Above Low-Viscosity Regions of the Upper Mantle. Geophysical Research Letters 2022 ;Volum 49.(17) UiO
105. Wei, Bitian; Cheng, Xin; **Domeier, Mathew Michael**; Jiang, Nan; Wu, Yiying; Zhang, Weijie; Wu, Ke; Wang, Baofeng; Xu, Pengxiang; Xing, Longyun; Zhang, Dongmeng; Li, Teng; Deng, Xiaohong; Liu, Feifan; Zhou, Yanan; Wu, Hanning. Placing Another Piece of the Tethyan Puzzle: The First Paleozoic Paleomagnetic Data From the South Qiangtang Block and Its Paleogeographic Implications. Tectonics 2022 ;Volum 41.(10) UiO
106. **Werner, Stephanie**; Bultel, Benjamin Gabriel Rene; **Rolf, Tobias**; Fernandes, Vera Assis. Orientale Ejecta at the Apollo 14 Landing Site Implies a 200-million-year Stratigraphic Time Shift on the Moon. The Planetary Science Journal (PSJ) 2022 ;Volum 3.(3) Suppl. 65. UiO
107. Wilkes, Elise B.; Sessions, Alex L.; Zeichner, Sarah S.; Dallas, Brooke; Schubert, Brian; **Jahren, Anne Hope Florine**; Eiler, John M.. Position-specific carbon isotope analysis of serine by gas chromatography/Orbitrap mass spectrometry, and an application to plant metabolism. Rapid Communications in Mass Spectrometry 2022 ;Volum 36.(18) UiO
108. Yu, Liang; Yan, Maodu; **Domeier, Mathew Michael**; Guan, Chong; Shen, Miaomiao; Fu, Qiang; Xu, Wanlong; Xu, Zunbo; Niu, Zhichao; Yang, Liye; Shi, Rendeng; Zhang, Weilin; Zan, Jinbo; Zhang, Dawen; Li, Bingshuai. New Paleomagnetic and Chronological Constraints on the Late Triassic Position of the Eastern Qiangtang Terrane: Implications for the Closure of the Paleo-Jinshajiang Ocean. Geophysical Research Letters 2022 ;Volum 49.(2) UiO
109. Zhang, Hongrui; **Torsvik, Trond Helge**. Circum-Tethyan magmatic provinces, shifting continents and Permian climate change. Earth and Planetary Science Letters 2022 ;Volum 584. UiO
110. Zhou, Haoyang; Müller, Axel; **Augland, Lars Eivind**; Kristoffersen, Magnus; Erambert, Muriel. Titanite links rare-element (meta-)pegmatite mineralization to Caledonian metamorphism. Geochimica et Cosmochimica Acta 2022 ;Volum 332. s.285 -306 UiO
111. Zuchuat, Valentin; **Augland, Lars Eivind**; **Jones, Morgan Thomas**; Sleveland, Arve R.N.; Twitchett, Richard; Tovar, Francisco J Rodríguez; Hammer, Øyvind; Senger, Kim; Betlem, Peter; Turner, Holly E; Midtkandal, Ivar; **Svensen, Henrik Hovland**; **Planke, Sverre**. The Permian-Triassic boundary across the Barents Shelf: an intricate record of climate change, mass extinction, recovery, and basin reorganisation. EGU General Assembly 2022 UiO UNIS
112. Zurkowski, C.C.; Lavina, B.; Brauser, N.M.; **Davis, A.H**.; Chariton, S.; Tkachev, S.; Greenberg, E.; Prakapenka, V.B.; Campbell, A.J. Pressure-Induced C 23– C 37 Transition and Compression Behavior of Orthorhombic Fe2S to Earth's Core Pressures and High Temperatures. Am. Mineral. 2022, 107, 1878–1885, doi:10.2138/am-2022-8187

Above: View on Fagradalsfjall 2021 lava flow, Reykjanes Peninsula (Iceland). Field trip before the 35th Nordic Geological Winter Meeting (Reykjavík, May 2022).

Below: Sunset on Mauna Loa shield volcano and Mauna Kea volcanic craters, Big Island (Hawaii, US). Field trip after the Goldschmidt Conference (Honolulu, July 2022).

Photos by: Manfredo Capriolo

Outreach activities

TV; radio; newspapers and magazines

1. Aakre, Gina. Rocks unravel the secrets of rhe Earth's magnetic field, profile on Titan [newspaper for science and technology at the University of Oslo] https://titan.uio.no/universet/2022/rocks-unravel-secrets-earths-magnetic-field
2. Callegaro, Sara. Consultancy and summer field trip in the Dolomites, Italy with Ashford, I. and Hartley, G. (BBC) for the episodes on the End Permian and Carnian Pluvial Event on the BBC series "Earth" [TV] (in preparation)
3. Heyn, Björn Holger, Forskere har undersøkt to enorme, mystiske strukturer i jordens indre, forskning.no [Interview] Forskere har undersøkt to enorme, mystiske strukturer i jordens indre (forskning.no)
4. Heyn, Björn Holger; Shephard, Grace. Revealing "invisible" plume tracks beneath continents. [Internett] 2022-04-06 UiO
5. Kulakov, E. Superkontinentet Rodina faktisk eksisterte, forskning.no [study presentation] https://forskning.no/geologi/ny-norsk-studie-stiller-sporsmal-ved-om-superkontinentet-rodinia-faktisk-eksisterte/2057821
6. Shan, Yutong et al. NASA's TESS mission [CEED blog] https://www.mn.uio.no/ceed/english/about/blog/2022/rocky-planets-discovered-nearby.html
7. Steinberger, B. Why are there continent-sized 'blobs' in the deep Earth? [BBC] https://www.bbc.com/future/article/20220510-why-are-there-continent-sized-blobs-in-the-deep-earth
8. Svensen, Henrik Hovland. Ny bok om bergarter i Norge. NRK P1+ Holm [Radio] 2022-10-19 UiO
9. Svensen, Henrik Hovland; Bøckmann, Petter; Bjorå, Charlotte Sletten. Abels tårn. EKKO; NRK P2 [Radio] 2022-05-13 UiO
10. van der Boon, Annique. Jordens magnetfelt betyr mer for hverdagen din enn du tror, Aftenposten [newspaper] https://www.aftenposten.no/meninger/kronikk/i/z7qv8q/jordens-magnetfelt-betyr-mer-for-hverdagen-din-enn-du-tror 2022-06-26

Other outreach activities

1. Andersen, Torgeir b.; Jerram, Dougal A. et al. Wilson Cycle release (4 episodes) [Internett] https://www.youtube.com/playlist?list=PLu_DCJwCuJPpiITgDQfN6pX09ZkagnVpx
2. Anell, Ingrid; Shephard, Grace. GEOlogic game. iEarth seed funds
3. Flatland, Annabel; Shephard, Grace. The faces behind Arctic features. [CEED Blog] https://www.mn.uio.no/ceed/english/about/blog/2022/arctic-naming-origins.html
4. Kiraly, Agnes. EGU GD [blog posts] https://blogs.egu.eu/divisions/gd/2023/03/16/geodynamics-101-viscous-anisotropy/ ; https://blogs.egu.eu/divisions/gd/2022/07/27/the-marie-sklodowska-curie-postdoctoral-fellowship/

5. Krzesinska, Agata M. Comets workshop during Ungforsk festival 2022-09-28 - 2022-09-29 UiO
6. Krzesinska, Agata M. Pint of Science. Norwegian meteorites – how to find them and why to study 2022-02-07
7. Marcilly, Chloé M. Global sea level in deep time [CEED blog] https://www.mn.uio.no/ceed/english/about/blog/2022/global-sea-level-in-deep-time.html
8. Selway, Katherine. Climate science on the Greenland Ice Sheet. https://www.youtube.com/watch?v=fLzWPcyAH7c [Internett] 2022-07-14 UiO
9. Shephard, Grace. Bubbles and bathymetry in the Barents. [CEED blog] https://www.mn.uio.no/ceed/english/about/blog/2022/bathymetry-and-bubbles-in-the-barents.html
10. Shephard, Grace. Ending rainbows but keeping the pots of Gold. MetOs Lavterskel. 2022-04-06 UiO
11. Shephard, Grace. Meeting place, Earth. Photo competition finalist.. European Geosciences Union 2022 UiO
12. Shephard, Grace. Modellering for en Digital Jord [Talk] Pedagogisk Dag 2022-11-11 UiO
13. Shephard, Grace. The seafloor is not a rainbow. CAGE UiT lunchtime seminar 2022-10-27
14. Shephard, Grace. What's lurking on the top of the below. [CAGE blog] https://cage.uit.no/2022/09/02/whats-lurking-on-top-of-the-below/
15. Shephard, Grace; Fabio Crameri. Create and Share Better Science Graphics. [Hybrid course]. iEarth seed funds 2022-09-12 - 2022-09-13
16. Svensen, Henrik Hovland. En verden under føttene. [Kunstnerisk og museal presentasjon] Kunstutstilling. Sirius kunstnerunion; Fredrikstad. 2022-11-25 - 2022-11-27 UiO
17. Svensen, Henrik Hovland. Redd for antropocen. [Kunstnerisk og museal presentasjon] Kunstutstilling / Novemberutstillingen. Buskerud bildende kunstnere; Drammen. 2022-11-20 - 2023-01-08 UiO

Abstracts (talks & posters at conferences)

1. Andersen, Torgeir Bjørge; Jakob, Johannes; Beyssac, Olivier; Mohn, Geoffroy. Tectonostratigraphy of the Scandinavian Caledonides and its role for understanding the Scandian Orogenu. Earth History, Dynamics and Planetary Habitability; 2022-11-12 - 2022-11-19 NGU UiO
2. Arnould, Maëlis; Rolf, Tobias; Manjon Cabeza Cordoba, Antonio. Exploring the effect of mantle composite rheology on surface tectonics and topography. EGU General Assembly; 2022-05-23 - 2022-05-27 UiO
3. Backhouse, N.; Thomson, A.; Brodholt, J.P.; Wilson, C. A lab-based method for Paris-Edinburgh Press seismic velocity measurements. Int. Mineral. Assoc. IMA2022-1786, P3_15
4. Ballo, Eirik Gottschalk. Lipid biomarkers in Lake Sagtjernet, Norway. Organic Geochemistry group guest talk at Lamont-Doherty Earth Observatory; 2022-02-21 - 2022- 02 -21 UiO
5. Ballo, Eirik Gottschalk; Bajard, Manon Juliette Andree; Bakke, Jostein; Støren, Eivind Wilhelm Nagel; D'Andrea, William J.; Høeg, Helge Irgens. Lake Sagtjernet hydrogen isotopes and pollen. VIKINGS project annual meeting; 2022-06-16 - 2022-06-16 UiO UiB
6. Belosa, Lea; Gaina, Carmen; Callegaro, Sara; Mazzini, Adriano; Meyzen, Christine M; Polteau, Stephane; Bizimis, Michael. Plume-Fracture Zone interactions in the NE Atlantic. EGU General Assembly 2022; 2022-05-23 - 2022-05-27 IFE UiO
7. Berndt, Christian; Planke, Sverre; Zarikian, Carlos A.; Bünz, Stefan; Karstens, Jens; Svensen, Henrik Hovland; Manton, Ben; IODP Expedition 396, Scientific P.. Shallow-water hydrothermal venting in the North Atlantic during the Paleocene Eocene Thermal Maximum. EGU General Assembly 2022; 2022- 05-23 - 2022-05-27 UiO UiT
8. Binde, Cornelia Mentzoni; Bünz, Stefan; Plaza-Faverola, Andreia; Planke, Sverre; Manton, Ben. Hydrothermal venting driving extreme global warming at the Paleocene-Eocene boundary. Methane in a changing Arctic; 2022-09-14 - 2022-09- 16 UiO UiT
9. Bjærke, Marit Ruge; Ekström, Anders; Hastrup, Frida; Svensen, Henrik Hovland. Bridging an epistemological gap: Roundtable on the importance of cooperation between the humanities and the natural sciences.. Gardening the Globe Opening Conference; 2022-05 -23 - 2022-05-23 UiB UiO
10. Boscaini, Andrea; Davies, Joshua H.F.L.; Sassi, Raffaele; Mazzoli, Claudio; Callegaro, Sara; De Min, Angelo; Marzoli, Andrea. Lifetime of the Early Permian giant caldera-system of Bolzano/Bozen (North-eastern Italy). Geosciences for a sustainable future SGI -SIMP conference; 2022-09-18 - 2022-09-21 UiO
11. Boscaini, Andrea; Marzoli, Andrea; Bertrand, Hervé; Chiaradia, Massimo; Jourdan, Fred; Faccenda, Manuele; Meyzen, Christine M; Callegaro, Sara; Serrano Durán, Lina Maria. The architecture of the lithospheric mantle controlled the emplacement of the Central Atlantic Magmatic Province. EGU General Assembly 2022; 2022-05-23 - 2022-05-27 UiO
12. Brodholt J.P. Ab initio calculations on Si diffusion suggest that CaSiO3 perovskite is very strong. Int. Mineral. Assoc. IMA2022-1759, OL19_3
13. Bultel,B.; Krzesinska, A.M.; Veneranda, M.; Loizeau, D.; Pilorget, C.; Hamm, V. et al. Micro-scale characterization of vermiculite-rich sample from Granby Tuff, an analogue to Oxia Planum clays. EGU General Assembly Conference Abstracts, EGU22-11272
14. Bögels, T.; Caracas, R. Critical point and supercritical regime of MgO. Int. Mineral. Assoc. IMA2022-1733, P4_44
15. Bögels, T.; Caracas, R. Refractory oxides at extreme conditions. Int. Mineral. Assoc. IMA2022-1729, OL19_1

16. Callegaro, Sara; Svensen, Henrik H.; Heimdal, Thea H.; Jerram, Dougal A.; Planke, Sverre; Polozov, Alexander; Deegan, Frances M.; Capriolo, Manfredo. Mineral-scale evidence for magma–evaporite interaction in basaltic sills from the Siberian Traps (Tunguska basin, Russia). The 35th Nordic Geological Winter Meeting 2022; 2022-05-11 - 2022-05-13 UiO
17. Callegaro, Sara; Svensen, Henrik Hovland; Deegan, Frances M.; Planke, Sverre; Polozov, Alexander. Magma-host rock interaction in basaltic sills from the Siberian Traps (Tunguska basin, Russia): mineral scale and whole-rock perspectives. Geosciences for a sustainable future, SGI-SIMP conference; 2022-09-18 - 2022-09-21 UiO
18. Callegaro, Sara; Svensen, Henrik Hovland; Heimdal, Thea Hatlen; Kjøll, Hans Jørgen; Harstad, Andreas Olaus; Neumann, Else Ragnhild. New insights on shallow intrusions from the early stage of the Oslo Rift.. The 35th Nordic Geological Winter Meeting 2022; 2022-05-11 - 2022-05- 13 UiO NGI
19. Capriolo, Manfredo. Carbon degassing from Large Igneous Provinces during mass extinction events: Insights from melt and fluid inclusions. Goldschmidt 2022; 2022- 07-10 - 2022-07-15 UiO
20. Capriolo, Manfredo. Melt and fluid inclusions to constrain LIPs emplacement. Earth`s History, Dynamics, and Planetary Habitability; 2022-11-13 - 2022-11-19 UiO
21. Capriolo, Manfredo; Callegaro, Sara; Dal Corso, Jacopo; Newton, Robert J.; Baker, Don R.; Renne, Paul R.; Storm, Malte; Marzoli, Andrea. Magma plumbing system of mass extinction-related Large Igneous Provinces: Insights from Synchrotron Light X-ray microtomography. The 35th Nordic Geological Winter Meeting 2022; 2022-05-11 - 2022-05-13 UiO
22. Capriolo, Manfredo; Callegaro, Sara; Dal Corso, Jacopo; Newton, Robert J.; Baker, Don R.; Renne, Paul R.; Storm, Malte; Marzoli, Andrea. Synchrotron Light X-ray microtomography data constrain the magma plumbing system of mass extinction-related Large Igneous Provinces. SGI- SIMP Conference "Geosciences for a sustainable future"; 2022-09-18 - 2022-09-21 UiO
23. Capriolo, Manfredo; Callegaro, Sara; Marzoli, Andrea; Aradi, László E.; Dal Corso, Jacopo; Newton, Robert J.; Bartoli, Omar; Szabo, Csaba. Different oxidation states of carbon in the end-Triassic Large Igneous Province. International School "Understanding Oxygen fugacity in Geoscience"; 2022-09-05 - 2022-09-09 UiO
24. Capriolo, Manfredo; Mills, Benjamin J.W.; Newton, Robert J.; Dal Corso, Jacopo; Dunhill, Alexander M.; Wignall, Paul B.; Marzoli, Andrea. Anthropogenic-scale CO2 emissions from the Central Atlantic Magmatic Province behind the end-Triassic crisis. SGI-SIMP Conference "Geosciences for a sustainable future"; 2022-09-18 - 2022-09-21 UiO
25. Caracas, R.; Martin, L.; Bethkenhagen, M.; Bögels, T.; Li, Z. Moon Impact – a geological story. Int. Mineral. Assoc. IMA2022-1746, OL10_3
26. Caracas, R.; Solomatova, N.; Kobsch, A.; Bögels, T.; Li, Z.; Schaan, R.; Solomatova, N. Analyzing melts and fluids from ab initio molecular dynamics simulations with the UMD package. Int. Mineral. Assoc. IMA2022-1750, P4_45
27. Caracas, R.; Stewart, S. Thermochemical state of the protolunar disk after the giant impact. Int. Mineral. Assoc. IMA2022-1660, OL62_6
28. Chidester, B. et al. (including R. Caracas). Experimental temperature measurements of Fe-bearing silicate minerals and glasses to 1.6 TPa. 22nd Biennial Conference of the APS Topical Group on Shock Compression of Condensed Matter. 2022. O04.00003
29. Davis A.H.; Solomatova, N.V.; Caracas, R.; Campbell, A. Densities and miscibilities of carbonate-silicate-metal melts in the lower mantle. Int. Mineral. Assoc. IMA2022-1608, OL53_4
30. Davis, A.H.; Caracas, R. Vaporization of He and C from a pyrolite melt: Implications for the early Earth's atmosphere. Am. Geophys. Union Fall Mtg. 2022. MR35B-0070

31. Davis, A.H.; Solomatova, N.V.; Caracas, R.; Campbell, A. Computational insights on carbonate-silicate-metal melt behavior in the lower mantle. Am. Geophys. Union Fall Mtg. 2022. D1025-08
32. de Boer, R.A.; van der Boon, A.; Königshof, P. and De Groot, L.V. Paleointensity estimates of the Middle Devonian obtained from German pillow lavas. 17th Castle Meeting, 2022. Croatia
33. de Boer, R.A.,;van der Boon, A.; Königshof, P. and De Groot, L.V. Paleomagnetism of Middle Devonian pillow lavas from Germany, EGU general assembly 2022
34. Domeier, M.; Arnould, M.; Eyster, A.; Gallo, L.C.; Gürer, D.; Király, Á.; Robert, B.; Rolf, T.; Sapienza, F.; Shephard, G.E.; Swanson-Hysell, N.; Vaes, B.; van der Boon, A.; Wu, L.; Zhang, Y. Frontiers in quantitative paleogeography and paleomagnetism, EGU general assembly 2022
35. Ebbing, J.; Fullea, J.; Root, B.; Conrad, Clinton Phillips; 3D Earth Study Team, The. 3D Earth – Towards a digital twin for the geosphere. Living Planet Symposium; 2022-05-23 - 2022-05-27 UiO
36. Figowy, S.; Dubacq, B.; Caracas, R. Crystal chemistry and partitioning of halogens in hydrous silicates, 2022.
37. Gallo, L.C.; Domeier, M. and Sapienza, F. On the feasibility of Paleomagnetic Euler Pole Analysis. In EGU General Assembly Conference Abstracts (pp. EGU22-8469)
38. Geng, Ming; Jónsson, Hannes. DFT Calculations and Thermodynamic Analysis of the Forsterite Mg2SiO4(010) Surface. 23rd International Mineralogical Association General Meeting; 2022-07-18 - 2022-07-22 UiO
39. Grishko, Elena V.; Yarushina, Viktoriya M.; Bobrova, Maria; Stanchits, Sergei; Minakov, Alexander; Stukachev, Vladimir. Experimental and numerical investigation of acoustic emission and its moment tensors in sandstones during failure based on the elastoplastic approach. EGU General Assembly 2022; 2022-05-23 - 2022-05-27 IFE UiO
40. Handford, B.; Biggin, A.; Rapalini, A.; Haldan M.; Langereis, C.; Monti, M.; de Luchi, M.L.; van der Boon, A.; Franceschinis, P. and Kugabalan, B.Characterising the Triassic Palaeomagnetic Field with an Aim to Investigate the Mesozoic Dipole Low, EGU general assembly 2022
41. Heyn, Björn Holger; Conrad, Clinton Phillips. Basal erosion and surface heat flux anomalies associated with plume-lithosphere interaction beneath conti-nents. EGU General Assembly; 2022- 05-23 - 2022-05-27 UiO
42. Jerram, Dougal Alexander. Understanding large igneous provinces and volcanic rift margins. Hertfordshire Geological Society Lecture Series; 2022-09-08 - 2022-09-08 UiO
43. Jerram, Dougal Alexander. Understanding the South Atlantic Volcanic Margin: Key Insights from Subaerial to Subaqueous Volcanic / Sedimentary Environments Onshore Namibia and Angola. Hydrocarbon Potential in Namibia; 2022-06-07 - 2022-06-09 UiO
44. Jerram, Dougal Alexander; Planke, Sverre; Millett, JM; Howell, John. Understanding volcanic margin prospectivity; insights from the north and south Atlantic margins. The impacts of volcanism on sedimentary basins and their energy resources; 2022-09-09 - 2022-09-09 UiO
45. Jones, Morgan Thomas. Tracing North Atlantic volcanism and North Sea connectivity across the Paleocene-Eocene Thermal Maximum (PETM). 12th International Conference on Climatic and Biotic Events of the Paleogene (CBEP12); 2022-08-22 - 2022-08-25 UiO
46. Kiraly, Agnes; Fraters, Menno; Gassmoeller, Rene. Implementing 3D anisotropic viscosity calculations into ASPECT. EGU General Assembly; 2022-05-23 - 2022-05-27 UiO
47. Kiraly, Agnes; Wang, Yijun; Fraters, Menno; Gassmoeller, Rene; Dannberg, Juliane; Hansen, Lars; Conrad, Clinton Phillips. Incorporating olivine CPO-related anisotropic viscosity into 3D geodynamics simulations. Ada Lovelace Workshop on Mantle and Lithosphere Dynamics; 2022-08-28 - 2022-09-02 UiO

48. Krzesinska, A.M.; Bultel, B.; Werner, S.C. Analogues for Martian crustal and aqueous processes: Lessons learnt from mineralogy and geochemistry of rocks in the PTAL collection. EGU General Assembly Conference Abstracts, EGU22-12286
49. Krzesinska, A.M.; Schofield, P.F.; Geraki, K.; Mosselmans, J.F.W.; Michalski, J.R. Trace Elemental Composition of Alteration Minerals in Nakhlites—Source and Nature of Aqueous Fluids. 85th Meteoritical Society Meeting, Glasgow. LPI Contributions 2695, 6191
50. Krzesinska, A.M.; Tyminski, Z.; Kmieciak, K.; Shrbeny, L.; Spurny, P.; Borovicka, J. The Antonin L5 Chondrite Fall (Poland): Mineralogy and Petrology of Meteorite, Bolide Trajectory and Meteoroid Orbit. 85th Meteoritical Society Meeting, Glasgow. LPI Contributions 2695, 6144
51. Kästle, Emanuel; Shephard, Grace; Paul, Anne. Vote maps of the Alpine upper mantle. 6th Annual AlpArray; 2022-10-12 - 2022-10-14 UiO
52. Larsen, H.C.; Blischke, A; Halldórsson, S.A.; Brandsdóttir,B.; Lesher, C.E.; Conrad, C.P.; Brown, E.L.; Coxall, H.K.; Frieling, J.; Dannberg, J.; Erlendsson, Ö.; McCarthy, A.; Steinberger, B.; Gautason, B.; Gaina, C.; Devey, C.; Peate, D.; Karner, G.D.; Hopper, J.R.; Planke, S. et al., "Rift propagation north of Iceland: A case of asymmetric plume dynamics?", Nordic Geologic Winter Meeting, Reykjavik, Iceland, May 2022
53. Lasabuda, Amando P. E.; Hanssen, Alfred; Laberg, Jan Sverre; Rydningen, Tom Arne; Patton, Henry; Faleide, Jan Inge; Abdelmalak, Mohamed Mansour; Kjølhamar, Bent. Underexplored continental shelf gateways: timing, mechanisms and role of SW Barents Sea Gateway, Norwegian Arctic. OCEANIC GATEWAYS: MODERN AND ANCIENT ANALOGUES AND THEIR CONCEPTUAL AND ECONOMIC IMPLICATIONS Conference; 2022-11-23 - 2022-11-25 UiO UiT
54. Li, Z.; Caracas, R.; Soubiran, F. Partial core vaporisation during giant impacts. Int. Mineral. Assoc. IMA2022-1736, OL60_4
55. Lord, O.T.; Drewitt, J.W.E.; Walter, M.J.; Brodholt, J.P.; Muir, J.M.R. Hydrous silicate melts and the deep mantle H2O cycle. Goldschmidt Conf. 2022. Abstr. 2bT1.
56. Luo, H.; Li, Y.; Vocadlo, L.; Brodholt, J.P. Ab initio calculations on metal-silicate partition coefficients of highly siderophile elements. Int. Mineral. Assoc. IMA2022-1751, OL19_2
57. Manjon Cabeza Cordoba, Antonio; Rolf, Tobias. The importance of Grain-Size Evolution for the tectonic regime divergence of Venus and Earth. Europlanet Science Congress; 2022-09-18 - 2022-09-23 UiO
58. Manjon Cabeza Cordoba, Antonio; Rolf, Tobias; Arnould, Maëlis. Feasibility of the mobile-lid regime controlled by grain size evolution. EGU General Assembly; 2022-05-23 - 2022-05-27 UiO
59. Marcilly, C.M.; Maffre, P.; Le Hir, G.; Pohl, A.; Fluteau, F.; Godderis, Y.; Donnadieu, Y.; Heimdal, T.H. and Torsvik, T.H. New constraints on early Paleozoic carbon cycle balance and climate change from modelling. Goldschmidt Conference 2022
60. Marcilly, Chloe M.. Understanding the early Paleozoic carbon cycle balance and climate change from modelling. Goldschmidt conference 2022; 2022-07-10 - 2022- 07-15 UiO
61. Ozgurel, O.; Caracas, R. Helium partitioning between the mantle and the core at the early Earth. Int. Mineral. Assoc. IMA2022-1711, OL03_5
62. Paul, Jyotirmoy; Conrad, Clinton Phillips; Becker, Thorsten W.; Ghosh, Attreyee. Self-induced craton compression: Potential implications for craton stability. AGU Fall Meeting; 2022-12-12 - 2022-12-16 UiO
63. Plaza-Faverola, Andreia; Cooke, Frances Ann; Vachon, Remi Elie Celestin; Waghorn, Kate Alyse; Koehl, Jean-Baptiste P.; Beaussier, Stefan Jon; Bünz, Stefan. Coupling between rifted oceanic crust and sedimentary deformation in the Fram Strait: implications

for seafloor seepage and gas hydrates dynamics. EGU General Assembly 2022; 2022-05-23 - 2022-05-27 UiT UiO

64. Ramirez, Florence Dela Cruz; Selway, Kate; Conrad, Clinton Phillips; Lithgow-Bertelloni, C.. Constraining Upper Mantle Viscosity Using Temperature and Water Content Inferred from Seismic and Mag-netotelluric Data. EGU General Assembl; 2022-05-23 - 2022-05-27 UiO
65. Robert, Boris; Conrad, Clinton Phillips; Steinberger, Bernhard; Domeier, Mathew Michael. Linking plate kinematics and true polar wander over the last 250 Myrs. Earth's History, Dynamics and Planetary Habitability; 2022-11-14 - 2022- 11-18 UiO
66. Rolf, Tobias; Crameri, Fabio; Heyn, Björn Holger; Thielmann, Marcel. Testing a (quasi -)free base for modelling core-mantle boundary topography. EGU General Assembly; 2022-05-23 - 2022-05-27 UiO
67. Rolf, Tobias; Manjon Cabeza Cordoba, Antonio. Convection in Europa's icy shell: numerical simulations with composite rheology and dynamic grain size evolution. Ada Lovelace Workshop on Numerical Modelling of Mantle and Lithosphere Dynamics; 2022-08-28 - 2022-09-02 UiO
68. Root, B.; Conrad, Clinton Phillips; Ebbing, J.; Fullea, J.; Lebedev, S.. 4D Deep Dynamic Earth project: Recommendations for future research. Living Planet Symposium; 2022 -05-23 - 2022-05-27 UiO
69. Ruggero, Livio; Sciarra, Alessandra; Tuccimei, P.; Galli, G.; Mazzini, Adriano; Mazzoli, Claudio; Tartarello, M; Florindo, F.; Wilson, G.; Anderson, J.; Worthington, R.; Giagnoni, M.; Bigi, Sabina; Sassi, R.; Ciotoli, Giancarlo. Study of the origin of soil 222Rn and 220Rn activities in Taylor Valley, Antarctica. Goldschmidt 2022; 2022-07-10 - 2022-07-15 UiO
70. Saurety, A.; Caracas, R. Study of self diffusion of noble gases in magma ocean. Int. Mineral. Assoc. IMA2022-1661, OL11_8
71. Schweitzer, J.25 Years of Earthquake Locations with HYPOSAT, IV. Assembly Latin American and Caribbean Seismological Commission, October 3 – 5, 2022, Quito, Ecuador
72. Schweitzer, J. 25 Years of Earthquake Locations with HYPOSAT, Joint Assembly of Asian & African Seismological Commissions, October 10 – 13, 2022, Hurghada, Red Sea, Egypt
73. Schweitzer, J. Seismic Station Troll, Dronning Maud Land, East Antarctica – the first 10 Years, 3rd ECEES; Bucharest, 4 – 9 September 2022
74. Schweitzer, J.; Paulsen, B.; Antonovskaya, G.N.; Fedorov, A.V.; Konechnaya, Y.V.; Asming, V.E.; Pirli, M.: The European Arctic Seismic Bulletin for the years 1990 – 2013, 82. Jahrestagung der Deutschen Geophysikalischen Gesellschaft, München, März 2022
75. Schweitzer, Johannes. 30 Years of Cooperation Between Central Asia and NORSAR. Final Norwegian Ministry of Foreign Affairs-Project Meeting; 2022-09-19 - 2022- 09-22 UiO
76. Shephard, Grace. Introducing the POLARIS project – uncovering deep-to-surface connections. International Conference on Arctic Margins (ICAM9); 2022-06-13 UiO
77. Shephard, Grace. Modellering for en Digital Jord. UiO faglig pedagogisk dag 2022; 2022-11-03 - 2022-11-03 UiO
78. Shephard, Grace. The seafloor is not a rainbow, implementing better colour choices in science. CAGE lunchtime seminar; 2022-10-27 - 2022-10-27 UiO
79. Shephard, Grace; Crameri, Fabio; Straume, Eivind Olavson. Introducing s-Ink.org; a community portal for sharing quality science graphics. EGU General Assembly 2022; 2022-05-23 - 2022-05-27 UiO

80. Shephard, Grace; Faleide, Jan Inge; Gaina, Carmen; Abdelmalak, Mohamed Mansour; Gac, Sebastien; Torsvik, Trond Helge. Building deformable plate models for the North-east Atlantic. NorthGreen MagellanPlus workshop; 2022-11-21 - 2022-11-23 UiO
81. Shephard, Grace; Gaina, Carmen; Heyn, Björn Holger; Conrad, Clinton Phillips; Anfinson, Owen; Schaeffer, Andrew; Senger, Kim. Exploring potential lower mantle structures and interactions for the origins of HALIP. International Conference on Arctic Margins (ICAM9); 2022- 06-13 - 2022-06-17 UNIS UiO
82. Smyrak-Sikora, A.; Augland, L.E.; Betlem, P.; Grundvåg, S.A.; Helland-Hansen, W.; Jelby, M.E.; Jensen, M.A.; Jochmann, M.M.; Johanessen, E.P.; Jones, M.T.; Vickers, M.L.; Koevoets-Westerduin, M. Deep-time paleoclimate archive in High Arctic, Svalbard, Norway (EGU22-7172). EGU General Assembly 2022, Vienna, Austria, May 2022
83. Stokke, Ella Wulfsberg; Liu, Emma J.; Jones, Morgan Thomas. Explosive hydromagmatic eruptions during the emplacement of the North Atlantic Igneous Province: A story of volcanic ash. Nordic Geological Winter Meeting; 2022-05-11 - 2022-05-13 UiO
84. Svensen, Henrik Hovland. Da Oslo eksploderte. Åpen dag Univ. Oslo 2022; 2022-03-10 UiO
85. Svensen, Henrik Hovland. Geologien i Oslo-området. Omvisning av skoleklasser fra vgs; 2022-04-02 - 2022-04-04 UiO
86. Svensen, Henrik Hovland. Geologisk vandring i Oslo sentrum. Geologisk vandring i Oslo sentrum ROM galleri; 2022-09-24 UiO
87. Svensen, Henrik Hovland. Hva skjuler seg under asfalten i Oslo?. Foredrag Oslo kommune bymiljøetaten; 2022-11-28 UiO
88. Svensen, Henrik Hovland. Oslo under asfalten. Medlemsforedrag Oslo guideforening; 2022-10-19 UiO
89. Svensen, Henrik Hovland. Oslos naturhistorie gjennom to milliarder år - og vulkanene på Ullern. Årsmøte, Ullern, Røa og Bygdøy historielag; 2022-03-14 UiO
90. Svensen, Henrik Hovland. Science and art: Experience from collaboration with artists - and using art in outreach. Undervisning i MNKOM9000, UiO; 2022-04-01 UiO
91. Svensen, Henrik Hovland. The Huken quarry and the resulting landscapes. Undervisning i EHS4000, Environm. Humanities; 2022-03-26 UiO
92. Svensen, Henrik Hovland. Under asfalten. Seminar Deichman bibliotek; 2022-04-06 UiO
93. Svensen, Henrik Hovland. Østfolds vakre bergarter og mystiske fortid. Foredrag; 2022-11-27 UiO
94. Svensen, Henrik Hovland; Müller, Reidar. Lanseringssamtale, Et land av stein. Boklansering; 2022-10-13 UiO
95. Svensen, Henrik Hovland; Torgersen, Eivind. Norske byggeklosser – bergartene som bygget landet. Litteraturfestivalen Popvit; 2022-11-10 UiO
96. Taschimowitz, I.; Brodholt, J.P.; Thomson, A.; van Driel, J.; Schofield, P. The mixing behavior of MgSiO3 and CaSiO3 melts. Int. Mineral. Assoc. IMA2022-1727, P4_41
97. Trønnes, Reidar G; Mohn, Chris Erik. Composition, evolution and structure of the deep mantle. Abstr. ESRF, GeoBridge Webinar, March 23, www.esrf.fr/home/events/webinars/content/area-events/past-online-seminars/composition-evolution-and-structure-of-the-deep-mantle-reidar-g□trnnes-university-of-oslo.htm. ESRF, GeoBridge Webinar, March 23 2022 UiO
98. van der Boon, A., Schubert, B.A., Hagopian, W.M., Domeier, M., Jahren, A.H., Possible Methane Release during the Middle Devonian: A New Carbon Isotope Record from the Mimerdalen Subgroup near Pyramiden, Svalbard, CAGE International Conference, Tromsø, September 2022
99. Vickers, M.L.; Bernasconi, S.M.; Peterse, F.; Sluijs, A.; Ullmann, C.V.; Longman, J.; Stokke, E.W.; Frieling, J.; Thibault, N.; Counts, J.W.; Schultz, B.P.; Jones, M.T., and IODP Expedition 396 Science Party. What drives the formation of glendonites in the

Paleogene? 12th International Conference on Climatic and Biotic Events of the Paleogene, Bremen, Germany, August 2022

100. Vickers, M.L.; Bernasconi, S.M.; Schultz, B.P.; Rogov, M.; Ershova, V.; Ullmann, C.V.; Chivas, A.R.; Dux, F.W. and Jones, M. Can glendonites be used as palaeothermometers? (EGU22-3797). EGU General Assembly 2022, Vienna, Austria, May 2022
101. Vickers, M.L.; Ullmann, C.V.; Hougaard., I.W.; Price, G.D.; Wilby, P.R.; Looser, N.; Korte, C.; Alsen, P.; Grafulha Morales, L.; Lode, S.; Bernasconi, S. What can belemnites tell us about Mesozoic ocean circulation patterns and temperatures. 14th International Conference on Paleoceanography, Bergen, Norway, August – September 2022
102. Wang, Yijun; Kiraly, Agnes; Conrad, Clinton Phillips; Fraters, Menno; Hansen, Lars. Olivine texture evolution under simple deformation: Comparing different numerical methods for calculating LPO and anisotropic viscosity. EGU General Assembly; 2022-05-23 - 2022-05-27 UiO
103. Wang, Yijun; Kiraly, Agnes; Conrad, Clinton Phillips; Hansen, Lars N.; Fraters, Menno. Olivine texture evolution under simple deformation: Comparing different numerical methods for calculating LPO and anisotropic viscosity. EGU General Assembly; 2022-05-23 - 2022-05-27 UiO
104. Wang, Yijun; Kiraly, Agnes; Fraters, Menno; Gassmoeller, Rene; Dannberg, Juliane; Hansen, Lars; Conrad, Clinton Phillips. Olivine texture evolution under a simple deformation scheme: Comparing different numerical methods of LPO calculations. Ada Lovelace Workshop on Mantle and Lithosphere Dynamics; 2022-08-28 - 2022-09-02 UiO
105. Wentzcovitch, Renata; Shephard, Grace; Houser, Christine; Hernlund, John; Trønnes, Reidar G; Valencia, Juan. Seismological expression of the iron spin crossover in ferropericlase in the Earth's lower mantle. Exploring High Pressure Science at the Extremes; 2022-07-17 - 2022-07-22 UiO
106. Werner, S.C.; Krzesińska, A.M.; Bultel, B.; PTAL Team. Planetary Terrestrial Analogues Library—Rock Collection and Spectral Database for Analogue Studies of Igneous and Aqueous Environments on Mars. 85th Meteoritical Society Meeting, Glasgow. LPI Contributions 2695, 6198
107. Wessel, Paul; Chase, Andrew; Frazer, L.N.; Conrad, Clinton Phillips. A method for examining recent drifts of Pacific hotspots. AGU Fall Meeting; 2022-12-12 - 2022-12-16 UiO

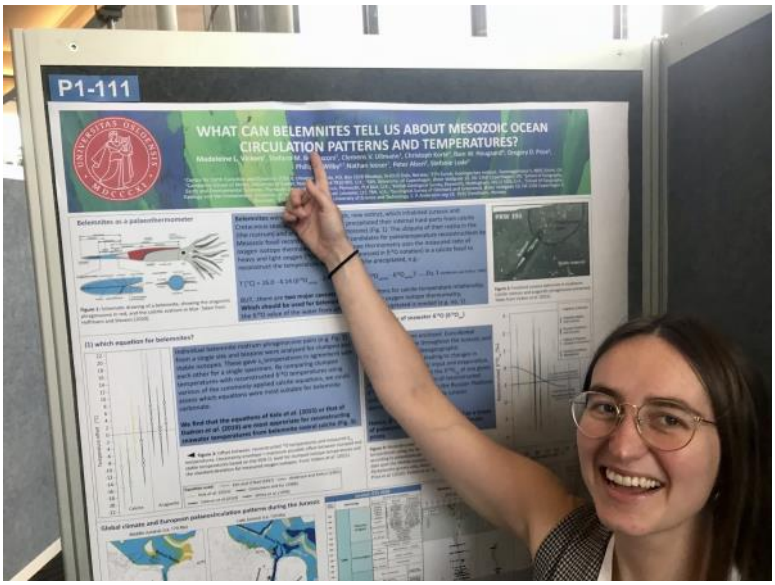

Madeleine Vickers presenting her poster at the 14th Conference on Paleoceanography in Bergen, August 22. Photo by: Madeleine Vickers

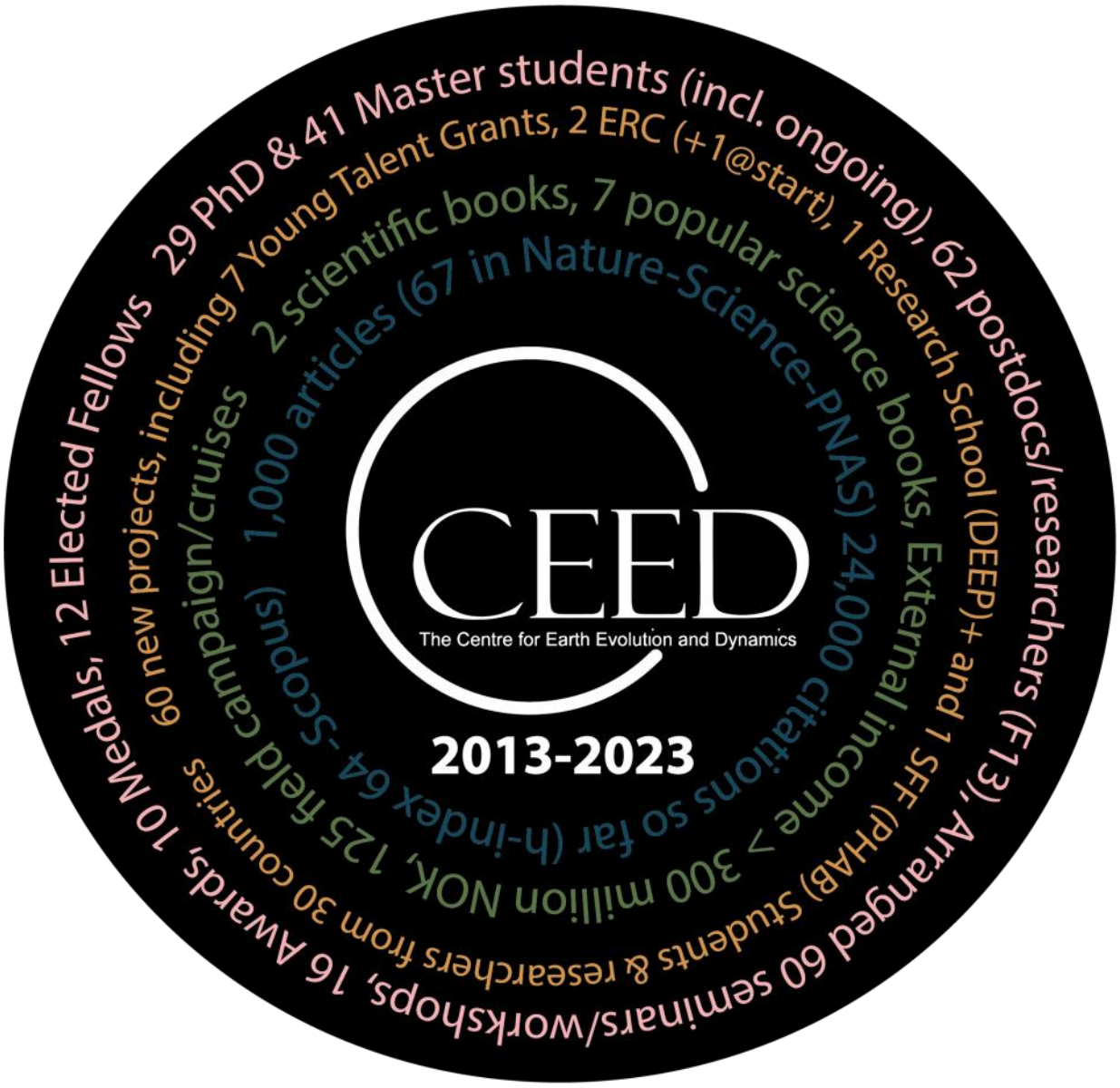

Some of the highlights of CEED, in classic concentric Earth layers with CEED at the core, featured the scientific colours.

Figure by: Grace Shephard.

Professors, Researchers and Adjunct Professors

Name	Title	Period at CEED	Man months in 2022
Abdelmalak, M. Mansour	Researcher	01.06.19-31.05.22	5,0
Andersen, Torgeir B.	Professor emeritus	01.03.18-30.04.20	
Augland, Lars Eivind	Researcher	13.20.21-28.02.23	1,5
Breivik, Asbjørn	Associate professor	01.03.18-28.02.23	6,0
Brodholt, John	Professor	01.03.18-28.02.23	2,4
Bultel, Benjamin	Researcher	15.01.19-31.01.22	1,0
Callegaro, Sara	Researcher	22.09.20-28.02.23	12,0
Caracas, Razvan	Researcher	01.09.18-28.02.23	2,4
Conrad, Clinton P.	Professor	01.08.16-28.02.23	12,0
Corfu, Fernando	Professor emeritus		
Domeier, Mathew	Researcher	07.08.16-28.02.23	12,0
Dubrovine, Pavel	Researcher	01.10.16-28.02.23	12,0
Faleide, Jan I.	Professor	01.03.18-28.02.23	3,6
Gac, Sebastien	Researcher	01.10.19-30.04.22	4,0
Gaina, Carmen	Professor	01.03.18-28.02.23	6,4
Heyn, Björn Holger	Researcher	15.09.16-28.02.23	12,0
Jahren, A. Hope	Researcher	01.09.16-28.02.23	12,0
Jerram, Dougal	Researcher	01.03.13-28.02.23	2,4
Jones, Morgan	Researcher	18.09.17-28.02.23	11,0
Kiraly, Agnes	Researcher	01.08.17-28.02.23	12,0
Kruger, Kirstin	Professor	01.11.18-28.02.23	1,2
Krzesinska, Agata	Researcher	15.10.20-28.02.23	12,0
Kulakov Evgeniy	Researcher	01.05.19-28.02.23	8,0
Luu, Jane	Adjunct professor	01.09.19-28.02.23	1,2
Magni, Valentia	Researcher	01.03.19-31.12.22	12,0
Maupin, Valerie	Professor	01.03.18-28.02.23	6,0
Mazzini, Adriano	Researcher	01.03.13-28.02.23	3,6
Medvedev, Sergei	Researcher	01.12.18-30.04.22	4,0
Minakov, Alexander	Researcher	01.10.20-28.02.23	12,0
Mohn Chris E.	Researcher	01.06.13-28.02.23	12,0
Neumann, Else Ragnhild	Professor emerita	01.03.13-28.02.23	
Niscancioglu, Kerim Hestnes	Adjunct professor	01.10.18-20.02.22	1,2
Planke, Sverre	Adjunct professor	01.07.18-28.02.23	1,8
Prieur, Nils Charles	Researcher	01.10.21-28.02.23	3,0
Rolf, Tobias	Researcher	01.12.18-31.05.22	10,5
Schweitzer, Johannes	Adjunct professor	01.09.15-28.02.23	2,4
Selway, Kate	Researcher	15.09.20-28.02.23	2,4
Shephard, Grace	Researcher	01.05.18-28.02.23	12
Steinberger, Bernhard	Researcher	01.05.16-28.02.22	2,4
Svensen, Henrik	Researcher	01.05.16-28.02.23	12
Torsvik, Trond H.	Professor	01.03.18-28.02.23	11
Trønnes, Reidar	Professor	01.03.18-28.02.23	6
Watson, Robin	Researcher	01.12.18-28.02.23	1,2
Werner, Stephanie	Professor	01.03.18-28.02.23	6

PhD candidates

Name	Funding Source	Period at CEED	Man months in 2022
Anzulović, Ana	CompSci (EU Horizon)	01.09.22-31.08.25	6,0
Ballo, Eirik	UiO	24.09.18-28.02.23	10,0
Beloša, Lea	UiO	04.11.19-05.11.23	12,0
Harrington, Elise	UiO	26.08.19-28.02.23	0,0
Hatalova, Petra	UiO	03.05.21-28.02.23	12,0
Jerkins, Anne E.	Project NNSN/Norsar	01.01.20-28.02.23	12,0
Marcilly, Chloé F.M.	UiO	05.08.19-04.08.22	12,0
Meza-Cala, Juan Camilo	NFR (project Dypole)	07.02.22-06.02.25	11,8
Ramirez, Florence	NFR (SFF CEED)	13.08.19-31.12.22	12,0
Wang, Yijun	NFR (project Anima)	07.09.21-28.02.23	12,0
Werdesteijn, Maaike	NFR (project Magpie)	28.05.19-15.02.23	12,0
Xue, Yi	ERC (project EPIC)	25.10.22-26.10.25	4,0

Postdoc fellowships

Name	Funding Source	Period at CEED	Man months in 2022
Capriolo, Manfredo	NFR (project Maples)	01.08.21-28.02.23	12,0
Cordoba, Antonio	NFR (project Platonics)	16.11.20-30.03.22	3,0
Davis, Anne Hope	NFR (project HIDDEN)	21.03.22-20.03.25	8,0
Dowding, Elizabeth	NFR (SFF CEED)	26.04.21-30.11.22	11,0
Figowy, Sarah	NFR (project HIDDEN)	28.06.22-27.06.25	6,0
Gallo, Leandro	MSCA (project Tango)	02.08.21-28.02.23	12,0
Geng, Ming	NFR (SFF CEED)	01.06.21-28.02.23	7,0
Heimdal, Thea Hatlen	NFR (SFF CEED)	07.01.19-26.03.22	3,6
Koehl, Jean-Baptiste	NFR (SFF CEED)	18.01.21-31.08.22	8,0
Neukirch, Maik	EEA (project Geysir)	01.06.21-28.02.23	12,0
Ozgurel, Ozge	NFR (SFF CEED)	03.02.20-02.03.22	12,0
Shan, Yu Tong	NFR (SFF CEED)	16.08.21-28.02.23	4,5
Stokke, Ella Wulfsberg	NFR (SFF CEED)	15.02.21-28.02.23	10,5
Van der Boon, Annique	NFR (SFF CEED)	14.06.21-28.02.23	12,0
Vickers, Madeleine Larissa	MSCA (project Icecap)	18.10.21-28.02.23	12,0

Techinical-administrative staff

Name	Title	Period at CEED	Man months in 2022
Hagopian, William	Senior Engineer	01.01.17-28.02.23	12,0
Nettum, Sara Asgari	Senior Executive Officer	01.12.20-28.02.23	12,0
Ryen, Sofie Hildegard	Senior Executive Officer	01.08.22-28.02.23	5,0
Thorud, Nina Mino	Head of Administration	01.01.22-31.03.22	3,0
Sannesmoen, Trine	Senior Executive Officer	01.02.22-28.02.23	11,0
Silkoset, Petter	Senior Engineer	01.01.16-28.02.23	12,0
Sørlie, Anita	Senior Exectuive Officer	15.06.16-31.07.22	7,0

Guest researchers at CEED

Name	Title	Period at CEED
Flatland, Annabel	Master student	27.06.22-24.08.22
Halvorsen, Erik	Dr. Philos	01.01.22-28.02.23
Saurety, Adrien	Master student	07.02.22-08.07.22

CEED: A CENTRE OF EXCELLENCE 2013-2023

Basic research relevant to society and industry

CEED
University of Oslo
PO Box 1028 Blindern
N-0315 Oslo
Norway

trine.sannesmoen@geo.uio.no
phone: +47 22 85 64 35

www.mn.uio.no/ceed